Report No. CDOT-DTD-R-2001-12

Performance of Geosynthetic-Reinforced Walls Supporting the Founders/Meadows Bridge and Approaching Roadway Structures

Report 2: Assessment of the Performance and Design of the Front GRS Walls and Recommendations for Future GRS Abutments

Naser Abu-Hejleh
Jorge G. Zornberg
Trevor Wang
Michael McMullen
William (Skip) Outcalt

October 2001

COLORADO DEPARTMENT OF TRANSPORTATION RESEARCH BRANCH

The contents of this report reflect the views of the authors, who are responsible for the facts and accuracy of the data presented herein. The contents do not necessarily reflect the official views of the Colorado Department of Transportation or the Federal Highway Administration. This report does not constitute a standard, specification, or regulation.

Technical Report Documentation Page

1. Report No.	2. Government Accession No.	3. Recipient's Catalog No.
CDOT-DTD-R-2001-12		

4. Title and Subtitle	5. Report Date
Performance of Geosynthetic-Reinforced Walls Supporting the Founders/Meadows Bridge and Approaching Roadway Structures Report 2: Assessment of the Performance and Design of the Front GRS Walls and Recommendations for Future GRS Abutments.	August, 2001 **6. Performing Organization Code**
7. Author(s) Naser Abu-Hejleh, Jorge G. Zornberg, Trevor Wang, Michael McMullen, and William (Skip) Outcalt	**8. Performing Organization Report No.** CDOT-DTD-R-2001-12
9. Performing Organization Name and Address Colorado Department of Transportation 4201 E. Arkansas Ave Denver, Colorado 80222	**10. Work Unit No. (TRAIS)** **11. Contract or Grant No.**
1. Sponsoring Agency Name and Address Colorado Department of Transportation 4201 E. Arkansas Ave Denver, Colorado 80222	**13. Type of Report and Period Covered** **14. Sponsoring Agency Code**
15. Supplementary Note	

16. Abstract The Founders/Meadows structure is the first major bridge in the United States built on footings supported directly by geosynthetic-reinforced soil (GRS) walls, eliminating the traditional use of deep foundations altogether. The performance of the front GRS walls, which support the bridge structure and embankment behind the abutment wall, was investigated by collecting data for the movements of the wall facing, settlement of the bridge footing, distributions of the vertical earth pressures and geogrid tensile strains inside the front GRS walls, and lateral earth pressures against the wall facing. Monitoring data was collected during six construction stages and while the structure was in service. This report provides a summary and analysis of the collected data, assessment of the performance and design of the front wall, and recommendations for design and construction of future GRS abutments. Compaction operations created large loads in the reinforcements and against the wall facing during interim construction stages of the front wall. The front GRS walls showed excellent performance because: (i) the monitored movements were significantly smaller than those expected in design or allowed by performance requirements, (ii) post-construction movements and geogrid strains became negligible after an in-service period of 1 year, (iii) measured loads in the reinforcements, connections, and on the wall facing were less than or around 50% of those estimated in the design, (iv) there is not any potential for overturning the structure (due to the flexibility of GRS wall system, resulting in the reduction of loads developed behind and against the wall facing), and (v) the measured bearing pressures were well below the allowable soil bearing capacity. The design employs a high creep reduction factor for the geogrid reinforcements although little if any long-term creep was observed.

Implementation The excellent performance of the Founders/Meadows GRS walls and other GRS abutment structures reported in the literature suggests that the use of GRS walls to support both the bridge and approaching roadway structure should be considered by CDOT design engineers as a standard alternative in future bridge abutment projects. The deformations and performance monitored at the Founders/Meadows GRS walls can be used as a reference for future projects. The features, limitations, and recommendations for the design and construction of future GRS abutments are presented. Recommendations to waive the design requirements for facing connection strength and to employ larger percent of the geosynthetic ultimate strength in the design are furnished.

17. Key Words	18. Distribution Statement
GRS abutments, design, performance, creep, connection, walls, MSE	

19. Security Classif. (of this report)	20. Security Classif. (of this page)	21. No. of Pages	22. Price

CONVERSION TABLE

U. S. Customary System to SI to U. S. Customary System

(multipliers are approximate)

Multiply (symbol)	by	To Get (symbol)	Multiply	by	To Get
		LENGTH			
Inches (in)	25.4	millimeters (mm)	mm	0.039	in
Feet (ft)	0.305	meters (m)	m	3.28	ft
yards (yd)	10.914	meters (m)	m	1.09	yd
miles (mi)	1.61	kilometers (km)	m	0.621	mi
		AREA			
square inches (in^2)	645.2	square millimeters (mm^2)	mm^2	0.0016	in^2
square feet (ft^2)	0.093	square meters (m^2)	m^2	10.764	ft^2
square yards (yd^2)	0.836	square meters (m^2)	m^2	1.195	yd^2
acres (ac)	0.405	hectares (ha)	ha	2.47	ac
square miles (mi^2)	2.59	square kilometers (km^2)	km^2	0.386	mi^2
		VOLUME			
fluid ounces (fl oz)	29.57	milliliters (ml)	ml	0.034	fl oz
gallons (gal)	3.785	liters (l)	l	0.264	gal
cubic feet (ft^3)	0.028	cubic meters (m^3)	m^3	35.71	ft^3
cubic yards (yd^3)	0.765	cubic meters (m^3)	m^3	1.307	yd^3
		MASS			
ounces (oz)	28.35	grams (g)	g	0.035	oz
pounds (lb)	0.454	kilograms (kg)	kg	2.202	lb
short tons (T)	0.907	megagrams (Mg)	Mg	1.103	T
		TEMPERATURE (EXACT)			
Farenheit (°F)	5(F-32)/9 (F-32)/1.8	Celcius (° C)	° C	1.8C+32	° F
		ILLUMINATION			
foot candles (fc)	10.76	lux (lx)	lx	0.0929	fc
foot-Lamberts (fl)	3.426	candela/m (cd/m)	cd/m	0.2919	fl
		FORCE AND PRESSURE OR STRESS			
poundforce (lbf)	4.45	newtons (N)	N	.225	lbf
poundforce (psi)	6.89	kilopascals (kPa)	kPa	.0145	psi

Performance of Geosynthetic-Reinforced Walls Supporting the Founders/Meadows Bridge and Approaching Roadway structures

Report 2: Performance and Assessment of the Design of the Front GRS Walls and Recommendations for Future GRS Abutments

by

Naser Abu-Hejleh
Jorge G. Zornberg
Trevor Wang
Michael McMullen
William (Skip) Outcalt

Report No. CDOT-DTD-R-2001-12

Prepared by
Colorado Department of Transportation
Research Branch

Sponsored by the
Colorado Department of Transportation
In Cooperation with the
U.S. Department of Transportation
Federal Highway Administration

October 2001

Colorado Department of Transportation
Research Branch
4201 E. Arkansas Ave.
Denver, CO 80222
(303) 757-9506

ACKNOWLEDGEMENTS

The Colorado Department of Transportation and the Federal Highway Administration provided funding for this study. The authors wish to acknowledge valuable input and comments provided by the study panel members, Rich Griffin, Hsing Cheng Liu, and Matt Greer. Special thanks are also extended to Dan Smith for his ongoing excellent surveying work.

EXECUTIVE SUMMARY

The Founders/Meadows structure is the first major bridge in the United States built on footings supported directly by geosynthetic-reinforced soil (GRS) walls, eliminating the use of traditional deep foundations altogether. The first report of this study (Abu-Hejleh et al., 2000) presented the design, materials, construction, and instrumentation of these GRS walls. The performance of the front GRS walls, which support the bridge structure and embankment behind the abutment wall, was investigated by collecting data for the movements of the wall facing, settlement of the bridge footing, distributions of the vertical earth pressures and geogrid tensile strains inside the front GRS walls, and lateral earth pressures against the wall facing. Monitoring data was collected during six construction stages and while the structure was in service. This 2nd report presents a summary and analysis of the collected data, assessment of the performance and design of the front GRS wall based on the reliable collected data, and recommendations for design and construction of future GRS abutments.

The maximum geogrid tensile loads, connection loads, and lateral earth pressures against the wall facing measured during placement and compaction of 1 meter of backfill are up to twice those estimated in the design. Measures to alleviate/contain the compaction influence during interim construction stages of the wall were furnished in Chapter 6.

The Founders/Meadows front GRS walls experienced excellent performance because:

- The monitored movements were smaller than those expected in design and less than a third of those allowed by AASHTO performance requirements. Post-construction movements and geogrid tensile strains became negligible after an in-service period of 1 year. Preliminary results suggest no signs of development of bridge bump problem.
- The measured maximum geogrid tensile loads range from 43% to 57% of the values estimated in design.
- The measured connection loads range from 19% to 47% of the values estimated in design. The measured lateral earth pressures against the wall facing range from 4.2 % to 36.4% of the values estimated in design. The measured vertical earth pressures behind the wall facing range from 2% to 67% of the vertical earth pressure values employed in design. The

placement of bridge superstructure had a small influence on the loads developed behind and against the upper zone of the wall facing.

- The measured eccentricity values of the resulting vertical forces acting at different horizontal levels inside the front GRS wall were negligible (i.e., there is not potential for overturning the Founders/Meadows structure). This was attributed to the flexibility/movements of the front GRS wall system that reduced the loads developed behind and against the wall facing.
- The measured bearing pressures at the base of the reinforced fill and below the bridge footing were below the expected design and allowable values of the soil bearing capacity.

If the post-construction geogrid strains were developed due to traffic loads only (not from creep), the design overestimated the reinforcement loads due to traffic load by almost two times. If the post-construction geogrid strains were developed due to creep (not from traffic load), they are relatively very small (zero to 0.09%), and they leveled out and became constant from January to June 2000. However, CDOT design procedure employs a creep reduction factor of 2.7 to determine the geogrid long-term design strength from the geogrid ultimate strength.

The findings of this study agree well with the research findings on three other GRS bridge supporting structures (FHWA, 2000; see Section 1.5.1). First, all four structures experienced acceptable level of movements under service surcharge pressure up to 200 kPa. Second, all structures showed negligible long-term lateral creep deformation under service load. Third, lateral earth loads against the relatively flexible wall facings and connections were small.

Implementation Statement

The excellent performance of the Founders/Meadows GRS walls and other GRS abutment structures reported in the literature suggests that the use of GRS walls to support both the bridge and approaching roadway structure should be considered by CDOT design engineers as a standard alternative in future bridge abutment projects. This application works well for multiple spans bridges and allows for construction in stages and within a small working area. GRS abutments can be considered at any time scour is not a significant problem. GRS abutments may be advantageous from cost basis whenever 1) a fill retaining structure is needed at an abutment and pile driving or drilled shafts are difficult or expensive, and 2) as a competitive measure to

alleviate the bridge bump problem resulting from *moderate* post-construction settlements (25 mm to 75 mm) of the approach slab. A settlement below 25 mm can be more economically dealt with by using an approach slab approximately 9 m long. A settlement of 75 mm would be a typical abutment settlement limit for a superstructure of a medium span bridge (see Chapter 2). When expected structure settlements exceed 75 mm, deep footings should be considered to support the bridge abutment. In all cases, the foundation soil for the leveling pad of the wall facing should be firm.

Future GRS abutments constructed and designed as in the Founders/Meadows structure are expected to experience a satisfactory performance. Abu-Hejleh et al. (2000) presented the layout, design, and material and construction specifications of the front GRS walls of the Founders/Meadows structures (see also Chapter 1). The recommendations that could be considered in the design and construction of future GRS abutments to enhance the performance and reduce the project costs are:

1) The maximum tension line can be assumed to be bilinear. It starts at the toe of the wall and extends through a straight line to the back edge of the bridge footing at the mid height of the wall, and from there extends vertically to the back edge of the bridge footing.
2) The displacements reported for the Founders/Meadows structure provide a reference of the order of magnitude of displacements anticipated in future GRS abutment projects.
3) To minimize wall deformations to the lowest level, it is preferred to: a) place backfill behind the abutment wall before placing the girders, b) place the GRS backfill during the warm and dry season, and c) the well-compacted granular backfill should have a friction angle of 40 degrees.
4) The Founders/Meadows project verifies this application for applied surcharge bearing pressures up to 150 kPa. Higher surcharge pressures up to 200 kPa are allowed that could require reinforcement with closer spacing than that employed in the Founders/Meadows structure.

Based on the performance of the Founders/Meadows structure and the findings of other research studies (see Section 1.5.1), the following additional recommendations could be made:

1) Place the blocks and reinforcements as in the Founders/Meadows structure but without mechanical connections between blocks (i.e., waive the requirements for facing connection strength). In this case, it may be preferred to utilize blocks having a raised lip along the block's outside face and to use setbacks 50% larger than those employed with the mechanical connections. In order to control/minimize the wall facing movements in the upper 1.6 m of the wall below the surcharge load, it is recommended for that zone to: 1) place reinforcements with a wrapped-around procedure, 2) attach the facing blocks to the reinforced soil mass through tail reinforcements that extend 1 m into the reinforced soil mass, and 3) dowel and grout with cement the top block layers (in lieu of gravel filled block cells).

2) Employ any type of geosynthetic reinforcements (not necessary geogrid) having a weight per area larger than 271 g/m^2 (from CDOT specification) that meet the design requirements and:

   a. Reinforcement spacing of 0.2 m (not 0.4 m as in the Founders/Meadows structure).

   b. Reinforcement stiffness consistent with those used in the Founders/Meadows structure in order to maintain small loads in reinforcements and an acceptable level of wall movements. In other words, for a vertical reinforcement spacing of 0.2 m, the tensile force at 1% of lateral tensile strain should be larger than 1000 kN/m, measured in accordance with ASTM D 4595 test method.

   c. Reinforcements long-term design strength estimated as high as 35% of the ultimate strength (17% employed in the Founders/Meadows structure for the geogrid). To reliably use this high value, it may be necessary to perform confined creep tests (FHWA, 1997; Wu and Helwany, 1996) on soil-geosynthetic specimens (materials and testing conditions as expected in the project) and show that the GRS composite will experience negligible long-term creep deformations.

TABLE OF CONTENTS

LIST OF FIGURES

LIST OF TABLES

1.0 BACKGROUND

1.1 Overview

The technology of geosynthetic-reinforced soil (GRS) systems has been used extensively in transportation systems to support the self-weight of the backfill soil, roadway structures, and traffic loads. The increasing use and acceptance of soil reinforcement has been triggered by a number of factors, including cost savings, aesthetics, simple and fast construction techniques, good seismic performance, and the ability to tolerate large differential settlement without structural distress. A comparatively new use of this technology is the use of GRS abutments in bridge applications, in which the reinforced soil mass would directly support both the bridge and approaching roadway structures. In this case, the reinforcement tensions and soil stresses are mobilized in a different manner than in the case of GRS walls supporting small surcharge loads. When compared to typical systems involving the use of deep foundations to support bridge structures, the use of geosynthetic-reinforced systems has the potential of alleviating the "bump at the bridge" problem caused by differential settlements between the bridge abutment and approaching roadway.

The most prominent GRS abutment for bridge support in the U.S. is the new Founders/Meadows Parkway structure, located 20 miles south of downtown Denver, Colorado. It carries Colorado State Highway 86 over U.S. Interstate 25. Figure 1.1 shows the segmental retaining wall system located at the southeast side of the new Founders/Meadows Bridge structure. This figure shows the bridge superstructure supported by the "front GRS wall," which extends around a 90-degree curve into a "lower GRS wall" supporting the "wing wall" and a second tier, "upper GRS wall." Figure 1.2 shows a plan view of the completed two-span bridge and approaching roadway structures. Each span of the new bridge is 34.5 m long and 34.5 m wide in order to accommodate six traffic lanes and sidewalks on both sides of the bridge. Figure 1.3 shows a typical cross-section through the "front GRS wall" and "abutment GRS wall." The figure illustrates that the front GRS wall provides direct support for the bridge and approaching roadway structures. The centerline of the bridge abutment wall and front edge of the foundation are located 3.1 m and 1.35 m, respectively, from the rear of the block facing of the front GRS wall (Figure 1.3). A short reinforced concrete abutment wall and two wing walls, resting on the spread foundation,

confine the reinforced backfill soil behind the bridge abutment (Figures 1.1, 1.2, and 1.3) and support the bridge approach slab.

The Founders/Meadows structure was the first major bridge in the United States built on footings supported directly by a geosynthetic-reinforced soil system, eliminating the use of traditional deep foundations (piles and caissons) altogether. A key element in the design was the need to support the high concentrated loads from the bridge footing and to alleviate the bridge bump problem. In addition, the construction allows for construction in stages and comparatively smaller construction working areas. The competent claystone bedrock formation below the base of the reinforced backfill and the use of an extended reinforced zone (Figure 1.3) significantly enhanced the overall stability and minimized settlements of the front GRS wall structure. The reasons listed above, other perceived advantages of GRS structures, and excellent performance of full-scale geosynthetic reinforced abutments and piers (see Section 1.5.1) convinced Mr. Trevor Wang and other Colorado DOT engineers to select GRS walls to support the Founders/Meadows superstructure. CDOT designed this structure in 1996, before FHWA published preliminary design details for bridge superstructures directly supported by MSE walls with panel facings (not blocks) and steel reinforcement (not geosynthetic reinforcement) in 1997 (Elias and Christopher 1997).

The performance of bridge superstructures supported by GRS abutments has not been tested under actual service conditions to merit acceptance without reservation in highway construction. Consequently, the Founders/Meadows structure was considered experimental and comprehensive material testing, instrumentation, and monitoring programs were incorporated into the construction operations. Three sections of the GRS system were instrumented to provide information on the structure movements, distribution of vertical earth pressures, lateral earth pressure on the wall facing, geogrid strains, and soil temperatures and moisture content. Performance data were collected during six construction stages and after opening the structure to traffic. Monitoring will continue until the structure's long-term movement becomes negligible. The overall objectives of this investigation are:

- To assess the performance of the structure (front and abutment GRS walls) under service loads using short- and long-term movement data.
- To evaluate the suitability of CDOT and AASHTO design procedures and assumptions for the use of front GRS wall as a measure to support the bridge footings, and, in conjunction with the abutment GRS wall, to alleviate the bridge bump problem.
- To collect performance data for future calibration and validations of numerical models.

The first report of this study (Abu-Hejleh et al., 2000) presented the design, materials, construction, and instrumentation of the Founders/Meadows structure. The focus of this second report is on the performance of the front GRS wall that supports the bridge structure and the embankment behind the abutment wall (see Figure 1.3). This report compiled herein presents a summary and analysis of all the data collected in the monitoring program for the front GRS wall, and assessment of the performance and design of this wall. The report recommendations for future design and construction of GRS abutments supporting directly bridge and approaching roadway structures were presented previously in the Executive Summary. This report is organized as follows:

- The rest of this chapter will present a brief description of the front GRS wall's design (Section 1.2), materials (Section 1.3), and instrumentation (Section 1.4). See Abu-Hejleh et al. (2000) for more detailed description of these issues. Findings of previous research studies referred to in the discussion of the results presented in this report are presented in Section 1.5.
- Chapter 2 presents a summary and discussion of the construction and post-construction induced movement data of the front wall facing and settlement of the bridge footing and comparison with the design and tolerable values.
- Chapter 3 presents a summary, analysis, and discussion of the collected measurements for the distribution of vertical earth pressure within the front GRS wall during six construction stages and one post-construction stage. The measured and analyzed data are compared with the design values and discussed.

- Chapter 4 presents a summary, analysis, and discussion of the collected measurements for lateral earth pressure against the wall facing during all monitored stages. The measured and analyzed data are compared with the design data and discussed.
- Chapter 5 presents a summary, analysis, and discussion of the collected measurements for the distribution of geogrid strains within the front GRS wall during six construction stages and one post-construction stage. The measured and analyzed data are compared with the design data and discussed.
- Chapter 6 presents a summary of all the study findings regarding the response and performance of the front GRS wall and an assessment of CDOT design of the front GRS wall.

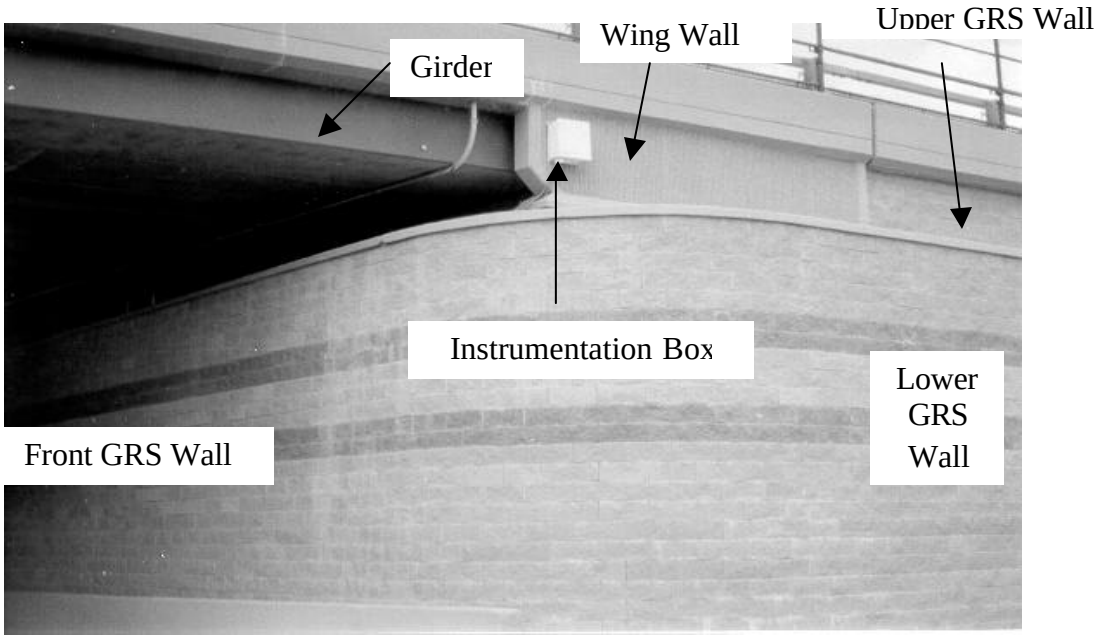

Figure 1.1 View of the Southeast Side of the Completed Founders/Meadows Bridge.

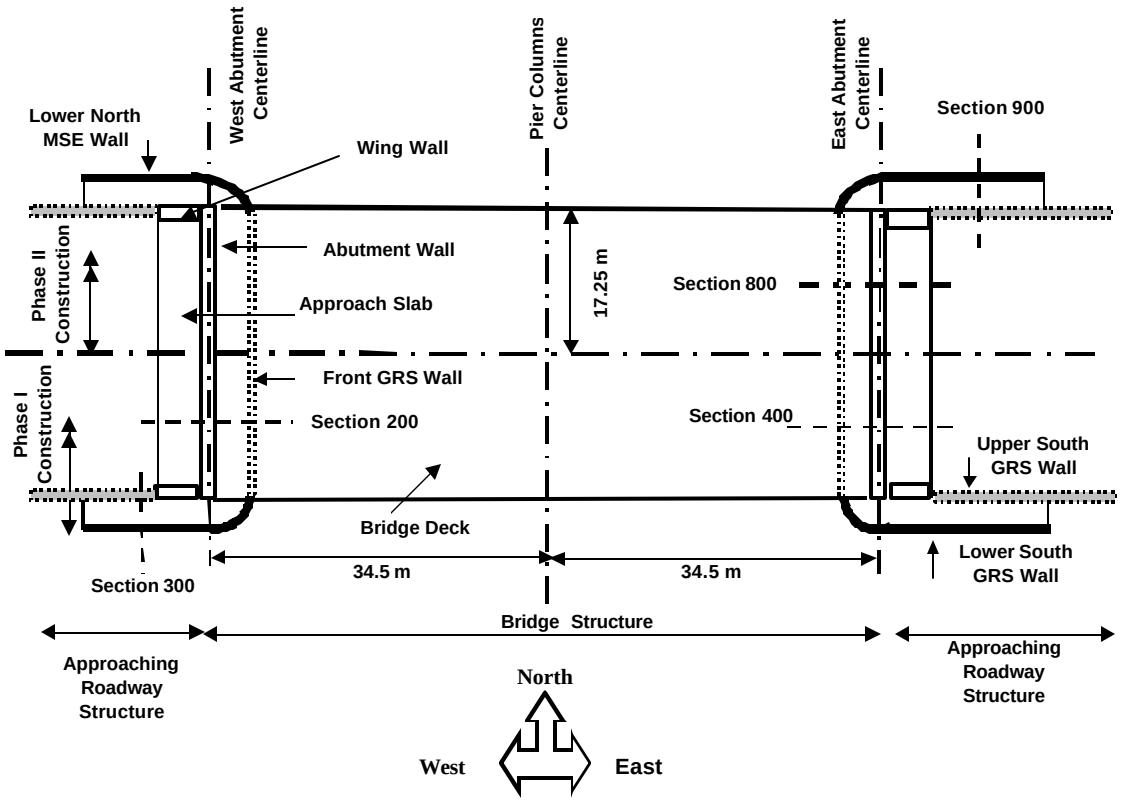

Figure 1.2 Plan View of the Completed Two-span Founders/Meadows Bridge and Approaching Roadway Structures.

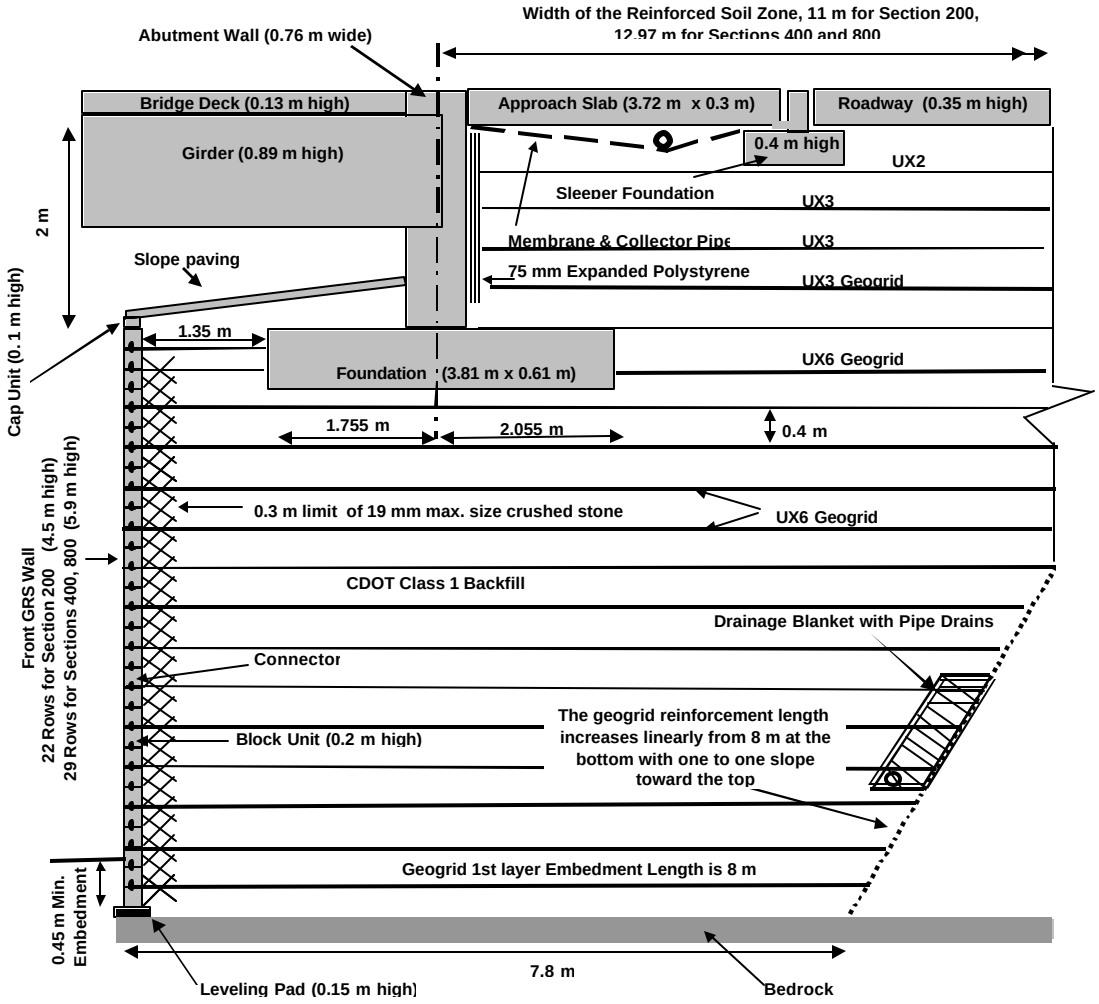

Figure 1.3. Typical Monitored Cross-Section (Sections 200, 400, and 800 in Figure 1.2) through the Front and Abutment GRS Walls.

1.2 Design of the Front GRS Wall

A comparatively long reinforced soil zone below the bridge and approaching roadway structure was considered (Figure 1.3) in order to address four design issues. First, integrating the roadway approach embankment and the bridge footing with an extended reinforced soil zone may alleviate the differential settlement problem. Second, enhancing the overall stability of the reinforced structure. Third, providing an additional margin of safety to alleviate concerns regarding a potential shear strength loss due to soaking of the claystone bedrock. Fourth, and in conjunction with the firm claystone foundation, significantly minimizing the settlement of the reinforced soil structure. The expected small settlements of the front GRS wall and the no scour potential made the design and construction of this structure possible.

The vertical earth pressure, $s_{v,}$ and lateral earth pressure, $s_{h,}$ employed for the calculation of the reinforcements maximum forces along the potential failure line at a depth z below the bridge footing (Elias and Christopher, 1997) are:

$$s_v = g\, z + Ds_v \qquad (1.1)$$

$$s_h = K_a\, s_v \qquad (1.2)$$

Where g is the backfill unit weight, K_a is the active earth pressure coefficient, and Ds_v is the stress increment induced within the soil mass by concentrated surcharge loads applied on the bridge footing. The value of K_a was estimated in the design as 0.31 for a backfill soil with friction angle of 34 degrees and a surcharge slope angle of 14 degrees (to account for backfill behind abutment wall). The maximum tensile force, $T_{max,}$ in each geogrid reinforcement layer (100% coverage) per unit width of wall was estimated as:

$$T_{max} = s_h\, S \qquad (1.3)$$

Where S is the reinforcement vertical spacing. For MSE walls supporting high surcharge load, Elias and Christopher (1997) recommended the use of Equations 1.2 to estimate the lateral earth pressures on the wall facing, s_{ho}, and Equation 1.3 to estimate the connection loads per unit width of wall, $T_{o,}$

$$\sigma_{ho} = K_a \sigma_v \quad (1.4)$$

$$T_o = \sigma_h S \quad (1.5)$$

1.3 Materials of the Front GRS Wall

The backfill soil used in this structure includes fractions of gravel (35%), sand (54.4%), and fine-grained soil (10.6%). The backfill met the material and construction (i.e., compaction level) requirements for CDOT Class 1 backfill (Abu-Hejleh et al., 2000). A friction angle of 34° and zero cohesion were assumed for the backfill material in the design of the front GRS walls. To evaluate the suitability of these design parameters for the gravelly backfill, conventional direct shear tests and large-size direct shear and triaxial tests were conducted. In the conventional tests, the 35% gravel portion was removed from the specimens per the test standards, but in the large-size triaxial and direct shear tests, the backfill soil specimens included the gravel portion. The results of conventional direct shear tests and large-size direct shear and triaxial tests indicate that assuming zero cohesion in the design procedure and removing the gravel portion from the test specimens lead to significant underestimation of the actual shear strength of the backfill. Hyperbolic model constitutive parameters were determined from the results of the large-size triaxial tests.

CDOT specifications imposed a global reduction factor of 5.82 to determine the long-term design strength (LTDS) of the geogrid reinforcements from their ultimate strength. This global reduction factor accounts for reinforcement tensile strength losses over the design life period due to creep, durability, and installation damage. It also includes a factor of safety to account for uncertainties. The Tensar Corporation manufactured the geogrid reinforcements. The long-term-design strength (LTDS) of the UX 6 geogrid reinforcements employed beneath the bridge footing (Figure 1.3) is 27 kN/m. Facing mechanical connectors between blocks layers and between blocks and reinforcements were employed in the front GRS wall (Figure 1.3). The measured connection strength for this system of connectors mobilized at a horizontal movement of 19 mm (service state), conducted in accordance with NCMA Test Method SRWU-1, was 57.7 kN/m. All of CDOT requirements for the geogrid reinforcements and connections were met (Abu-Hejleh et al., 2000).

1.4 Instrumentation and Monitoring Program

A number of reliable instruments and techniques were employed in this study to monitor the performance of the front GRS wall. Surveying was employed to determine the movements of the facing of the front GRS wall and settlement of the bridge footing. An inclinometer (Geokon Model 6000) was employed to measure lateral movement of the fill material behind the facing of the front GRS wall, both parallel and or perpendicular to the wall. Geokon Model 4800 pressure cells were used to measure the distribution of vertical earth pressure inside the front GRS wall. Geokon Model 4810 pressure cells were employed to measure profiles of lateral earth pressure against the rear facing of the front GRS wall. Geokon Model 4420 Crackmeters and Geokon Model 4050 strain gages were employed to measure distribution of geogrid strains inside the front GRS wall. Refer to Geokon manuals and Abu-Hejleh et al. (2000) for a detailed description of these gages and reduction of the gages data.

The instrumentation program was conducted in two phases: Phases I and II, which correspond, respectively, to the construction of the Phase I Structure (from July to December 1998) and Phase II Structure (from January to June 1999). Construction was implemented in two phases to accommodate traffic needs (Figure 1.2). Monitored Sections 200 and 400 are located at the center of the Phase I Structure and Section 800 (identical to section 400) is located at the center of the Phase II Structure (Figure 1.3). The layouts of the instrumented Sections 200, 400, and 800 are shown in Figures 1.4, 1.5, and 1.6, respectively. All these sections were instrumented with survey targets as shown in Figures 1.4, 1.5, and 1.6. As a pilot investigation, Section 400 of Phase I structure was additionally instrumented with two pressure cells, two crackmeters, and one inclinometer (Figures 1.4 and 1.5). Abu-Hejleh et al (2000) presented the results of these four gages. There were some concerns with geogrid strain results obtained from the crackmeters (Abu-Hejleh et al., 2000) and so their results are not presented in this report.

Along Phase II Structure, Section 800 also was heavily instrumented with pressure cells and strain gauges (Geokon 4050 gages) along four critical Location Lines: Location Line A close to the wall facing, Location Line B close to the centerline of the bridge abutment wall, Location Line C close to the back edge of the bridge footing, and Location Line D behind the bridge footing (see Figure 1.6). Table 1.1 lists the location of these gages, where Y is the height of the

gage above the leveling pad, and X is the distance of the gage from the rear side of the block facing. The gages in Table 1.1 are designated through one or two digits and two or three letters (e.g., 10VBN, 11HN, and 6SBN). The first digit indicates the number of the closest geogrid layer to the gage (Figure 1.6). The first letter indicates the gage type: V= pressure cell to measure vertical pressure, H= pressure cell to measure lateral earth pressure, and S= Strain gage. The 2nd letter indicates the closest Location Line to the gage. The third letter (optional, N or S) is used when two gages are placed at the same location, one north of the control section (N) and one south of the control section (S). Two gages were placed at the same location to check on the consistency of the measured data and the suitability of assuming plain strain conditions. The 1st (reference) readings for each gage and the date and fill height when these reading were collected are also summarized in Table 1.1. For most of the gages, reference readings were collected when there was no backfill over the gage (i.e., gage location in Table 1.1 matches the fill height when the 1st reading was collected).

The collected performance data is organized according to the loading sequence (Figures 1.4 and 1.5) as follows:

Stage I. Construction of the front GRS wall up to the bridge footing elevation. The Stage I structure provides support for the bridge and approaching roadway structures.

Stage II. Placement of the bridge footing and girders seat.

Stage III. Placement of girders.

Stage IV. Placement of the reinforced backfill behind the abutment wall from the bridge footing elevation to the bottom of the sleeper footing.

Stage V. Placement of the of bridge deck.

Stage VI. Placement of the approaching roadway structure (including approach slab) and other minor structures. By the end of this stage, the total average vertical pressure exerted directly underneath the bridge footing was estimated as 115 kPa. This stage was completed on December 16, 1998 for the Phase I Structure and on June 30, 1999 for the Phase II Structure.

Stage VII. Post-Construction Stage until June 2000 (lasted 1 year for the Phase I Structure and 18 months for the Phase II Structure). The total vertical contact pressure exerted directly underneath the bridge footing during this stage was estimated to be 150 kPa.

Table 1.2 shows the start and completion date of each stage along Sections 200 and 400 (Phase I) and Section 800 (Phase II). Note that Stage IV occurred before Stage III on the Phase I Structure. The estimated average applied vertical earth pressures underneath the bridge footing and on the base of the reinforced fill (7.5 m wide) along Sections 400 and 800 are summarized in Table 1.3. Data from Section 800 gages were collected automatically every 6 minutes during Stage I and every half hour during Construction Stages II to VI. After opening the structure to traffic (Stage VII), data was collected every 10 minutes over the first two months and every 36 hours after that. Data for all gages were lost from days 320 to 355 and from days 439 to 483 (days counted from January 1, 1999). All the instrumentation results collected until the end of Stage VII (June 2000) are presented and discussed in this report. Subsequent publications will summarize the results from long-term monitoring results obtained after June 2000.

Table 1.1 Location and Reference Readings for Gages Placed along Section 800.

Gage #	Data logger Channel	Gage Location		Information for Reference Readings			
		X	Y	Date of Collection (# of Days from Jan. 1, 1999)	Height of Fill (m)	Gauge Reading	Temp., C
Pressure Cells to Measure Vertical Earth Pressure							
0VA	3	1.00	-0.15	23	-0.15	9644	0.2
0VD	5	7.50	-0.15	23	-0.15	8888	-0.1
3VA	11	0.60	1.52	28	1.52	8976	11.5
6VA	16	0.60	2.33	36	2.33	8988	14.4
6VBN	17	3.10	2.33	36	2.33	9026	17.2
6VBS	18	3.10	2.33	36	2.33	8995	21.1
6VC	19	5.50	2.33	36	2.33	8952	18.3
6VD	20	7.50	2.33	36	2.33	8420	17.8
10VA	28	0.60	3.95	49	3.95	9190.8	-0.9
10VBN	29	3.30	3.95	49	3.95	8787	-2.7
10VBS	30	3.30	3.95	49	3.95	8753	-0.2
10VC	31	5.00	3.95	49	3.95	9362	-0.5
10VD	32	7.60	3.95	49	3.95	8507	-0.7
12VD	41	7.30	4.95	51	5.28	9326	0.7
13VA	42	1.85	5.05	55	5.28	9090	2
13VB	43	3.25	5.05	55	5.28	9046	2.9
13VC	44	4.65	5.05	55	5.28	8889	3.7
Pressure Cells to Measure Lateral Earth Pressure on the Facing							
7H	21	0	4.27	46	4.27	9171	3.43
9H	22	0	3.75	48	3.75	9558	9.70
11HN	33	0	4.57	50	4.57	9101	10.8
11HS	34	0	4.57	50	4.57	9269	10.3
12H	40	0	4.97	55	5.28	8615	4.42
Strain Gages to Measure Lateral Geogrid Strain							
2SA	7	0.39	0.6	23	0.9	7076	3.1
2SB	8	3.6	0.6	23	0.9	7373	3.3
2SC	9	5.8	0.6	23	0.9	8122	3.3
6SA	12	0.38	2.23	35	2.23	4120	20.2
6SBN	13	3.35	2.23	35	2.23	4560	12.3
6SBS	14	3.35	2.23	35	2.23	3328	17.2
6SC	15	5.5	2.23	35	2.23	3923	14.6
10SA	23	0.33	3.85	50	3.85	2741	4.9
10SB	25	3.25	3.85	50	3.85	3080	4
10SC	26	5	3.85	50	3.85	3640	4
10SD	27	7.6	3.85	50	3.85	3576	3.9
12SB	36	3.17	4.67	51	4.67	2845	10.2
12SD	38	7.43	4.67	51	4.67	3375	8.3

Table 1.2. Time Progress of the Monitored Construction and Post-Construction Stages.

Monitored Stages	Phase I Structure		Phase II Structure, Section 800	
	Section 200 Date	Section 400 Date	Starting Date	# Days from Jan. 1, '99
Leveling Pad	7/16/98	8/15/98	1/19/99	19
Stage I Construction	8/ 15/98	9/12/98	2/ 24/99	19-55
Stage II Construction	9/12/98	9/26/98	3/8/99	55-67
Stage III Construction	10/6/98	10/12/98	3/10/99	67-69
Stage IV Construction	9/19/98	10/3/98	3/26/99	69-85
Stage V Construction	11/25/98		5/25/99	85-125
Stage VI Construction	12/15/98		6/29/99	125-179
Post-Construction Stage (VII)	12/16/98		6/30/99	180-545

Table 1.3. Estimated Average Applied Vertical Earth Pressure Beneath the Bridge Footing and on the Base of the Reinforced Fill along Sections 400 and 800.

	Estimated Average Applied Vertical Earth Pressure (kPa)	
	Bridge Footing	Base of the Reinforced Fill
Stage I Construction	0	117
Stage II Construction	22	134
Stage III Construction	64	155
Stage IV Construction	84	180
Stage V Construction	101	189
Stage VI Construction	115	199
Stages VII and VIII (Bridge in service)	150	223

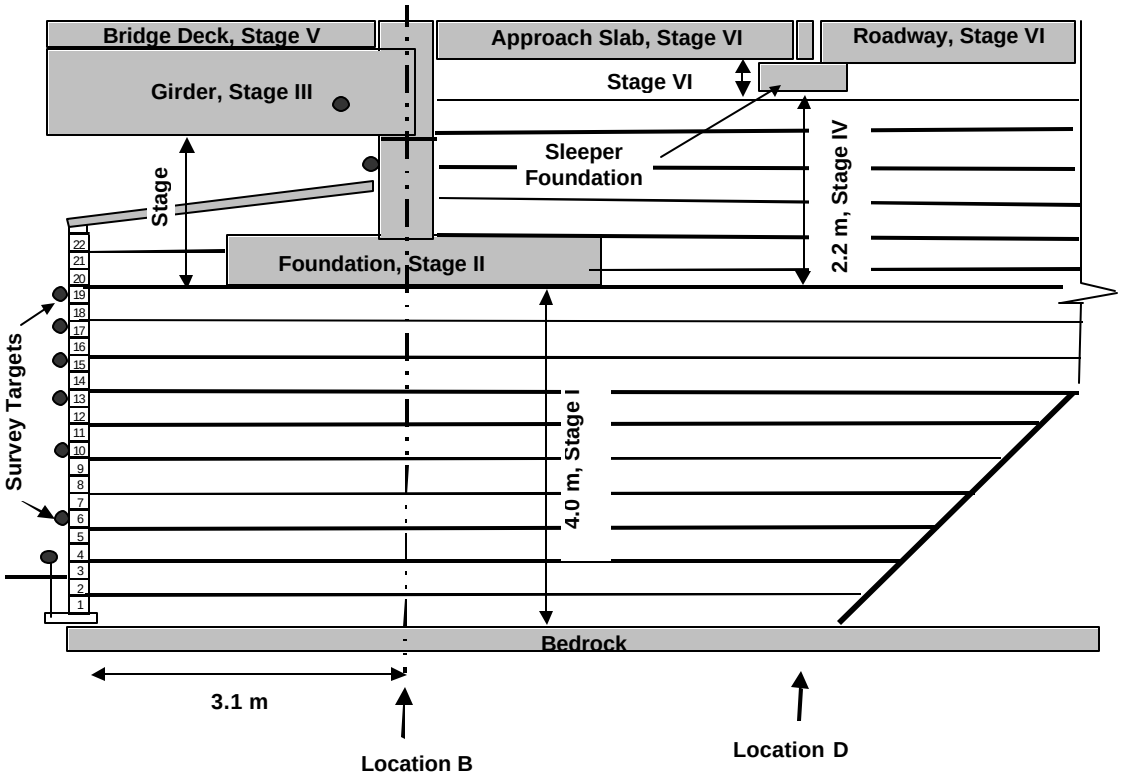

Figure 1. 4 Instrumented Section 200 Indicating Construction Stages.

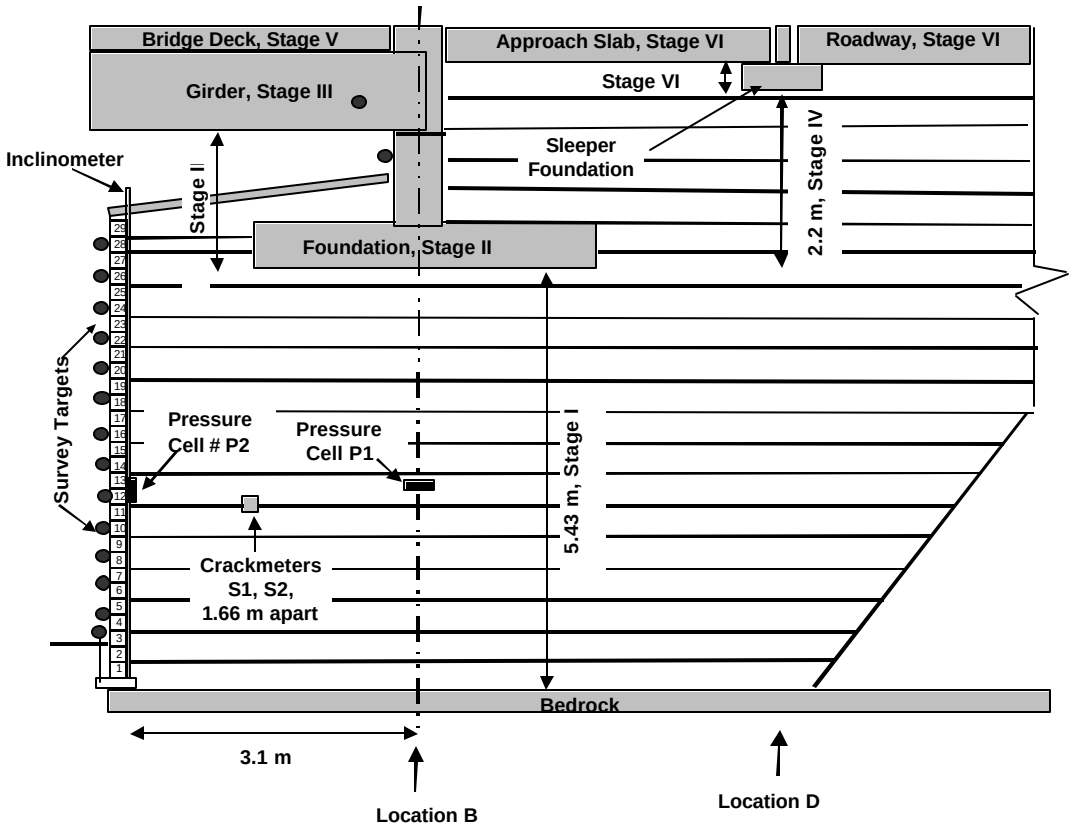

Figure 1.5. Instrumented Section 400 Indicating Construction Stages.

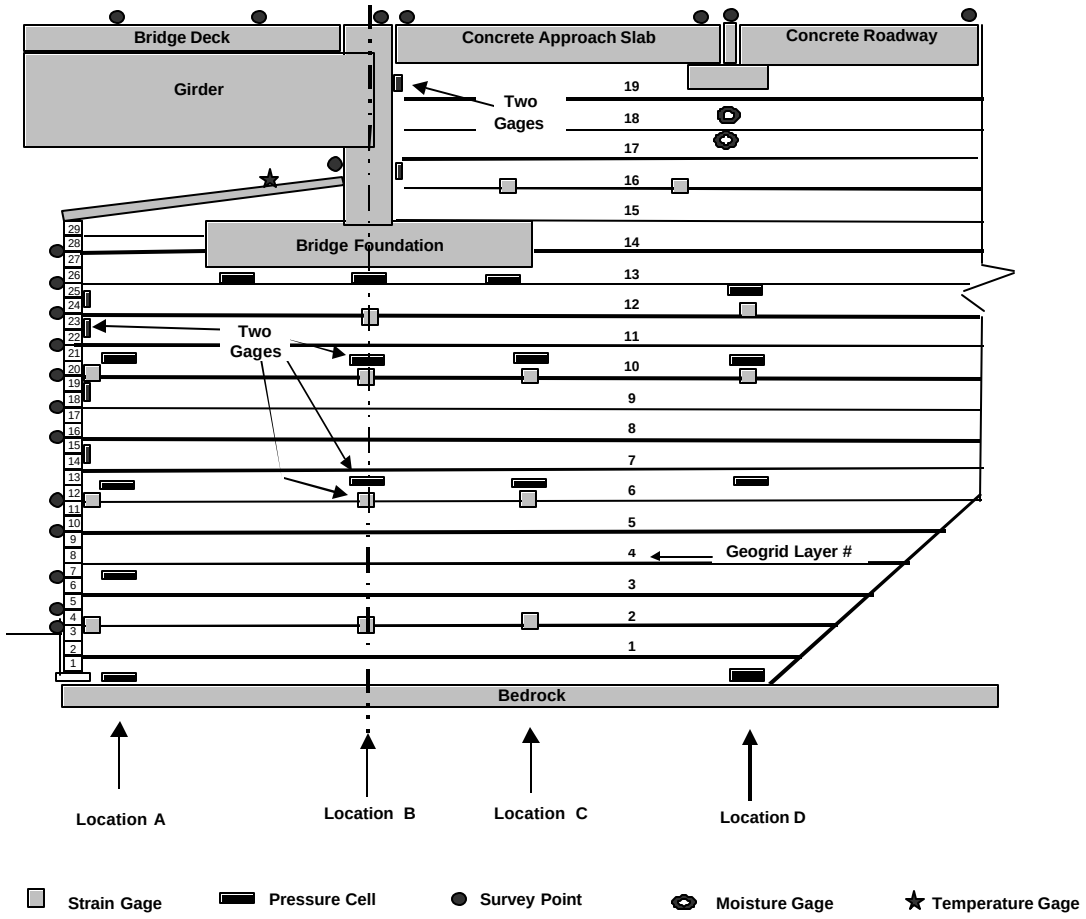

Figure 1.6 Layout of Instrumented Section 800.

1.5. Summary of Relevant Findings from Previous Research Studies

This section will present findings of previous research studies referred to in the discussion of the results presented in this report.

1.5.1 Use of GRS Wall Structures as Bridge Support

A recently published FHWA report (FHWA, 2000) describes three studies on GRS bridge supporting structures: load test of the Turner-Fairbank pier, load test of the Havana Yard piers and abutment in Denver, Colorado, and pre-loading of the Black Hawk abutment. Findings and conclusions of each study were presented. The findings of these studies that relevant to the study presented herein on the Founders/Meadows GRS walls are as follows:

- GRS abutments constructed using closely spaced (0.2 m to 0.3 m) and sufficiently stiff geosynthetic reinforcements, well-compacted granular backfill, and strong blocks will experience satisfactory performance under an average surcharge pressure of 200 kPa. The long-term creep deformations under service load of such GRS abutment structures were negligible. Small vertical reinforcement spacing and good compaction of the granular backfill significantly contribute to the satisfactory performance of the GRS bridge supporting structures.
- The use of concrete blocks as facing without mechanical connections between blocks results in satisfactory performance of the structures under service loads (i.e., the requirements for the connection strength could be waived). In this case, reinforcement layers were extended between block layers and the hollow concrete blocks were filled with uniform size gravel. The facing system developed its connection capacity by interface friction between blocks and reinforcement and between reinforcements and gravel.
- GRS abutments are clearly viable and adequate alternatives to bridge abutments supported by deep foundations or by metallic reinforced soil abutments.

Although the performance of the Turner Fairbank GRS pier and the Havana GRS abutment were excellent, this was not the case for the loaded Havana GRS pier. The GRS pier loaded in Havana Yard in Denver was a relatively slender structure when compared to the Turner Fairbank GRS pier (Abu-Hejleh et al., 2001). Four to five months after the Havana pier was loaded, excessive

movements of the top several block layers and severe cracking of the block facing were noticed. Therefore, it was decided to remove the applied surcharge load, dismantle the large-scale GRS abutment and pier structures, and perform a forensic investigation and a facing connection stability analysis. Abu-Hejleh et al. (2001) summarized the results of this forensic and stability investigations and identified possible causes for the excessive deformation and cracking experienced by the loaded GRS pier structure.

Abu-Hejleh et al. (2001) concluded that the friction-based connection strength for the facing of the Havana loaded pier was adequate for levels deeper than 1.6 m from the level of surcharge load. For future construction of piers and abutments with a high surcharge load, Abu-Hejleh et al. (2001) recommended the following construction measures to prevent the excessive facing movements in the upper 1.6 m of the structure: 1) place reinforcements with a wrapped-around procedure behind the facing, 2) attach the block facing to the reinforced soil mass through placement of tail reinforcements between block layers that extend 1 meter into the reinforced soil mass, and 3) dowel and grout with cement the block layers (in lieu of gravel filled block cells).

1.5.2 Influence of Temperature and Seasonal Changes on GRS Walls

Buttry et al. (1996) reported the influence of temperature and seasonal changes on the response of a 3.5 m high GRS segmental retaining wall constructed at the University of Wisconsin. This wall was instrumented to measure movements, earth pressures, forces between segmental units, temperatures and strains in the geogrid reinforcements. Monitoring was done during construction (October to December of 1993) and after construction. The observed behavior of the wall can be divided into two stages:

- From October of 1993 until March of 1994. The measured normal forces acting on the facing unit were about twice the weight of units above the load cell by the end of construction (December 1994) and remained until March of 1994. The difference was attributed to the downward frictional forces applied by the backfill soil to the rear of the block facing units. The geogrid strains increased during construction but leveled out and remained constant or increased slowly until April 1994.

- From March to October of 1994. Starting March of 1994, the normal forces began to decrease until August 1994 when the normal forces measurements approached the weight of the units. In April of 1994, the geogrid strains readings increased significantly at all locations and continued increasing through the summer months and into October 1994. Also during this time period, the wall facing moved outward approximately 2 mm. One explanation for these observations (Buttry et al., 1996) is that the wall system was rigid during the winter season and began to move, settle, and adjust during the spring thaw, when any ice in the backfill was melting and the soil may have been temporarily wet. As the wall moved and reached a more stable form, the downward frictional forces applied by the backfill soil to the rear of the block facing units dissipated, thus reducing the normal forces between facing units.

The front GRS wall of the Founders/Meadows structure along Section 800 also experienced a response that seems to be related to the seasonal changes of moisture and temperature (presented in Chapters 2, 3, 4, 5). Construction Stages I, II, III, and IV of section 800 occurred during the winter season and Construction Stages V and VI occurred during the spring season.

1.5.3 Strains and Stresses in GRS Wall Structures

At the at rest conditions (i.e., the lateral soil strain is zero) the lateral earth pressure is at its highest level. For this case, the ratio of lateral to vertical earth pressure, K_o, for a soil with friction angle of 34 degrees (assumed for the soil of the front wall) was estimated as 0.44. At the active limit state, the soil mass stretches in the lateral direction and the lateral tensile soil strain reaches the tensile strain at failure. This fully mobilizes the friction resistance of the backfill, thus reducing the horizontal lateral earth pressure to its lowest level. For this case, the ratio of lateral to vertical earth pressure for the soil of the front GRS wall was estimated as 0.31 (see section 1.2).

In a reinforced soil system, the measured reinforcement strains and forces give insight into changes of the lateral soil strains and stresses (see McGown et al., 1998). A common assumption made for geosynthetic reinforcement, due to their high level of bond, is that the tensile strains in the soil and reinforcement are equal in the direction of the reinforcement (Jewel, 1985). This

means that the geogrid reinforcement and the surrounding soil, both initially resting at zero strains, will expand to the same level of lateral tensile strains. When a soil element tends to expand in the lateral direction, it is resisted by both the reinforcement and the adjacent soil. At rest conditions (zero lateral soil strain), the lateral boundary of the soil element is fully confined by the adjacent soil elements. In this case, upper limit of lateral earth pressure is applied on the reinforced soil system, fully resisted by soil, and zero tensile force is mobilized by reinforcement. This is approximately the case for soil elements located far away from the wall facing (e.g., along Location Line D) where very small geogrid strains are measured. When the soil element stretches in the lateral direction, some of the reduced lateral (compression) earth pressure will be carried/supported by the reinforcement tensile stresses. If the soil yields sufficiently in the lateral direction, it is possible that the reinforcement tensile forces will balance all the lateral earth pressure. This provides the lower limit case for lateral earth pressure supported by adjacent soil element (theoretically zero) and the upper limit case for the reinforcement tensile force.

According to McGown et al. (1998), two limiting cases must be considered for lateral earth pressure on the facing of MSE walls. First, if the lateral boundary of the wall is not allowed to yield, the resulting pressure will be equal to or greater than those obtained under at-rest conditions. This case produces the upper limit of the lateral earth pressure on the wall. Secondly, if the lateral boundary is allowed to yield sufficiently to mobilize large tensile resistance in the reinforcement, and if the required forces and available forces balance, theoretically there will be no lateral earth pressure acting on the wall. This provides the lower limit case. However, even for this lower limit case, the soil masses between the reinforcing layers may have a tendency to produce localized stresses near the facing. These develop because each soil layer between reinforcements tends to act separately, causing the wall to be subjected to active horizontal pressure over the depth of that layer. For the front GRS wall of the Founders/Meadows structure, this lower limit earth pressure is expected to be smaller than 3 kPa.

Ingold (1979) investigated the effects of compaction on soil backfill behind rigid retaining walls. It was found that due to compaction stresses, the assumption of at-rest lateral earth pressures at the back of rigid retaining walls may be an underestimation of the actual horizontal stresses

within the soil mass. Compaction induces significant lateral earth pressures that are locked–in after removal of the vertical compaction stresses. Thus, due to compaction, ratios between horizontal to vertical earth pressures exceed those at the at-rest condition (larger than 0.44 in our case). Ingold (1979) developed an analytical model to estimate lateral earth pressure caused by compaction at the back of rigid retaining walls.

In GRS Walls, compaction also induces locked-in strains in the reinforcements after removal of the compaction loads. This is called *Static Interlock* based on the soil particles being locked into the geogrid due to static load (McGown et. al., 1998). Another mechanism called *Dynamic Interlock* (McGown et al., 1998) is also available and could be developed by repeated compaction loading in soil masses containing geogrid reinforcements with integral junctions (as used in the GRS walls of the Founders/Meadows structure). During compaction of a backfill soil containing a geogrid with integral junction, the compaction load forces soil particles into the apertures of the grids. When the compaction load is released, the grid attempts to return to its initial conditions, but is resisted by the particles within apertures. These locked-in strains have an effect similar to a confining stress on the soil (i.e., they increase the strength of the soil and reduce the lateral earth pressure).

The research conducted by Andraws and Yogarajah (1994) indicated that for stiff connection between the reinforcement elements and the facing, the tensile strain distribution was linear with maximum strains occurring close to the facing. For flexible connection, the maximum tensile strain occurred far from the facing. For the later case, larger shear resistance was mobilized in the soil and this resulted in reduced lateral earth pressure on the facing units.

2. MOVEMENTS OF THE FRONT GRS WALL STRUCTURE

2.1 Introduction

Direct measurements of the movements of the facing of the front GRS wall and settlement of the bridge footings were obtained from surveying and an inclinometer. Indirect measurements for the outward facing displacement of the front wall were obtained from the results of strain gages at geogrid layers 6 and 10 of Section 800 (Figure 1.6). Average geogrid strains at layers 6 and 10 of Section 800 were calculated using the geogrid strain values measured along Location Lines A, B, C, and D (Figure 1.6). The geogrid outward displacements at the facing were obtained by integrating the geogrid strains measured along each layer, and assuming that the retained backfill did not move and that there was no reinforcement slippage. The displacements calculated in this way were then compared to direct measurements of the wall outward displacements from surveying and the inclinometer. Complete details of the geogrid strain measurements are presented in Chapter 5.

Instrumented sections 200 and 400 are located at the center of Phase I Structure and Section 800 is located at the center of Phase II Structure (see Figures 2.2 to 2.6). The height of the front GRS wall (i.e., elevation above leveling pad) is 5.9 m for Sections 400 and 800 (identical), and 4.5 m for section 200. The bridge footing is located 5.28 m above leveling pad for Sections 400 and 800 and 3.86 m above the leveling pad for Section 200. The collected displacement data is organized according to the loading sequence, as follows: construction of the front GRS wall (Stage I), placement of the bridge superstructure (Stages II to VI), and post-construction stage (VII). Movements induced during wall construction (Stage I) can be compensated during wall construction (i.e., before placement of the bridge superstructure).

2.2 Facing Outward Displacements during Wall Construction (Stage I)

Monitoring data on the outward displacements of the wall induced during construction of the front GRS wall is summarized in Figure 2.1. The figure shows the outward wall displacements measured by surveying Section 400 along the lower 14 facing block layers (up to 2.75 m above leveling pad). These displacements resulted from construction of the front GRS wall from elevation 3.65 to 5.5 m. Figure 2.1

also shows the outward wall displacements measured by surveying Section 800 along the lower 10 facing block layers (up to 2.0 m above the leveling pad). These displacements resulted from construction of the front GRS wall from elevation 2.44 to 5.5 m. Estimated outward wall displacements along Section 800 inferred from strain gage results collected along geogrid layers 6 and 10 are shown in Figure 2.1. The inferred outward displacement obtained for geogrid layer 6 resulted from construction of the front GRS wall from elevation 2.23 m to 5.28 m; while the inferred outward displacement obtained for geogrid layer 10 resulted from construction of the GRS wall from elevation 3.85 m to 5.28 m. It is important to note that the sets of movement data shown in Figure 2.1 were not collected during construction of the same reinforcement lifts and, consequently, a direct comparison is not possible. Nevertheless, they show a consistent trend and provide an order of magnitude of the expected outward displacements during construction of GRS walls. The maximum outward wall displacements measured during construction of the front GRS wall of sections 400 and 800 were 8.5 mm, and 11.5 mm, respectively.

Additional insight on the characteristics of the outward wall displacements can be gained from the strain gage measurements collected during construction of the walls. Figure 2.2 shows the estimated average geogrid lateral strains and the outward displacements of the front wall facing obtained along geogrid layers 6 and 8 of Section 800. The information is presented as a function of the estimated vertical earth pressure applied on these layers (Equation 1.1) during all construction stages. Construction of the front wall itself (before placement of the bridge structure) corresponds to the first three data points shown in Figures 2.2a and 2.2b.

Figure 2.2a shows a good agreement between the average geogrid strains at different depths when the strain values are plotted as a function of the applied vertical earth pressures. However, for the same level of applied vertical earth pressure, Figure 2.2b shows that the wall outward displacements for layer 10 are higher than for layer 6. This is an expected behavior because the width of the active zone (defined by the locus of maximum tension line) increases with the height above the leveling pad. The second data point in Figures 2.2a and 2.2b was collected after compaction and placement of approximately 1 m of backfill (corresponding to approximately 20 kPa of vertical earth pressure) over

the gages. Strain gage monitoring results shown in Figure 2.2 indicate that, in spite of the surcharge loads due to the bridge superstructure, the largest components of wall outward displacements occurred during placement and compaction of a few lifts of soil above the geogrid layers (i.e., approximately 2 m of soil or 40 kPa).

2.3 Facing Outward Displacements Induced by Placement of Bridge Superstructure (Stages II to VI)

Monitoring data on the outward wall displacements induced during placement of the bridge superstructure is summarized in Figure 2.3. The data was obtained from surveying and strain gage records. As observed in the figure, the maximum wall outward displacements experienced along sections 200, 400, and 800 during placement of the bridge were approximately 7, 9, and 10 mm, respectively. The maximum outward displacements occurred within the upper third of the wall, directly below the bridge footing. In spite of the different height of the three sections (Section 200 is 4.5 m high, while Sections 400 and 800 are 5.9 m high), all three sections show a similar pattern. A maximum outward displacement of approximately 9 mm was induced by placement of the bridge superstructure (Figure 2.3). Although the outward displacements obtained for Sections 400 and 800 are of the same order of magnitude (these sections have identical configuration), it can be observed that displacements induced in Section 800 are somehow higher. Possible explanations for the difference in outward displacements between these two sections are:

- *Different construction season.* Most of the Phase I Structure (Section 400) was constructed during a warm season while the front GRS wall of Phase II Structure (Section 800) was constructed during a cold season (Table 1.1). Placement of the bridge superstructure along Section 800 occurred mostly in March and April of 1999 when thawing and wet seasons started (Table 1.1). This may have led to softening of the backfill and comparatively larger deformations.

- *Different construction sequence*. The backfill behind the abutment wall was placed before placement of the girders during construction of Section 400. Instead, the girders were placed before

placing backfill behind the abutment wall during construction of Section 800 (Table 1.1). This induced, most probably, larger lateral displacements and reinforcement strains within the GRS backfill along Section 800.

Additional insight on the outward movements induced by placement of the bridge superstructure can also be gained from assessment of the strain gage measurements shown in Figure 2.2. The label shown next to each data point in Figure 2.2 indicates the construction stage to which the data point corresponds (4^{th} data point corresponds to Stage II, 5^{th} corresponds to Stage III and so on). During Stages II to VI, the GRS system responded with comparatively small deformations to the increasing vertical earth pressures. A possible reason for this behavior is the influence of compaction experienced in the previous stage (Stage I). An additional potential justification is the fact that Construction Stages II to IV took place during the winter season. Buttry et al. (1996) reported a comparatively more rigid behavior for a GRS structure during the winter season (Section 1.5.2). During Stages V and VI (last three data points in Figures 2.2a and 2.2b), the GRS system appears to have responded with comparatively large strains and displacements to the increasing level of applied vertical earth pressures. Thawing and wetting of the backfill, as well as disappearance of the compaction influence, may have led to softening of the backfill in these stages (see Section 1.5.2).

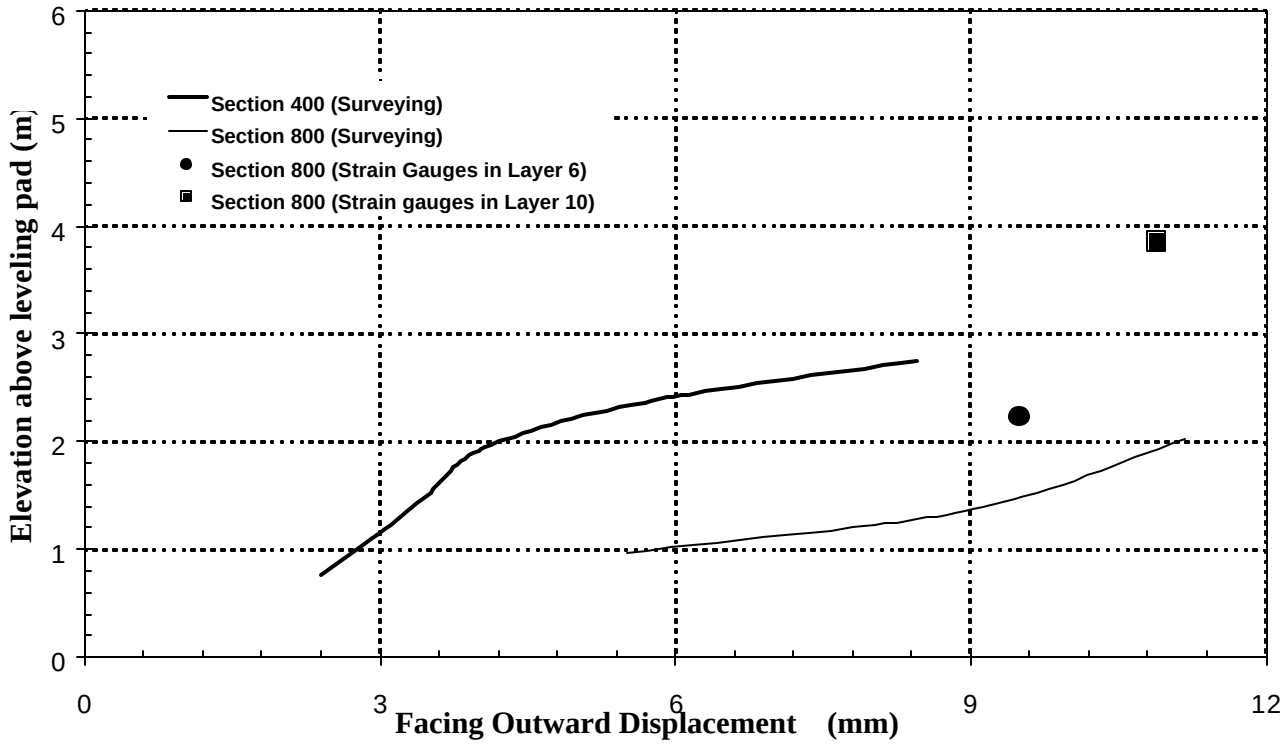

Figure 2.1. Measured Outward Displacements of the Front Wall Facing Induced during Construction of the Front GRS Wall. Note: sets of data correspond to different loading conditions.

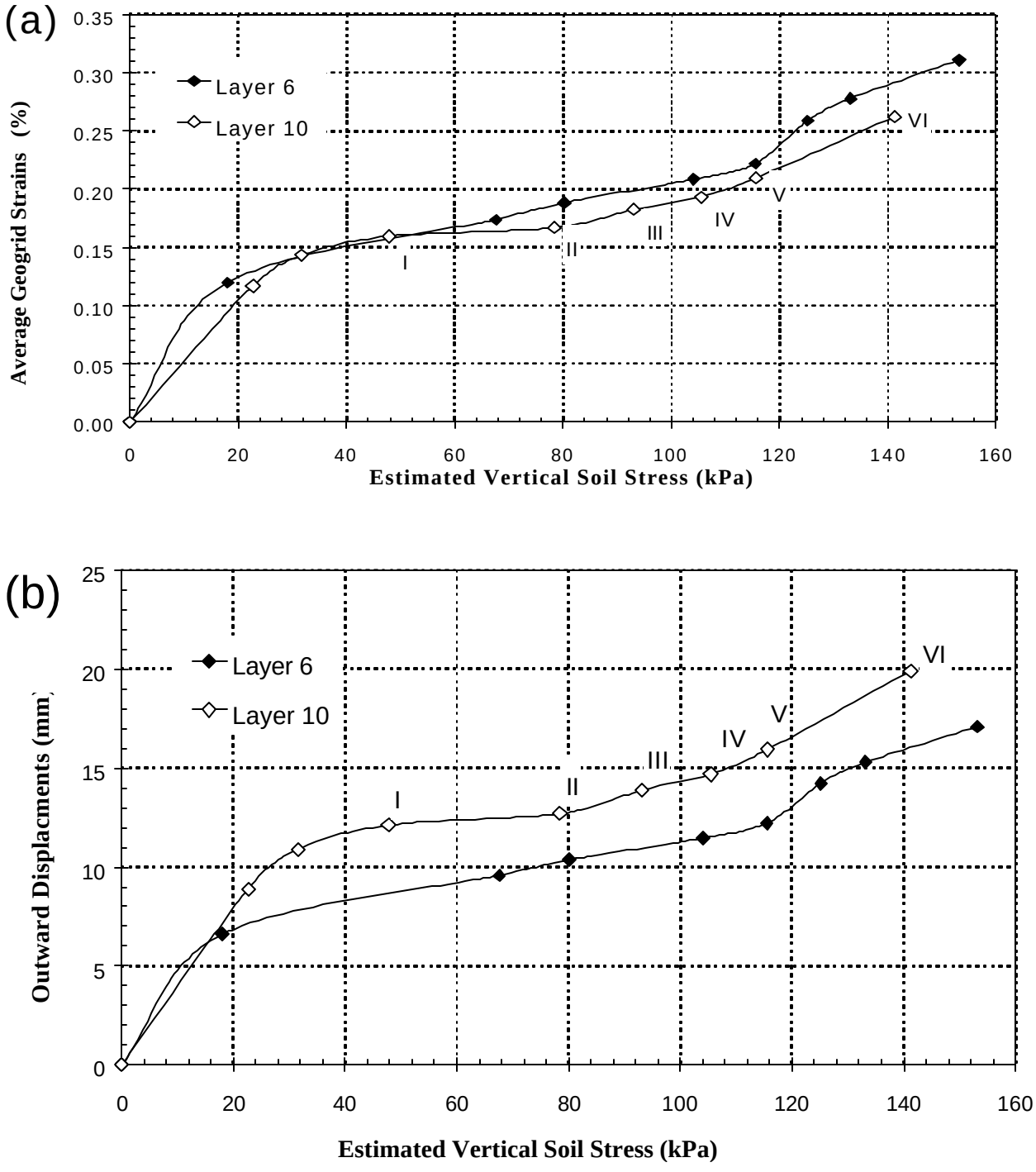

Figure 2.2. Strain Gage Results from Geogrid Layers 6 and 8 of Section 800 during all Construction Stages: a) Average Geogrid Strain; b) Estimated Outward Displacements at the Facing. Note: The label shown next to each data point indicates the construction Stage (I to VI) to which the data point corresponds (shown for Layer 10 data only).

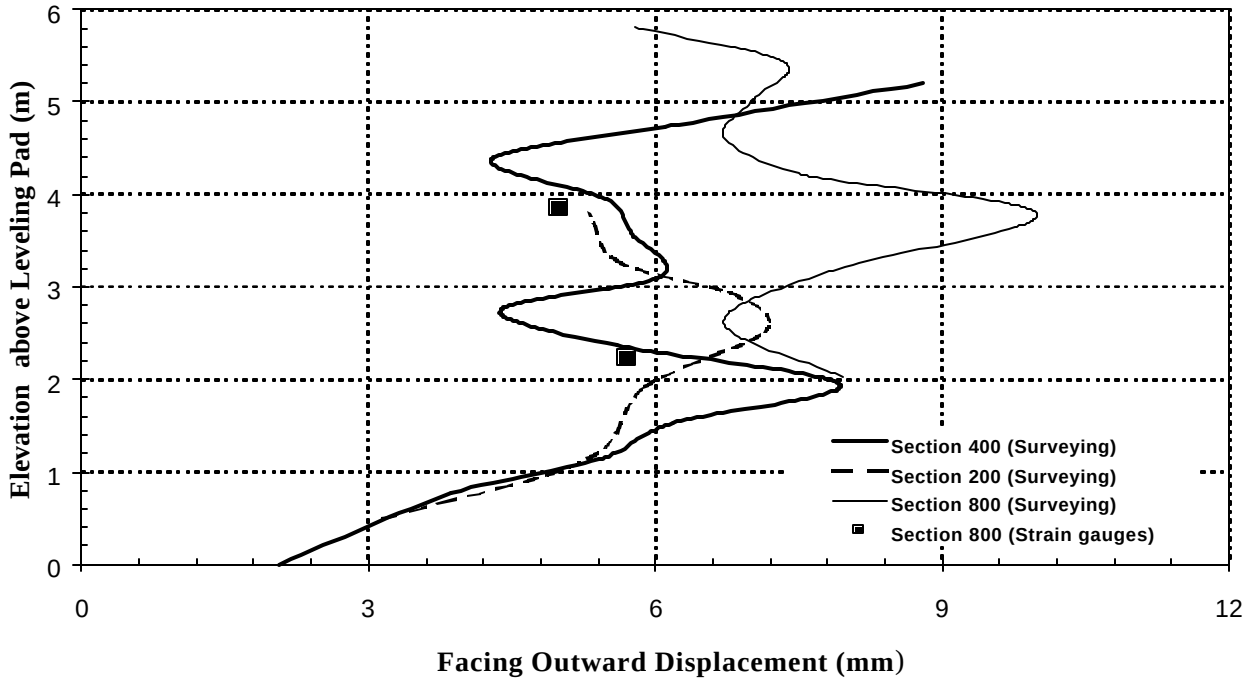

Figure 2.3. Measured Outward Displacements of the Front Wall Facing Induced by Placement of the Bridge Superstructure.

2.4 Facing Outward Displacements Induced while Bridge in Service

Monitoring Stage VII, which corresponds to the movements induced after opening the bridge to traffic, covers the period from December 1998 to June 2000 for the Phase I Structure (Sections 200 and 400) and from June 1999 to June 2000 for Section 800 of the Phase II Structure (see Table 1.1). The outward displacements of the front wall measured from surveying during Stage VII along Sections 200 and 800 are shown in Figures 2.4a and 2.4b, respectively. Figure 2.4c shows the outward displacement profile along Section 400 measured from the inclinometer at different times during Stage VII. The data obtained from the inclinometer along Section 400 represent the movements of the wall relative to the leveling pad (i.e., not the total "absolute" movements of the wall). However, since the outward displacements of the leveling pad during placement of the bridge superstructure were comparatively small (see Figure 2.3), leveling pad displacements were neglected in the interpretation of inclinometer data. Surveying results for Section 400 from December 1998 to June 1999 are not presented because

the surveying control point used in Section 400 was relocated during this period. Surveying results for Section 400 displacements from June 1999 to January 2000 and from June 1999 to June of 2000 are shown in Figure 2.4d. Figure 2.4d indicates good correlation between the surveying and inclinometer movement results obtained over similar monitoring periods.

The data shown in Figure 2.4 suggests that the outward wall displacements induced while the bridge was in service tended to decrease toward the leveling pad. The maximum outward wall displacement seemed to occur directly below the level of the bridge footing. The results in Figures 2.4 indicate that the structures continued to move after opening the bridge to traffic (Monitoring Stage VII). Although movements were not negligible, these displacements were relatively small for Sections 200 (Figure 2.4a) and 800 (figure 2.4b) and comparatively larger for Section 400 (Figures 2.4c and 24.d). Possible causes for these post-construction movements are traffic load, creep, and seasonal and temperature changes.

Figure 2.5 shows the time history of some of the collected geogrid strain measurements. The strain data shown in the figure was collected from strain gages placed in Section 800 during one year after opening the structure to traffic (i.e., June 1999 to June 2000 or days 180 to 545 from Jan. 1, 1999). Excellent agreement can be observed between the displacements inferred from strain gages placed in geogrid layers 6 and 10 and the displacements obtained from surveying (see Figure 2.4b). Geogrid strain results shown in Figure 2.5 support observations made regarding the outward displacements shown in Figure 2.4, which showed relatively small (though not negligible) post-construction displacements from June 1999 to January 2000, and negligible post-construction movements from January to June 2000. As shown in Figure 2.5, the geogrid strains measured from January to June 2000 (approximately days 365 to 540 from Jan. 1, 1999) leveled out and remained approximately constant.

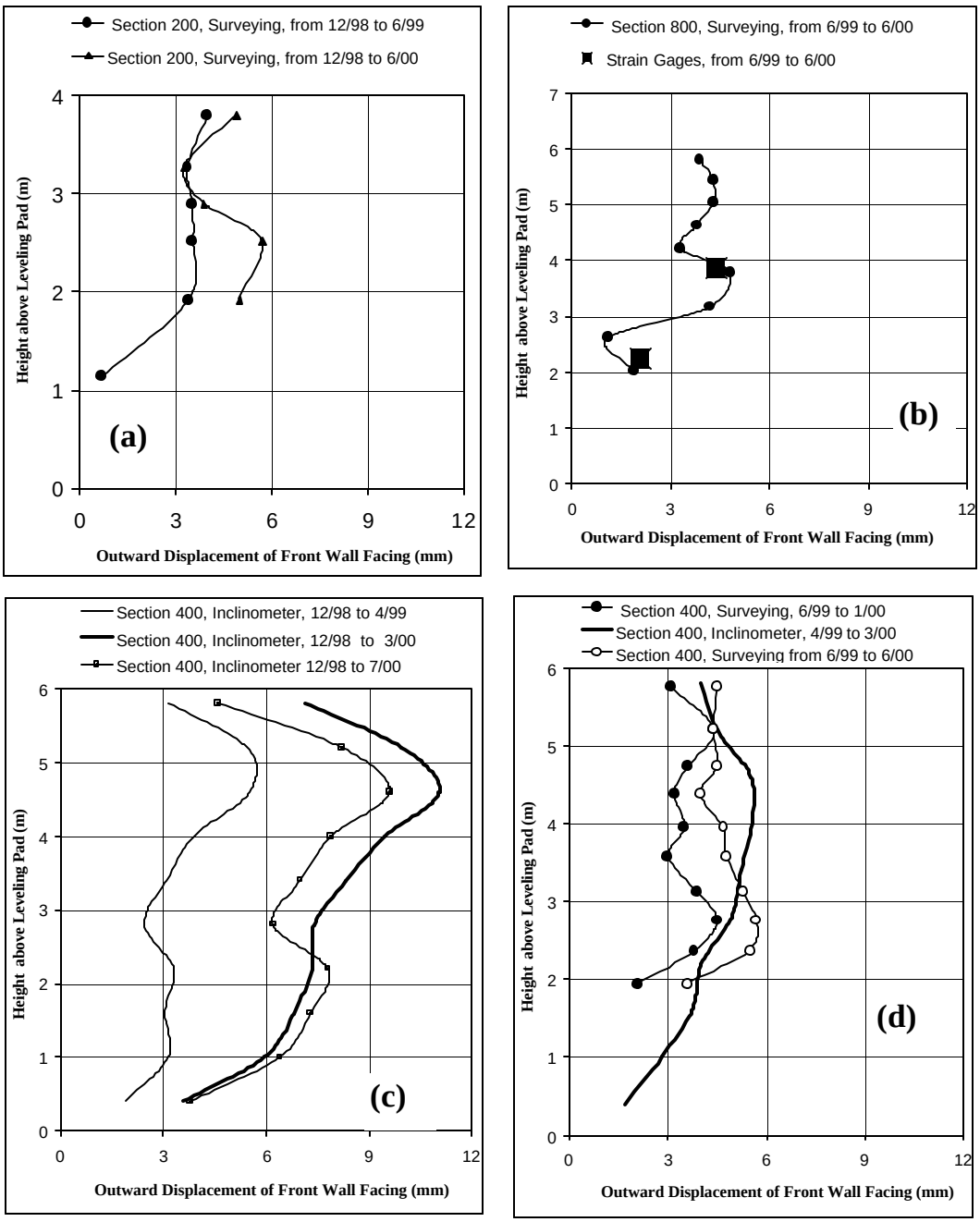

Figure 2.4. Measured Outward Displacements of the Front Wall Facing Induced while the Structure was in Service: (a) Section 200 from Surveying; (b) Section 800 from Surveying and Strain Gages; (c) Section 400 from the Inclinometer; (d) Section 400 from the Inclinometer and Surveying.

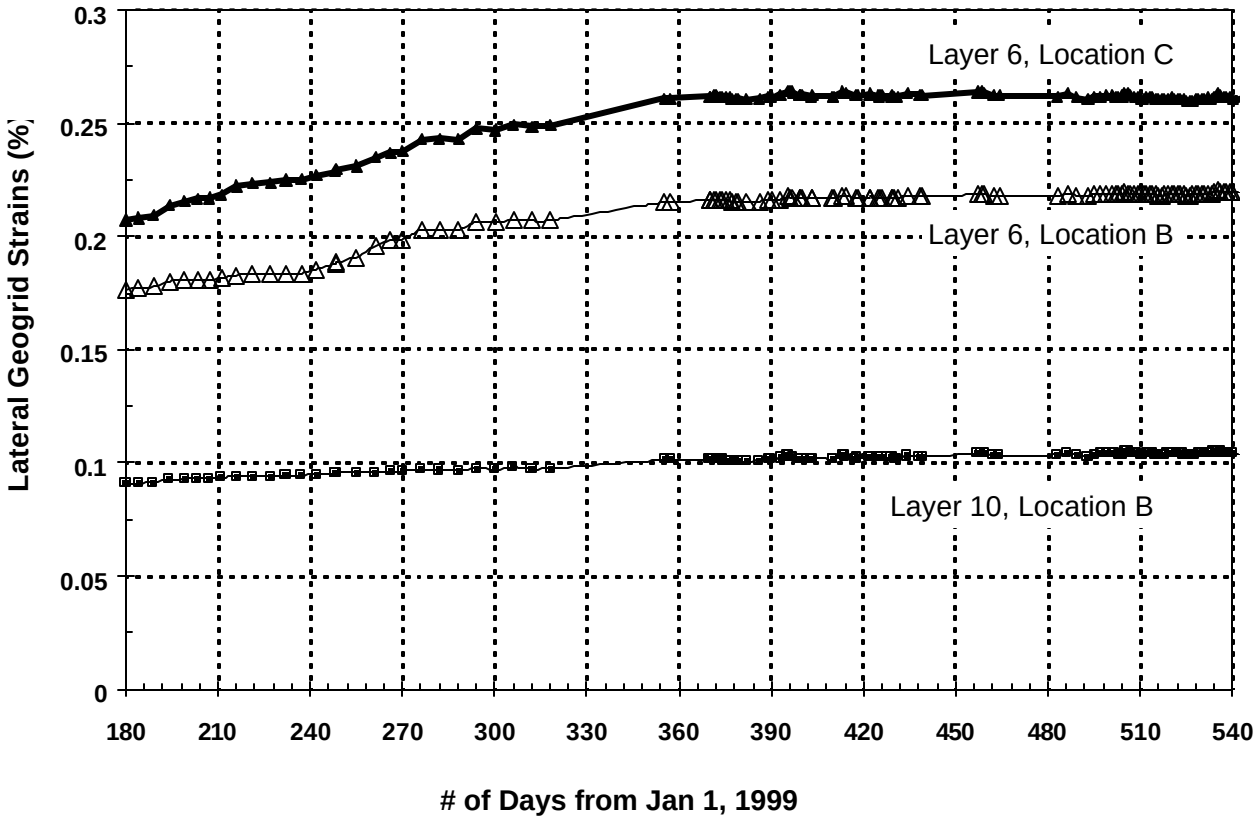

Figure 2.5. Geogrid Strain Gage Results Obtained along Section 800 below the Bridge Footing while Bridge was in Service (Stage VII). Note: The period shown in the horizontal axis ranges from June 1999 (180 days from Jan 1 1999) to June 2000 (540 days from January 1, 1999).

2.5 Settlement of the Bridge Footing

The maximum measured vertical settlements of the bridge footing, due to the placement of the bridge superstructure (Stages II to VI), were 13 and 12 mm on Sections 200 and 800, respectively. The maximum measured vertical settlements of the bridge footing induced while the bridge was in service (Stage VII) on Sections 200, 400, and 800 were 7, 11, and 10 mm respectively. The post-construction settlements of the bridge footing of the Phase I Structure on Section 400 took place during the first year in service (December 1998 to January 2000), but became negligible from approximately January to

June 2000. This correlates very well with the measured negligible front wall outward displacements along Section 400 during the same period of time (Figures 2.4c and 2.4d).

2.6 Summary and Discussion of the Front GRS Structure Movements

Table 2.1 summarizes the maximum recorded outward displacements and vertical settlements of the front GRS wall facing along Sections 200, 400 and 800, obtained from surveying, inclinometer, and strain gages. Surveying results for the bridge footing settlements along sections 200, 400, and 800 are also summarized in Table 2.1. The movements shown in the table were induced during construction of the front GRS wall (Stage I), during placement of the bridge superstructure (Stages II to VI), and during different periods after opening the structure to traffic (Stage VII). Although not shown in the table, the component of the facing displacements parallel to the wall, measured from surveying during all stages, was also collected. These displacements were essentially negligible. The more sensitive inclinometer results along Section 400 also indicated negligible displacements parallel to the wall. These findings support the assumption of a plain strain condition at the middle of the Phase I and Phase II Structures. The vertical settlement of the wall facing was approximately the same at different heights. This indicates that most of the wall vertical settlements were due to the settlement of the leveling pad and compression of the joint materials located between the leveling pad and first row of facing blocks.

The maximum displacement values obtained from all monitoring techniques and along all monitored sections during different stages are also shown in Table 2.1. These movements are normalized with respect to the wall design height. Careful analysis of the summary in Table 2.1 and Figure 2.2 leads to the following observations regarding the overall deformation response of the front GRS wall:

- Movements induced during construction of the front GRS wall. The wall experienced comparatively large movements and geogrid strains during this stage. This was attributed primarily to the influence of compaction that created large locked-in lateral geogrid and soil strains after removal of the compaction vertical loads. Strain gages results for geogrid layers 6 and 10 suggest that, out of the total wall outward displacements induced during all monitored stages (Stages I to VII),

approximately 50% occurred during placement and compaction of the initial 2 m of backfill (approximately 40 kPa vertical earth pressure) above these geogrid layers (Figure 3.2 and Table 2.1). The maximum measured front wall outward displacement induced by wall construction was 12 mm, which corresponds to 0.2 % of the front wall height. The measured settlement of the leveling pad supporting the front wall facing was approximately 8 mm.

- Movements induced during placement of the bridge superstructure. The total average vertical contact pressure directly underneath the bridge footing due to placement of the bridge superstructure was estimated as 115 kPa. The maximum front wall outward displacement and bridge footing settlement induced by placement of the bridge superstructure were 10 and 13 mm, respectively. These movements correspond, respectively, to 0.17% and 0.29 % of the front wall height (0.29% is normalized in relation to a wall height of 4.5 m). The measured settlement of the leveling pad supporting the front wall facing was approximately 7 mm.

- Movements induced after opening of the structure to traffic. The total average vertical contact pressure directly underneath the bridge footing due to placement of the bridge superstructure and the traffic load was estimated as 150 kPa. The maximum front wall outward displacement and bridge footing settlement induced while the bridge was in service (Stage VII) were 13 and 10 mm, respectively. These movements correspond, respectively, to 0.22 % and 0.17 % of the front wall height. The measured settlement of the leveling pad supporting the front wall facing was approximately 5 mm. From the time of opening the bridge to traffic (December 1998 for Phase I Structure and June 1999 for Phase II Structure) until January 2000, the structure showed continued movements. However, from January 2000 to June of 2000, the monitoring results suggest that the front GRS wall and bridge footing experienced negligible movements. Geogrid strain readings leveled out and remained approximately constant during this period.

CDOT engineers expected that the maximum outward displacement of the front GRS wall and settlement of the bridge footing due to placement of the bridge superstructure would not exceed, respectively, 20 mm (measured maximum displacement is 11 mm) and 25 mm (measured maximum

displacement is 13 mm). According to guidelines from the American Association of State Highway and Transportation Officials (AASHTO 1996), the two-span Founders/Meadows Bridge supported at its abutments by GRS walls could safely tolerate a maximum long-term differential settlement (due to placement of the bridge superstructure and after opening the bridge to traffic) of 70 mm without serious structural distress. An additional consideration was the need to maintain a 4.95 m minimum clearance between I-25 and the bottom of the bridge superstructure, which implies that the settlement of the bridge footing should not exceed 100 mm. The maximum settlement recorded for the bridge footing is 23 mm (13 mm induced by placement of bridge superstructure plus 10 mm induced after 18 months of service, as indicated in Table 2.1). This is roughly one-third the tolerable differential settlement (70 mm).

Based on the overall recorded deformation response so far, it can be concluded that the Founders/Meadows structure has showed excellent short- and long-term performance. Specifically, the monitored movements were significantly smaller than those expected in design or allowed by performance requirements, there were no signs of any structural damage, and post-construction movements became negligible after an in-service period of one year.

Table 2.1. Summary of the Maximum Movements of the Front Wall Facing and of the Settlements of the Bridge Abutment Footing

	Induced *Only* by GRS Wall Construction (Stage I)	Induced *Only* by Placement of Bridge Superstructure (Stages II to VI) [1]	Induced *Only* While Bridge was in Service (Stage VII) [2]		
			6 months	12 months	18 months
A. Maximum Outward Displacement (mm) of the Front Wall Facing					
Section 200, Surveying		7	4		6
Section 400, Surveying	9	9	8 [3]	12 [3]	13 [3]
Section 400, Inclinometer			6	11	10
Section 800, Surveying	12	10		5	
Section 800, Strain Gages	11	6	4	4	
Maximum Displacements (mm) (% of Wall Height)	12 (0.2 %)	10 (0.17 %)	8	12	13 (0.22 %)
B. Settlement (mm) of the Leveling Pad Supporting the Front Wall Facing					
Section200, Surveying		7	4		5
Section 400, Surveying	6	7	2	5	5
Section 800, Surveying	8	3		3	
Maximum Settlement (mm)	8	7	4	5	5
C. Bridge Abutment Footing Settlement (mm)					
Section 200, Surveying		13	7		6
Section 400, Surveying			7	11	10
Section 800, Surveying		12		10	
Maximum Settlement (mm) (% of Wall Height)		13 (0.29 %)	7	11	10 (0.17 %)

Notes: [1] Estimated surcharge is 115 kPa; [2] Months in service are counted from December 1998 for Sections 200 and 400, and from June 1999 for Section 800. Estimated surcharge is 150 kPa; [3] Displacements are estimated based on surveying and inclinometer data

3.0 VERTICAL EARTH PRESSURES IN THE FRONT GRS WALL

3.1 Introduction

Figure 1.6 and Table 1.3 show the locations of all pressure cells placed along Section 800 (Phase II Structure) to measure distribution of vertical earth pressures inside the front GRS wall below the bridge footing during all monitored stages. Gages placed between the 6th and 7th geogrid layers will be referred as layer 6 gages (Figure 1.6). Layers 0, 6, 10, and 13 gages are located at depths of 5.43 m, 2.95 m, 1.33 m, and 0.23 m, respectively, below the bottom of the bridge footing. Layer 0 gages were placed at the base of the reinforced fill (depth of 5.43 m). Layer 13 gages were placed directly below the bridge footing (at depth of 0.23 m). One Gage (3VA) was placed close to the facing (location line A) between geogrid layers 3 and 4 (Figure 1.6).

3.2 Typical Vertical Earth Pressure Results during Placement and Compaction of the Backfill

Figure 3.1 shows the vertical earth pressures measured during construction of the front GRS wall (Stage I) from layer 6 gages (Figure 3.1a) and from layer 10 gages (3.1b). The measured data shown in Figure 3.1 was collected every six minutes to monitor the soil response to compaction and construction operations of the wall. Note that in Figure 3.1, 51.5 day refers to the midday of the 52nd day from Jan. 1, 1999 and 52.0 refers to the midnight of that day. As expected, changes in the measured vertical earth pressures occurred during the day working hours and no changes occurred during the evening and night hours. The sudden changes of the measured vertical earth pressures (20 to 35 kPa) shown in this figure are most likely due to compaction-applied loads. Figure 3.1 also shows the estimated average vertical earth pressures (from Eq. 1.1) at the level of the measuring pressure cells at different stages. The measured response from the pressure cells correlates very well with the applied backfill self-weight loads during construction of the front wall (Figure 3.1).

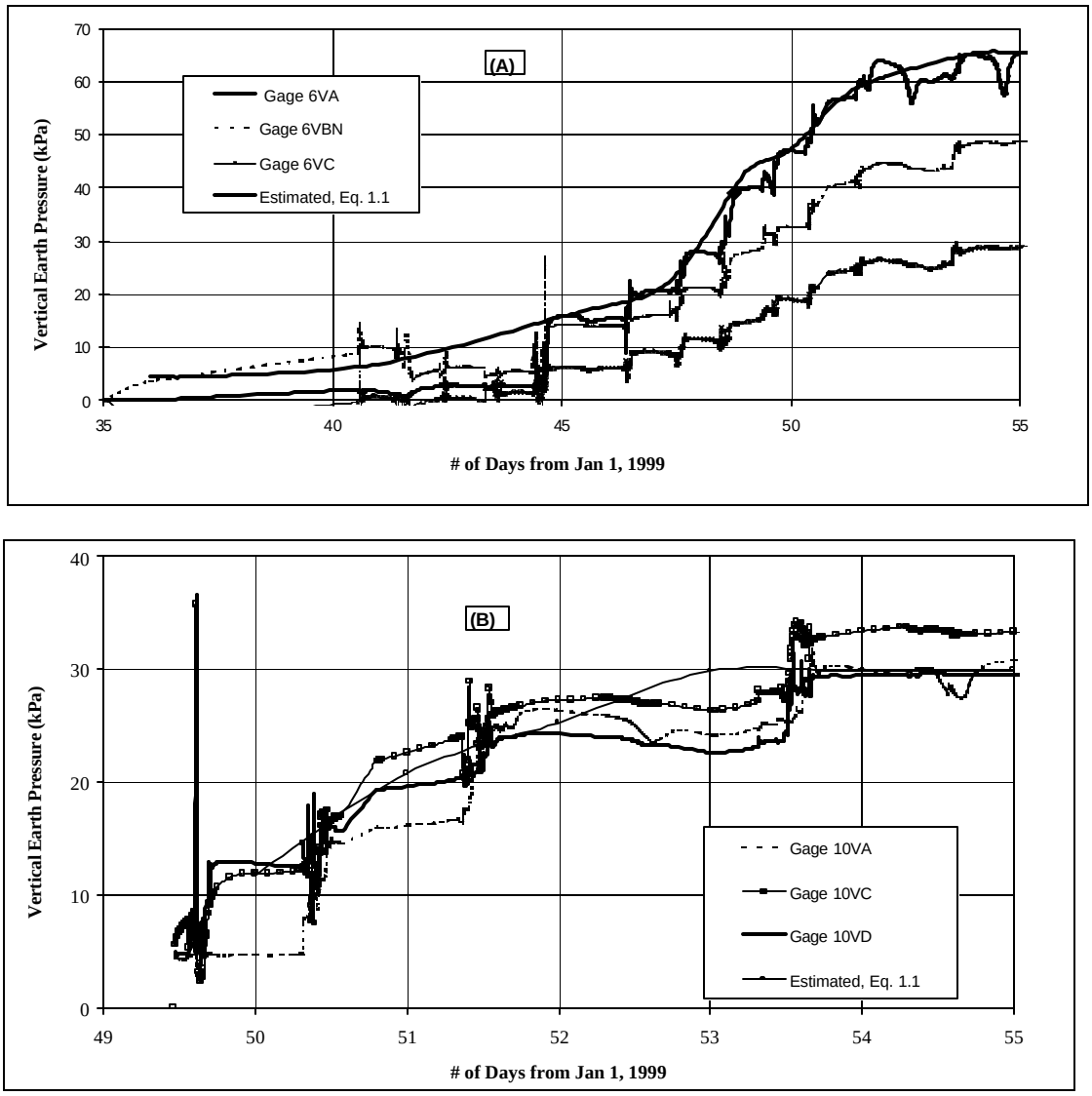

Figure 3.1. Typical Measured and Estimated Vertical Earth Pressure during Placement and Compaction of the Backfill from: (a) Layer 6 Gages, and (b) Layer 10 Gages.

3.3 Results of Vertical Earth Pressures during all Construction Stages

3.3.1 Measured Vertical Earth Pressures

Figure 3.2 shows time records of the vertical earth pressures measured by the pressure cells placed at the base of the reinforced soil mass along location lines A and D during all construction stages (Stages I to VI, till 180 days from Jan. 1, 1999). At the base of the reinforced fill, no pressure cells were placed at location lines B and C (Figure 1.6). Vertical earth pressures value at these missing locations were estimated by vertical and horizontal extrapolation of the measured vertical earth pressures around these two missing locations. Horizontal profiles of the vertical earth pressures at the base of the reinforced fill by end front wall construction (Stage I) and end of all construction stages (Stage VI) are given in Figure 3.3.

Figures 3.4 and 3.5 show time records and horizontal profiles of the measured vertical earth pressures from layer 6 gages during all construction stages. Figures 3.6 and 3.7 show time records and horizontal profiles of the measured vertical earth pressures from layer 10 gages during all construction stages. Figure 3.8 shows horizontal profiles of the measured changes in the vertical earth pressures from layers 6 and 10 gages induced by placement of the bridge superstructure (Stages II to VI, changes from Stage I values).

Figure 3.9 show time records of the vertical earth pressures measured directly beneath the bridge footing (from layer 13 gages) during placement of the bridge superstructure (Stages II to VI). The data of Figure 3.9 was recorded from pressure cells placed (see Figure 1.6) at location line A (close to the exterior edge of the bridge footing from Gage 13VA), location line B (from Gage 13VB), location line C (from Gage 13VC), and location line D (from gage 12VD). Horizontal profiles of the measured vertical earth pressures beneath bridge footing during placement of the bridge superstructure (Stages II to VI) are given in Figure 3.10.

Time records for the vertical earth pressures measured from all gages placed close to the wall facing (location line A) during all construction stages are summarized in Figure 3.11.

Table 3.1 summarizes the vertical earth pressures measured from all gages during all construction stages. Table 3.1 also summarizes changes in measured vertical earth pressures developed due to the placement of the bridge superstructure (Stages II to VI, like in Figure 3.8), referred to as "changes from Stage I." The measured changes in vertical earth pressures along different location lines (A, B, C, and D) induced by placement of the bridge superstructure (Stages II to VI) are summarized in Figure 3.12.

3.3.2 Discussion of the Results measured during Construction

By the end of Stage I (front wall construction) at depths of 5.43 m (layer 0) and 2.95 m (layer 6), the vertical earth pressures close to the wall facing exceeded those at other locations (see Figures 3.3 and 3.5). The reinforced fill at a depth of 1.33 m (layer 10) showed almost uniform distribution of vertical earth pressures at the end of Stage I Construction (Figure 3.7).

Sharp increases in measured vertical earth pressures were observed at all levels along location lines A, B, and C during Stage III construction (placement of girders) in two days (see Figures 3.2, 3.4, 3.6, and 3.9). As expected, the pressure cell placed along location line D at the base of the fill (Gage 0VD) recorded small changes in vertical earth pressure (Figure 3.2 and Figure 3.12d), but the pressure cell along location line D beneath the bridge footing (Gage 12VD) recorded no change in the vertical earth pressure (Figure 3.9 and Figure 3.12d). During Stages II and III, measured vertical earth pressures beneath the edges of the bridge footing are higher than at the center of the footing (Figure 3.10). This is a typical pressure diagram for rigid footing resting on any material. The results of gages placed at deeper depths (layers 0, 6 and, 10) during stages II and III suggest the following:

- Location line B along the center of the bridge abutment footing experienced the highest increase in vertical earth pressures during these stages followed by location C (Figures 3.8 and 3.12).
- The changes in vertical earth pressures along location lines B and C during these stages decreased with the depth below the bridge footing as expected (Figures 3.8 and Figure 3.12), but such a trend was not noticed for changes in vertical earth pressures along location lines A (close to the facing, Figure 3.12a) and D (Figure 3.12d).

The pressure cell placed along location lines D and C responded to loading during Construction Stage IV, when the overlying backfill was placed behind the abutment wall (see Figures 3.2 to 3.9 and Figures 3.12c and 3.12d). As expected also, location line B showed a small response near to the bridge footing (Gage 12VB) and showed larger responses at deeper levels (Figure 3.12b). Location line A showed a response to loading during Stage IV only in the zone close to the base of the fill as expected (Figure 3.12a).

During Stage V, there was a severe and reduction in the measured vertical earth pressures close to the wall facing along location line A (see Figures 3.2 to 3.8 and 3.11) and in the zone beneath the bridge footing (Figures 3.9 and 3.10). This can be attributed to the comparatively large lateral movements of the front wall facing (see Chapters 2 and 5) and possible settlement of the bridge footing during Stage V. The results along location line A behind the wall facing shown in Figures 3.11 and 3.12a and Table 3.1 indicate that the largest reduction occurred at the base of the fill (40 kPa, Figure3.12a), the reduction was 23 kPa, 12 kPa, and 13 kPa at depths 3.76 m (Gage 3VA), 2.95 m (Layer 6), and 1.33 m (Layer 10), respectively. Directly below the bridge footing (depth 0.23 m), the measured reduction was 10 kPa at location line C and 17 kPa at location line A (Figure 3.10). Note that although the vertical earth pressure at these locations dropped down, the total vertical earth pressures remained in compression (Table 3.1). During Stage V, the pressure cells placed along location line D showed almost no change beneath the bridge footing (from Gage 12VD, see Figure 3.12d) and small increases at layers 6 and 10 gages (Figure 3.12d). As the vertical earth pressures close to the wall facing were dropping for layers 6 and 10 gages during Stage V, the vertical earth pressures along location line B (along the bridge abutment centerline) and to a lesser degree along location line C were increasing at a relatively high rate (Figure 3.4 to 3.8 and Figure 3.12). This behavior suggests transfer of vertical earth pressures at layers 6 and 10 from the zone close to the wall facing to a zone deeper in the reinforced soil.

The loading response at different locations during Stage VI is very similar to that presented for Stage IV.

By the end of all construction stages (Stage VI), the measured vertical earth pressures at location line A became very close to or even less than the values measured by the end of Stage I Construction (see Figures 3.11 and 3.12a). In other words, the measured changes in vertical earth pressure behind the wall facing that were induced by placement of the bridge superstructure were very small (less than 15 kPa). The distribution of vertical earth pressures directly beneath the bridge footing was almost uniform: 28 kPa along location line B, 34 kPa along location line A, and 39 kPa along location line C (Figure 3.10). At other levels (layers 0, 6, and 10), the vertical earth pressure distribution within the reinforced soil mass below the bridge footing differed significantly from location to location (Figures 3.3, 3.5, and 3.7). The lowest vertical earth pressure occurred close to the facing and the highest vertical earth pressure occurred along location line B, the centerline of the bridge abutment. This distribution was close to symmetrical around the center of the reinforced soil zone (~3.75 m from rear side of the facing), especially for layers 0 and 10 (Figure 3.3 and 3.7).

Table 3.1: Measured Vertical Earth Pressures (kPa) during all Construction Stages.

Stage #	I	II		III		IV		V		VI	
		Ch. = Change from Stage I (Wall construction) Values									
Gage #		Ch.	Total	Ch.	Total	Ch.	Total	Ch.	Total	Ch.	Total
Layer 0 Gages											
0VA	136	13	149	25	161	36	172	-3	133	2	138
0VD	75	6	81	12	87	37	112	50	125	62	138
3VA*	61	7	68	12	73	13	74	-11	51	-11	50
Layer 6 Gages											
6VA	66	13	79	24	90	26	92	15	81	9	75
6VBN	49	21	70	54	103	77	126	122	171	135	184
6VBS	36	20	56	47	83	63	99	94	130	99	135
6VC	29	6	35	18	47	39	68	58	87	71	100
6VD	47	3	50	7	54	41	88	51	98	66	113
Layer 10 Gages											
10VA	31	8	39	14	45	14	45	0	31	-1	30
10VBN	18	28	46	59	77	70	88	98	116	92	110
10VBS	29	38	67	85	114	100	129	142	171	139	168
10VC	33	10	43	30	63	62	95	86	119	106	139
10VD	30	-1	29	-2	28	36	66	39	69	54	84
Layer 13 Gages**											
12VD**	0	1	1	0	0	18	18	19	19	27	27
13VA	0	16	16	53	53	55	55	38	38	34	34
13VB	0	13	13	29	29	32	32	39	39	28	28
13VC	0	8	8	33	33	41	41	30	30	39	39

*Gage 3VA placed between geogrid layers 3 and 4

** Gage 12VD placed between geogrid layers 12 and 13

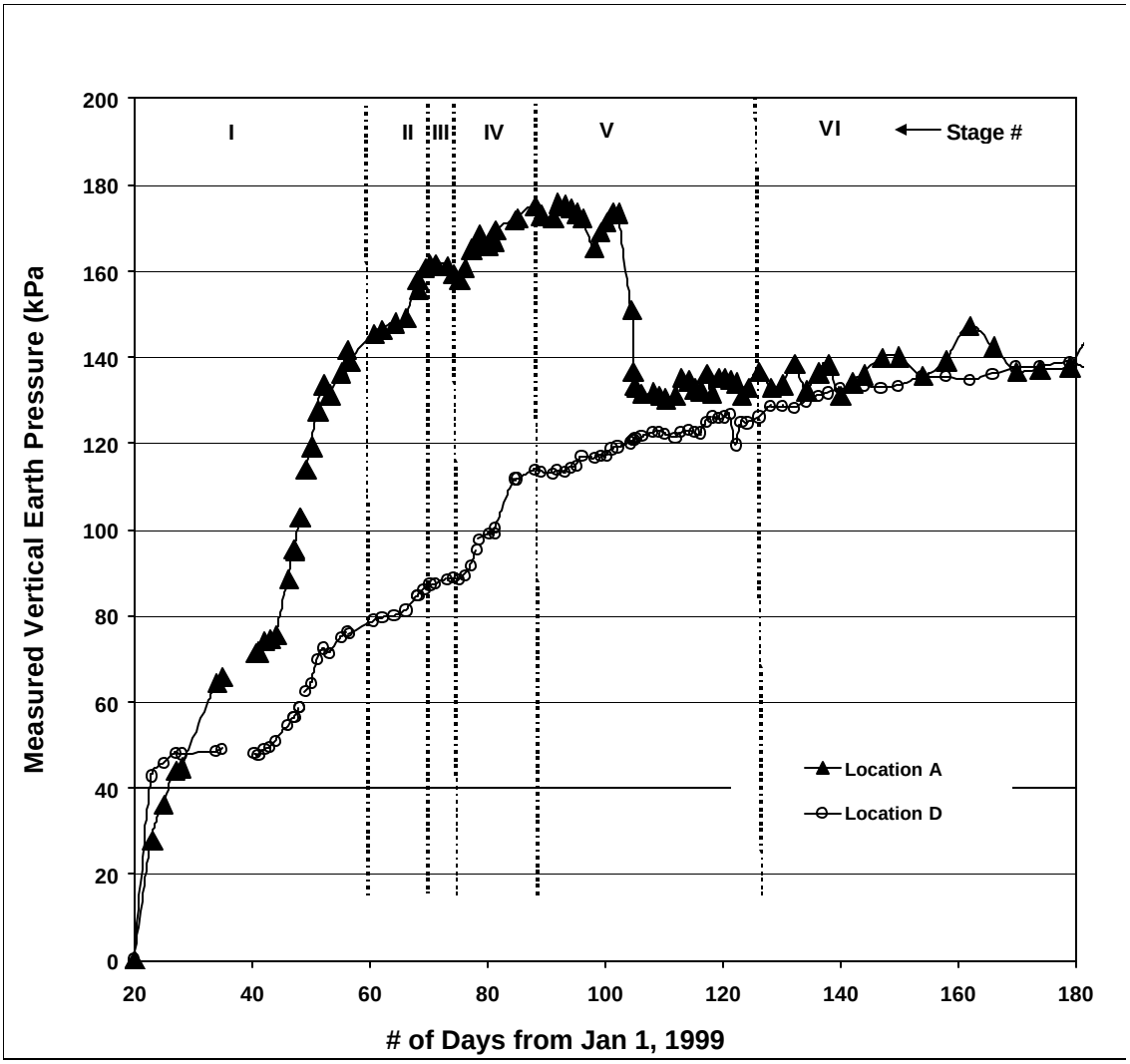

Fig. 3.2. Time Records for the Vertical Earth Pressure Measured from Gages Placed at the Base of the Fill during all Construction Stages.

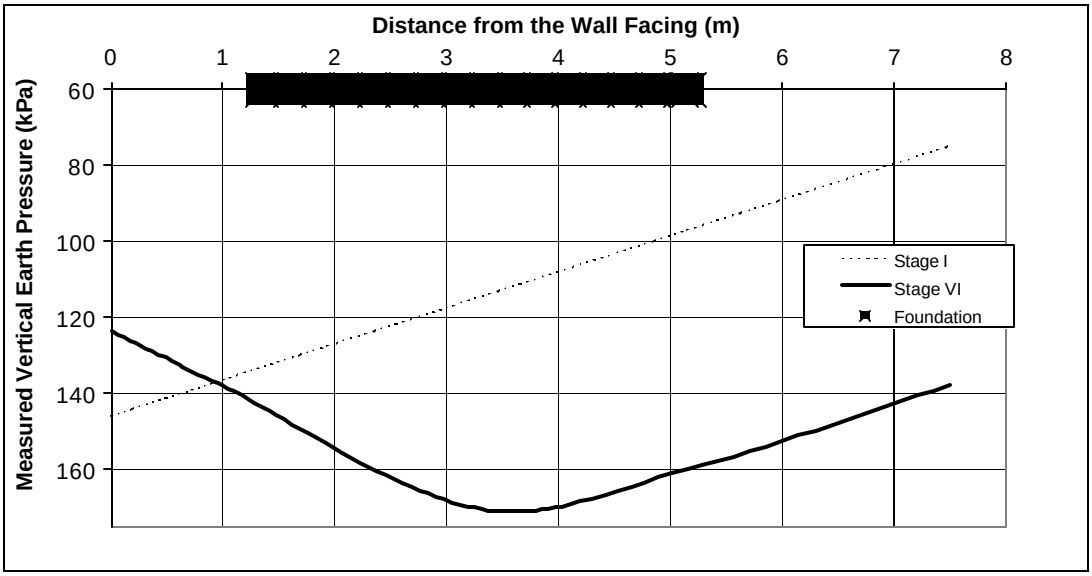

Fig. 3.3. Horizontal Profiles of the Vertical Earth Pressures Measured at the Base of the Reinforced Fill during Construction Stages.

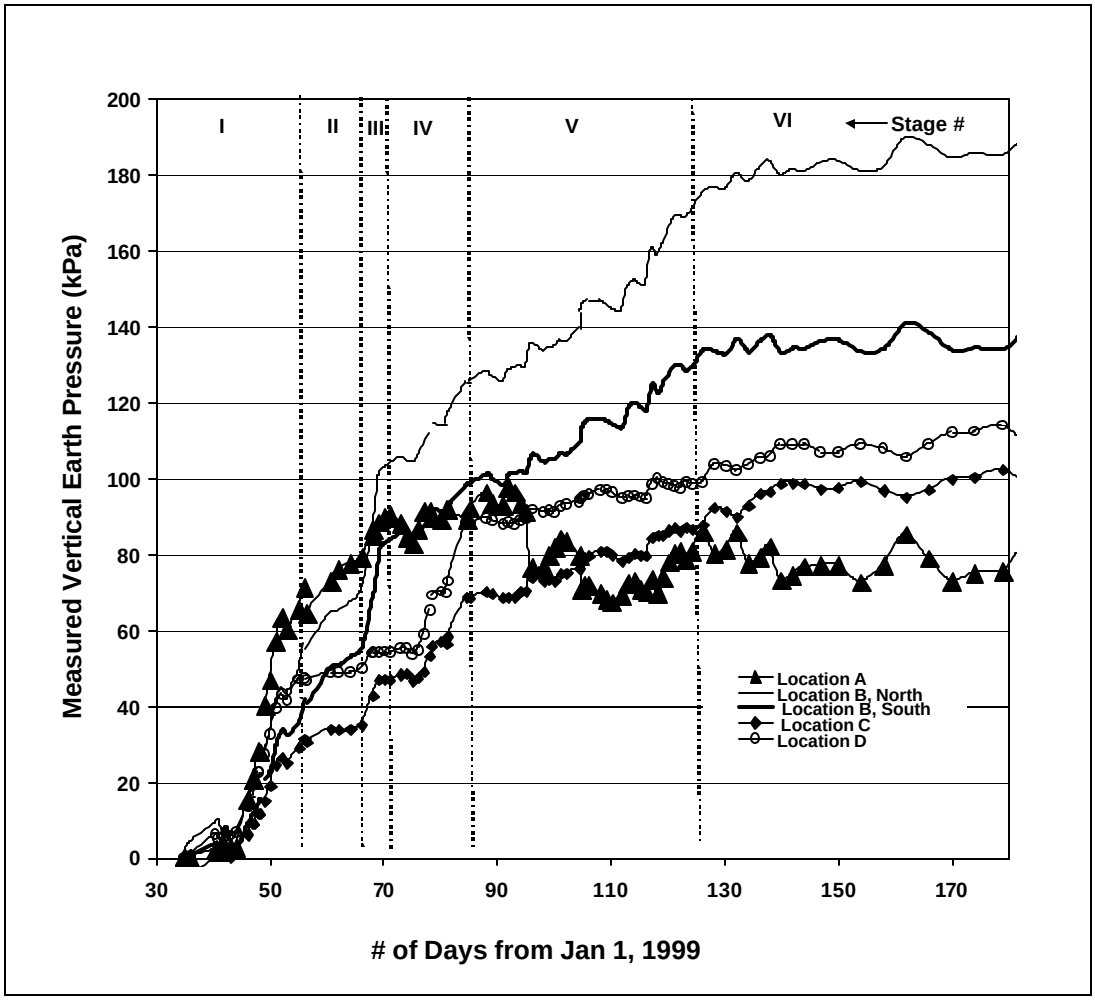

Fig. 3.4. Time Records for the Vertical Earth Pressures Measured from Layer 6 Gages during all Construction Stages.

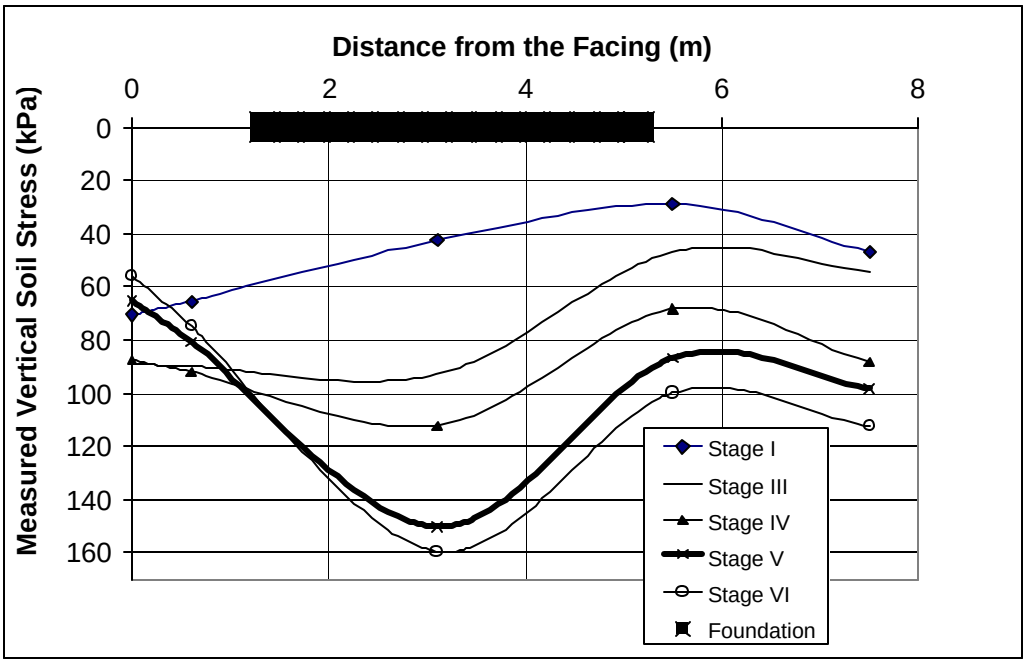

Fig. 3.5. Horizontal Profiles of the Vertical Earth Pressures Measured from Layer 6 Gages during Construction Stages.

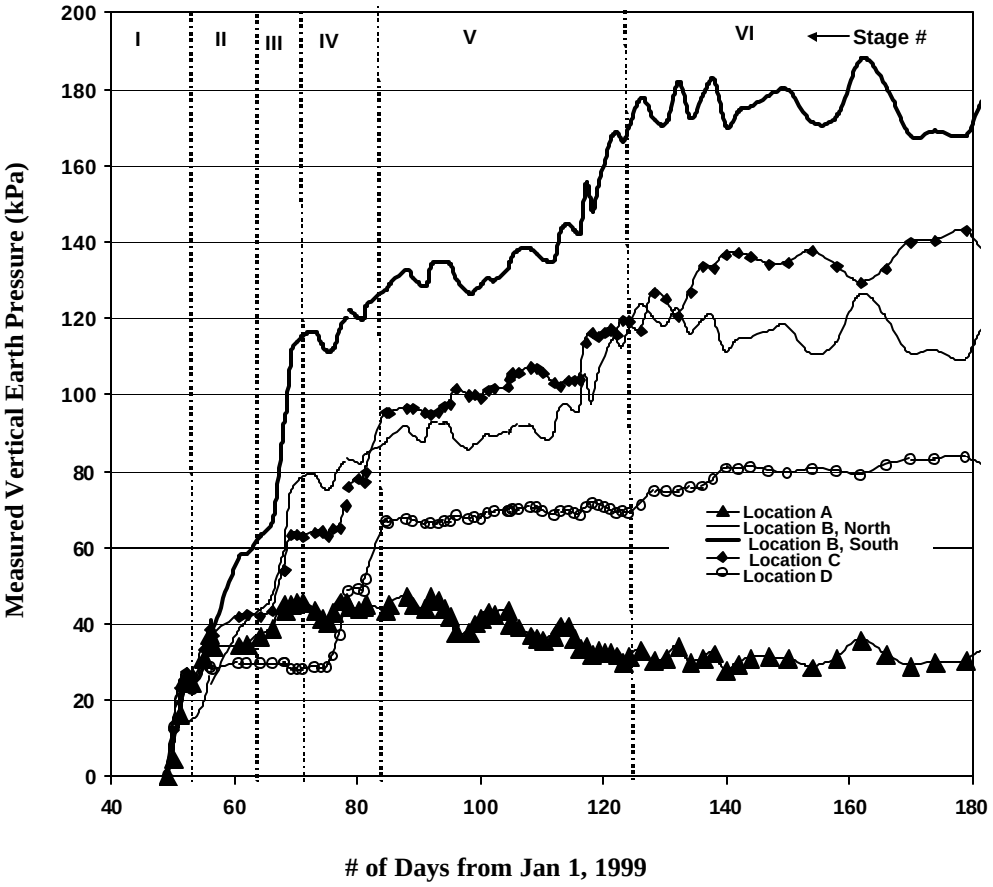

Fig. 3.6. Time Records for the Vertical Earth Pressures Measured from Layer 10 Gages during all Construction Stages.

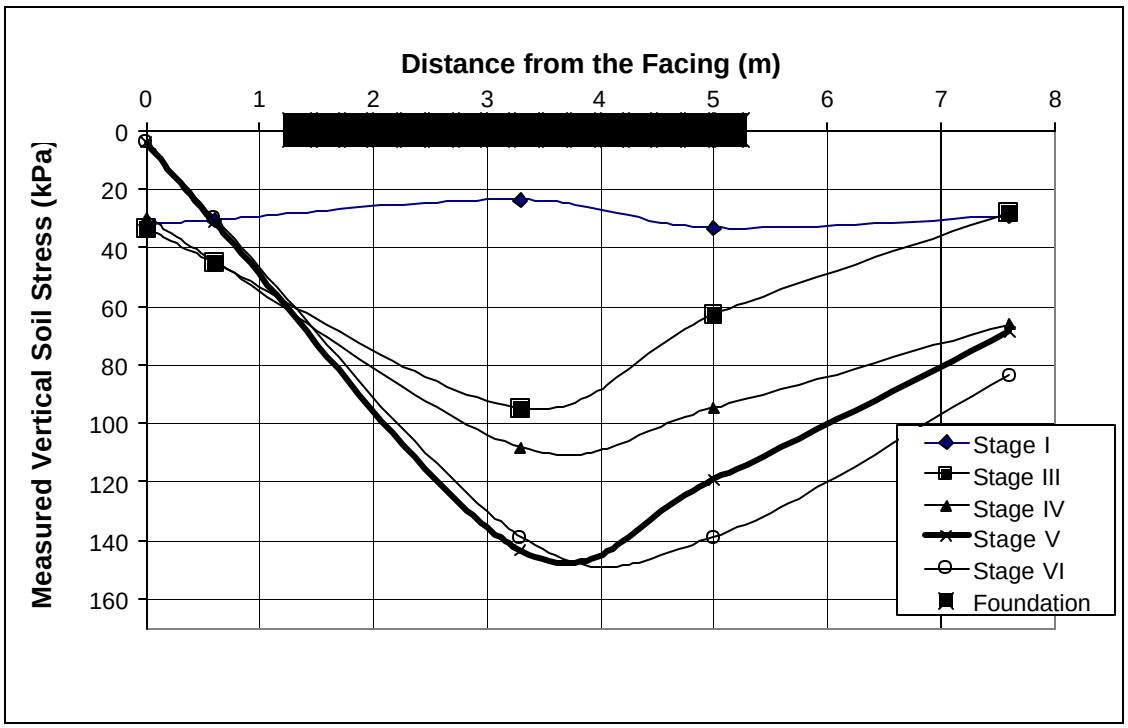

Fig. 3.7. Horizontal Profiles of the Vertical Earth Pressures Measured from Layer 10 Gages during Construction Stages.

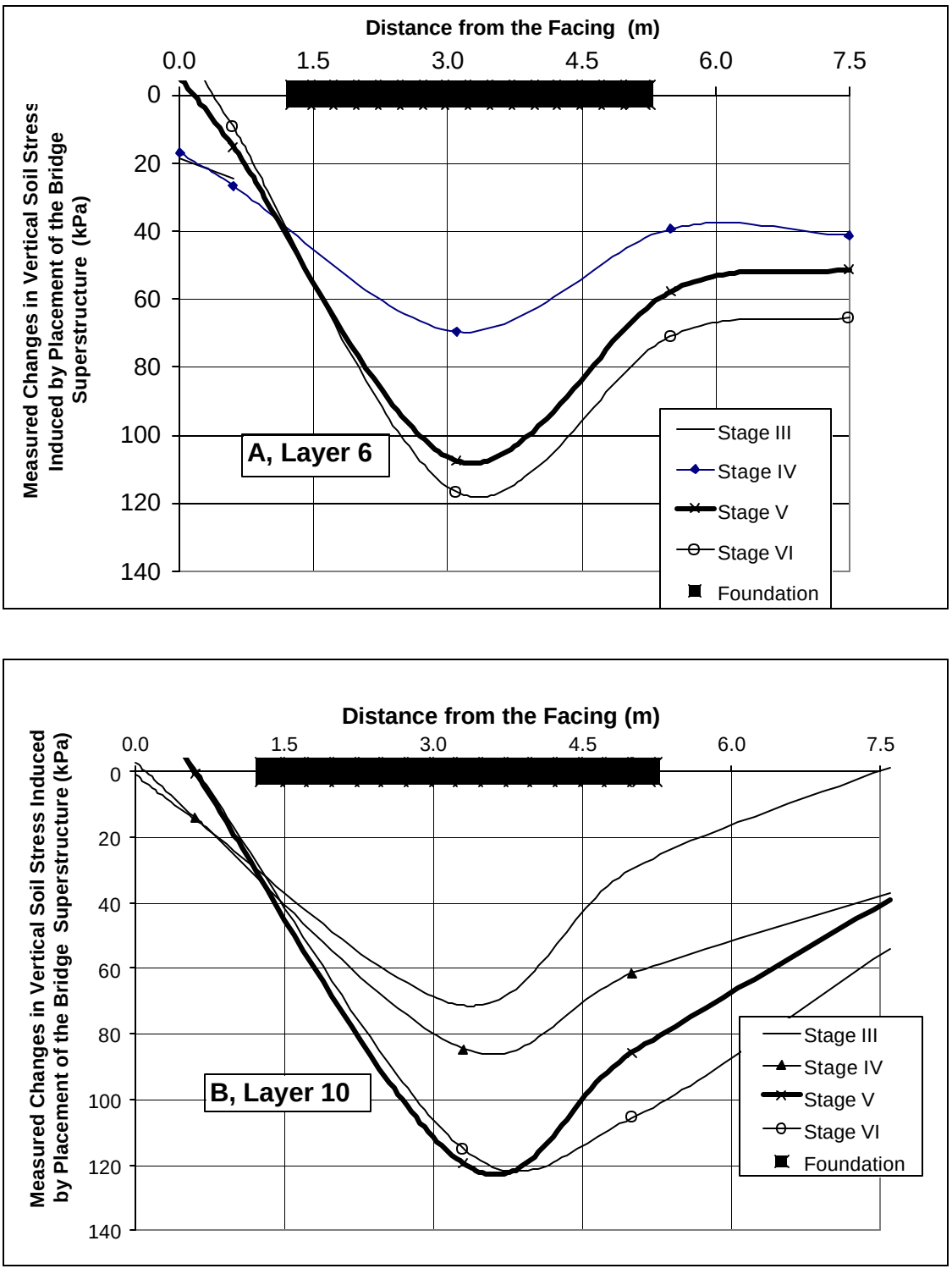

Fig. 3.8. Horizontal Profiles of Measured Changes in Vertical Earth Pressure Induced by Placement of the Bridge Superstructure (Stages II to VI from Stage I).

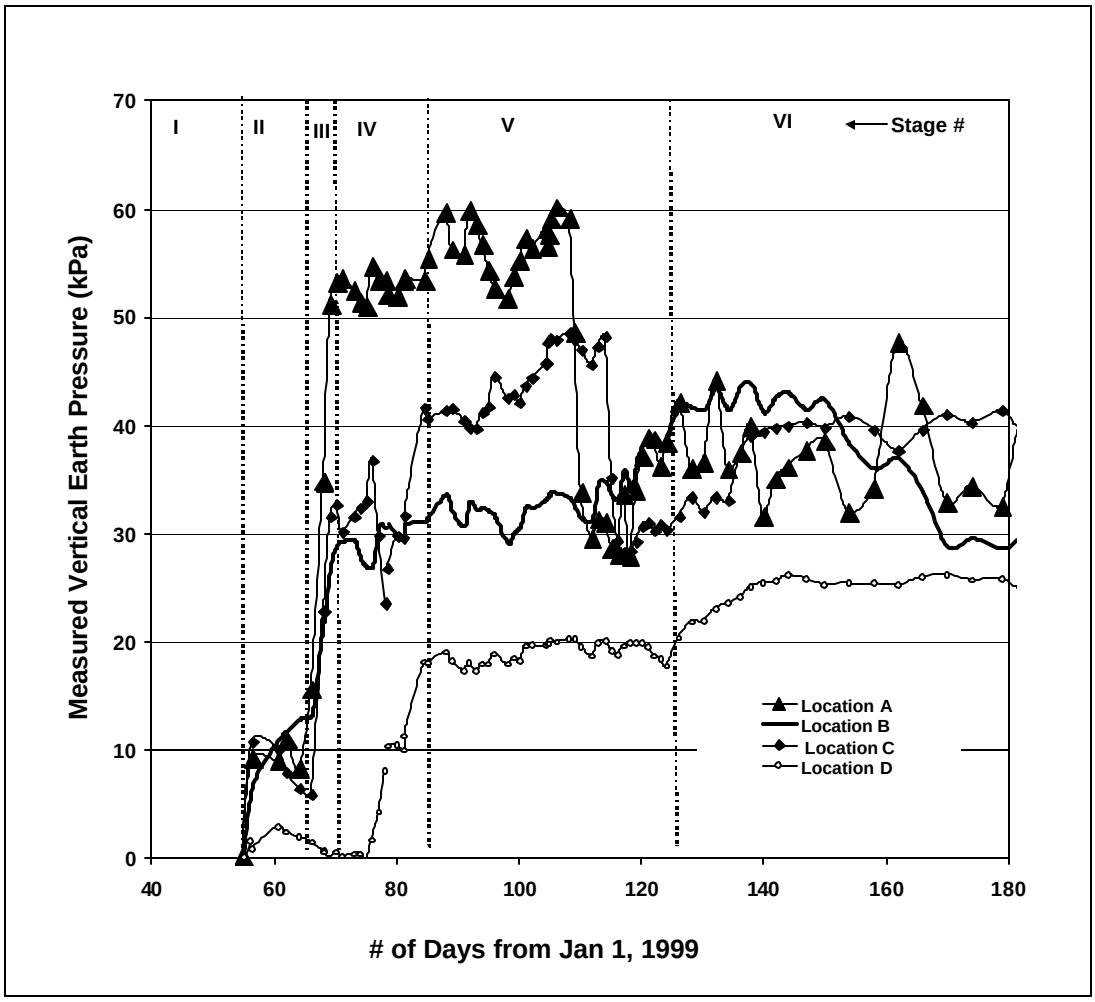

Fig. 3.9. Time Records for the Vertical Earth Pressures Measured from Layer 13 Gages Placed Beneath Bridge Footing during Construction Stages.

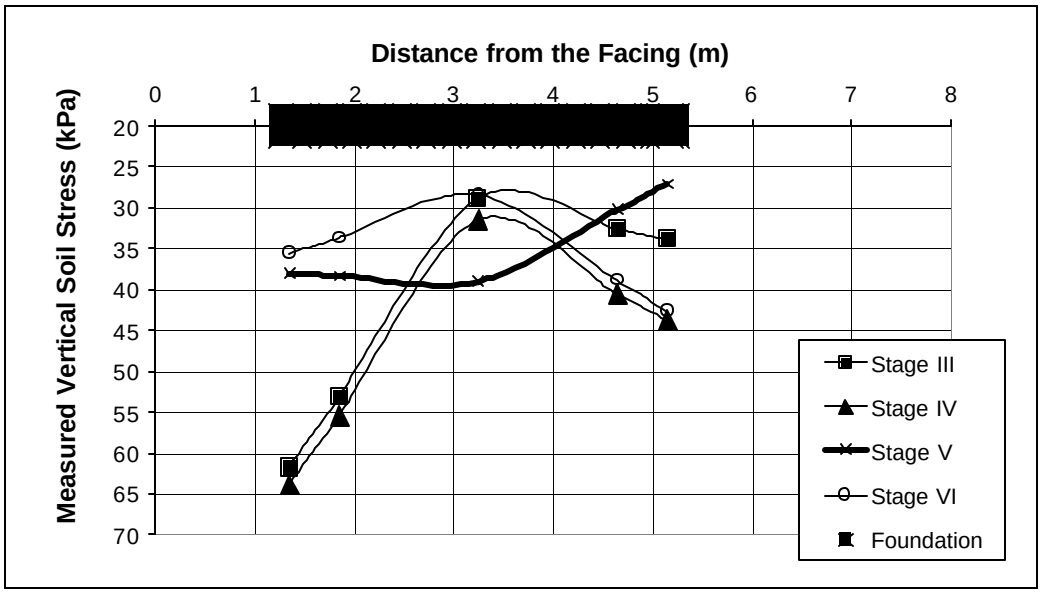

Fig. 3.10. Horizontal Profiles of the Vertical Earth Pressures Measured from Layer 13 Gages Placed Beneath Bridge Footing during Construction Stages.

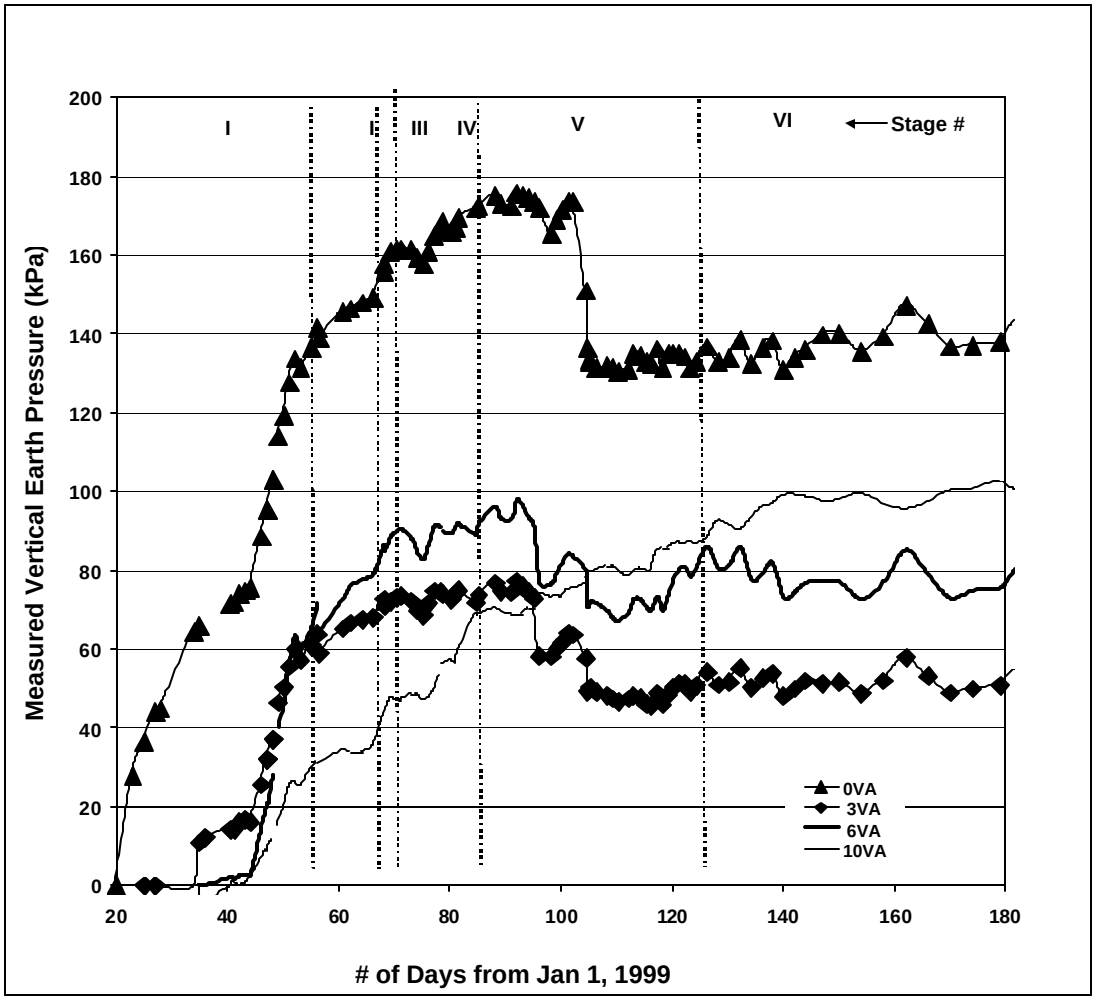

Fig. 3.11. Time Records for the Vertical Earth Pressure Measured during all Construction Stages from Gages Placed along Location Line A Close to the Wall Facing.

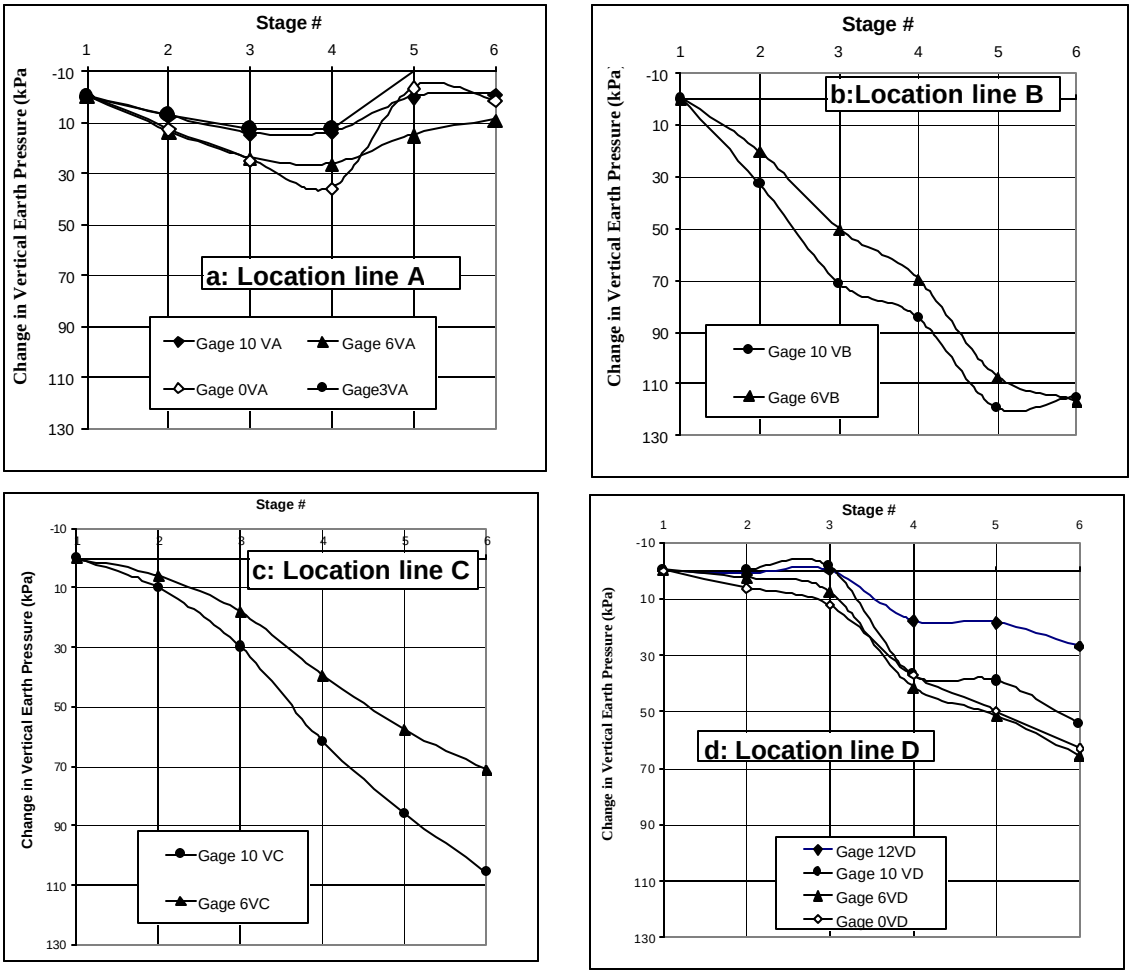

Fig. 3.12. Measured Vertical Earth Pressure along Different Location Lines due to Placement of the Bridge Superstructure.

3.4 Results of Vertical Earth Pressures while the Structure was in Service

Figure 3.13 shows selected samples of time records of measured vertical earth pressures after opening the structure to traffic during Stage VII (from days 180 to 545 from Jan. 1, 1999). Table 3.2 summarizes the vertical earth pressures measured by the end of the construction stages (Stage VI) and after opening the bridge to traffic (Stage VII). Table 3.2 also summarizes changes in vertical earth pressure developed after opening the bridge to traffic, referred to as "changes from Stage VI." As seen in Table 3.2, only six gages registered small changes in the measured vertical earth pressures after opening the structure to traffic (0VA, 6VBS, 6VD, 10VBS, 13VA, 10VC) ranging from -11.3 kPa (a decrease) to 14.5 kPa (an increase). These small changes occurred immediately after opening the bridge to traffic (see Figure 3.13), possibly due to placement of minor structures on the bridge structure (even after opening the bridge to traffic). All other gages (15 gages) showed very small change in the measured vertical earth pressures after opening structure to traffic (Table 3.2). As expected, live loads from traffic do not seem to leave behind "locked-in" vertical earth pressures.

Table 3.2: Measured Vertical Earth Pressure while Structure was in Service.

Monitored Stage #	End of Construction (Stage VI)	While Structure in Service (Stage VII)	
Gage #		Change from Stage VI	Total
0VA	138	14	152
0VD	138	-4	134
3VA	50	5	55
6VA	75	3	78
6VBN	184	-1	183
6VBS	135	-11	124
6VC	100	-6	94
6VD	113	-8	105
10VA	30	2	32
10VBN	110	7	117
10VBS	168	15	183
10VC	139	-11	128
10VD	84	-3	81
12VD	27	-1	26
13VA	34	8	42
13VB	28	0	28
13VC	39	-2	37

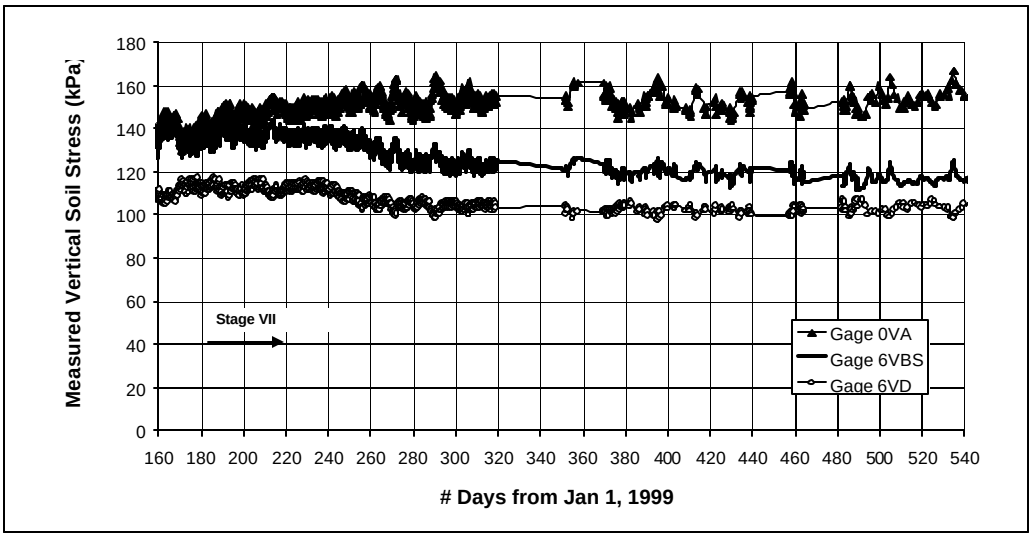

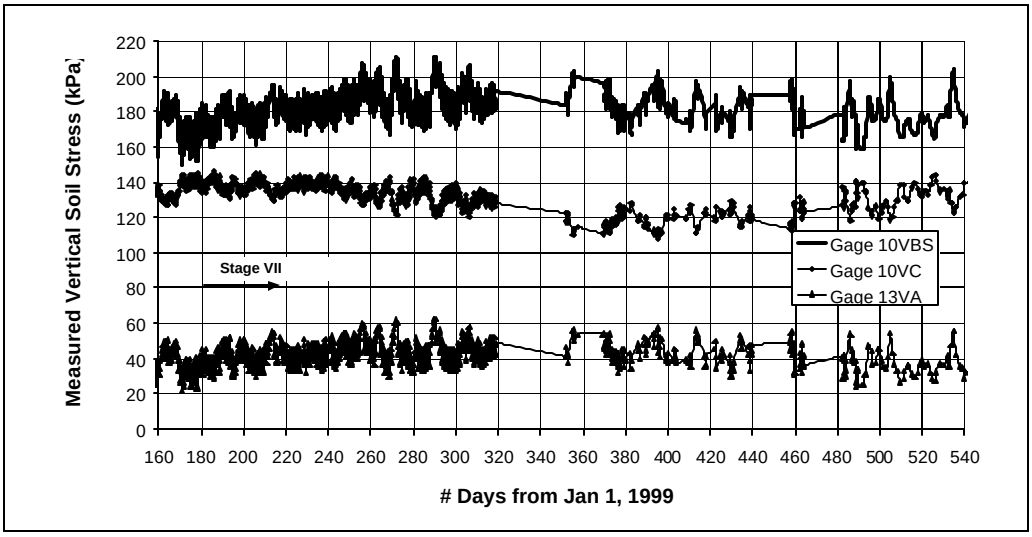

Fig. 3.13. Time Records for Measured Vertical Earth Pressures While Bridge was in Service (Stage VII).

3.5 Consistency of the Measured Data

The results from pressure cell gages placed at the same location (North and South in Figures 3.4 and 3.6) ran close to each other during Stage I when uniform backfill self-weight loading was applied, and almost parallel to each other during Stages IV through VI. The parallel behavior indicates almost similar response to different levels of loading by these two gages. The difference between these two gages ran up to almost 30%. The placement of girders on the abutment wall of Phase II Structure in two days starting from the south side, and the variability in soil properties between these two locations (e.g., variable soil stiffness due to variable compaction) might have contributed to this difference.

The measured response from the pressure cells correlates very well with the applied backfill self-weight loads during construction of the wall and during all subsequent construction stages. Sharp increases in measured vertical earth pressures were registered during Stage III construction (placement of girders). As expected, the pressure cells placed along location line D responded to loading during Construction Stages IV and VI when the overlying backfill and approach slab were placed, but showed very small response when the bridge structure was placed (Stages II, III and V). There is a close agreement between the results of pressure Cell P1 (118 kPa by end of Stage VI) placed along Section 400 of the Phase I Structure (Figure 1.5) and Gage 6VBS (135 kPa by end of Stage VI), both placed at the same elevation and distance from wall facing. Results of the next sections will demonstrate excellent agreement between the measured and applied total earth loads on geogrid layers 6 and 10 during different construction stages and along location line D. As will also be discussed in the next two chapters, the measurements for vertical earth pressures are strongly correlated with the measured lateral earth pressures against the wall facing and geogrid lateral strains. Based on the above discussion, it is fair to conclude that the measured results for the vertical earth pressures during construction are consistent and representative of the actual vertical stresses experienced by the structure.

3.6 Analysis and Design Implication of the Measured Results

When two gages are placed at the same location, their average value is used in analyzing the results.

The width of the reinforced soil zone is approximately 7.5 m at the bottom of the reinforced fill and increases on 1H: 1V slope toward the top (see Figure 1.3). To simplify the data analysis, the width of the reinforced soil zone is taken as 7.5 m (from the rear side of the facing to approximately location line D, see Figure 1.6). Vertical earth pressure data across the reinforced soil zone were obtained from pressure cells placed along location lines A, B, C, and D (Figure 1.6).

Very small change in the measured vertical earth pressures occurred while the structure was in service. Live loads due to traffic loading means accounting for a scenario such as a line of fully loaded trucks suddenly stopping on top of the bridge during a traffic jam. If this scenario happened during Stage VII, the instruments certainly did not capture it. Therefore, the collected data while the structure was in service cannot verify or be employed to investigate design assumptions regarding the effect of live load on the vertical loading of the structure. Therefore, these data will not be utilized herein for assessment of the design procedure. The data measured by end of construction stages will be utilized in the assessment of the design procedure of the front GRS wall. These data were proven reliable in the previous section.

3.6.1 Overturning Stability Analysis of the Front GRS Wall

The center location of the reinforced soil zone assumed in the analysis is 3.75 m from the facing. Positive eccentricity means that the location of the resulting vertical force acting on the reinforced soil zone is shifted from the center location of the reinforced soil zone toward the wall. The horizontal profiles of the vertical earth pressures measured from layer 0, 6, and 10 gages (Figures 3.3, 3.5, and 3.7) were employed to determine the eccentricity values of the resulting vertical earth forces acting, respectively, at: 1) the base of the reinforced fill, 2) the horizontal level within the reinforced soil zone at depth of 2.95 m (Layer 6), and 3) the horizontal level within the reinforced soil zone at depth of 1.33 m (Layer 10). The horizontal profiles of the vertical earth pressures measured just beneath the bridge footing (from front edge to back edge) from Layer 13 gages (Figure 3.10) were employed to determine the eccentricity value of the resulting vertical earth force acting on the bridge footing. Results for these measured eccentricity values at different stages and locations are shown in Figure 3.14 and Table 3.3. Also shown in Table 3.3 are the maximum eccentricity values measured during all construction stages.

By the end of Stage I Construction, the reinforced fill at depth 1.33 m (layer 10) experienced almost uniform distribution of vertical earth pressures but for layers 0 and 6 larger vertical earth pressures developed close to the wall facing (Figures 3.3, 3.5 and 3.7). This caused very small eccentricity on layer 10 (close to zero) and larger eccentricity values for layers 0 and 6 (see Figure 3.14). Eccentric loading of the bridge footing during Stages II and III was felt mostly beneath the bridge footing and at depth of 1.33 m (Figure 3.14). The placement of backfill behind the bridge abutment during Stage IV increased the loads in the interior side of the reinforced soil zone. This stabilized the reinforced soil mass against overturning and reduced the eccentricity values at all levels below the bridge footing (Figure 3.14). With the redistribution of vertical earth pressure that occurred during Stage V (i.e., reduction of vertical earth pressure close to the facing and increase of vertical earth pressure along the bridge abutment centerline), the eccentricity values were further reduced during Stage V (Figure 3.14). By the end of all construction stages, the eccentricity values of the resulting vertical forces at most locations were around zero. This is because the distributions of vertical earth pressures at different horizontal levels were uniform or close to symmetrical around the center of the reinforced soil zone as was discussed in a previous section (see Section 3.3.2 and Figures 3.3, 3.5, 3.7 and 3.10).

To meet the overturning stability requirements, the eccentricity of the resulting force must be less than L/4 for rock and L/6 for soil, where L is the width of the footing (Christopher and Elias, 1997). The allowable eccentricity is 0.64 m for the bridge footing (3.8/6), 1.25 m for the resulting force acting on the reinforced soil mass (7.5/6), and 1.88 m for the rocky base of the fill (7.5/4). Based on this information and the measured eccentricity values (Figure 3.14 and Table 3.3), the following can be concluded:

- The eccentricity values of the resulting vertical forces acting within and at the base of the front GRS wall is almost zero, well below the tolerable and design values (i.e., the factor of safety against overturning of the Founders/Meadows Bridge is very high, significantly exceeding the value estimated in the design).
- The most critical stage for the overturning stability occurred at the end of Stage III (the placement girders). The backfill behind the bridge (placed during Stage IV) should be placed before placement of the girders to increase the forces resisting potential overturning of the reinforced soil structure.

- The movement of the front GRS wall during Stage V (see Chapters 2 and 5) resulted in the reduction of high vertical earth pressure developed behind the wall facing. This enhanced the overturning stability of the Founders/Meadows Bridge structure.

Table 3.3. Measured Eccentricity Values for the Resulting Vertical Forces Acting below the Bridge Footing, Inside the Reinforced Fill, and at the Base of the Reinforced Fill.

Location	Measured Eccentricity by end of Construction, Stage VI, (m)	Maximum Measured Eccentricity during all Stages (m)
Bridge Footing	-0.05	0.20
Layer 10, Depth of 1.33 m	-0.43	0.23
Layer 6, Depth of 2.95 m	-0.1	0.4
Base of the Fill	0	0.4

3.6.2 Bearing Capacity Analysis for the Reinforced Soil Mass

The horizontal profiles of vertical earth pressures measured from layers 0, 6, and 10 gages across the 7.5 m wide reinforced soil zone (Figures 3.3, 3.5, and 3.7) were employed to determine the average measured value of vertical earth pressure acting on these layers. The corresponding estimated applied average vertical earth pressures at the horizontal level of these layers were estimated using the information summarized in the third column of Table 1.3. Applied and measured average vertical earth pressures on these layers during various construction stages are shown in Figure 3.15. The average measured vertical earth pressure values give insight into the loads resisted by the reinforced soil mass. The difference between the applied (estimated) and measured values provides insight into amount of vertical soil loads transferred through side shear to the structures alongside the reinforced soil mass. Most of this side shear is developed due to the settlement of the reinforced soil mass relative to the surrounding structures. By the end of Stage I Construction, the applied and measured average vertical earth pressures matched at a depth of 1.33 m, were very close at the base of the fill, and around 20-kPa difference occurred at depth of 2.95 m (Figure 3.15). During all subsequent construction stages, the measured changes in average vertical earth pressures for layers 6 (depth 2.95 m) and 10 (depth 1.33 m) were very close to those estimated (Figure 3.15). This implies that most of the applied vertical loads during placement of the bridge structure at depths of 1.33 m to 2.95 m below the bridge footing

were supported by the reinforced soil mass (i.e., very small loads if any were transferred to the wall facing).

Allowable bearing capacity of 480 kPa was recommended for the claystone bedrock supporting the front GRS walls (Abu-Hejleh et al., 2000). The measured average vertical earth pressure on the base of the reinforced fill (depth of 5.43 m) by the end of Construction Stage VI was 154 kPa, less than the estimated value of 199 kPa (Figure 3.15). To account for eccentric loading and calculate the bearing pressure, the Meyerhof approach assumes that eccentric loading results in a uniform redistribution of pressure over a reduced width equal to the width of the footing (L) less twice the eccentricity (Elias and Christopher, 1997). The measured eccentricity of the resulting force acting on the base of the fill by the end of the construction stages was zero (see Table 3.3). Thus, it can be concluded that the measured bearing pressure at the base of the reinforced fill is below the expected design value and well below the tolerable soil bearing capacity.

3.6.3 Bearing Capacity Analysis of the Bridge Footing

The horizontal profiles of vertical earth pressures measured from the three gages placed 0.23 m beneath the bridge footing (Figure 3.10) were employed to determine the average measured value of vertical earth pressure beneath the bridge footing. The corresponding estimated applied average vertical earth pressures were estimated using the information summarized in the second column of Table 1.3 and Equation 1.1. The estimated applied and measured vertical earth pressures beneath the bridge footing during different construction stages are shown in Figure 3.16. This figure indicates there is a 40-kPa difference between the applied and measured vertical earth pressures by the end of Stage IV. During subsequent stages, especially Stages V and VI, the difference between the measured and applied loads beneath the bridge footing increased significantly (Figure 3.16). It is possible that the difference between the applied and measured loads beneath the bridge footing was transferred to the wall facing through side shear due to the settlement of the reinforced soil mass beneath the bridge footing relative to the more rigid wall facing.

Allowable bearing capacities on the reinforced soil masses of 240 kPa and 200 kPa were recommended by, respectively, CDOT engineers (Abu-Hejleh et al., 2000) and the FHWA (Elias and Christopher, 1997). The measured average vertical earth pressure beneath the bridge footing by the end of the construction stages was 34 kPa, significantly below the estimated value of 119 kPa. The measured eccentricity of the resulting force acting on the bridge footing by the end of the construction stages was very close to zero (see Table 3.3). Thus, it can be concluded that the measured bearing pressure below the bridge footing is way below the expected value from the design and the allowable bearing capacity value.

3.6.4 Vertical Earth Pressure Distributions for Internal and External Stability Analyses

It was found from the results of strain gages (Section 5.4.4) that the potential failure line extends from the toe of the wall to the back edge of bridge footing (location line C). The vertical earth pressure employed for the calculation of maximum reinforcements forces along the potential failure line was estimated through Equation 1.1 (see Figure 3.17). Also shown in Figure 3.17 are three vertical profiles of measured vertical earth pressures 1) average of earth pressures from the wall facing to location line C (back edge of the bridge footing), 2) maximum of earth pressures measured along location line B, and 3) vertical earth pressures directly behind the wall facing. The results shown in Figure 3.17 suggest:

- The vertical earth pressure distribution within the potential failure zone differs significantly from location to location. The lowest vertical earth pressure occurred close to the wall facing and the highest vertical earth pressure occurred along the centerline of the bridge abutment (see Figures3.5 and 3.7).
- Equation 1.1 used in the design procedure provides good estimation of the average vertical earth pressure acting within the potential failure zone, not along the potential failure line. The design procedure might underestimate the vertical earth pressures acting on the potential failure line beneath the bridge footing by approximately 20%. The design procedure overestimates the vertical earth pressure acting on the potential failure line close to the toe of the wall by approximately 33%.

- The measured vertical earth pressure behind the wall facing is smaller than the estimated vertical earth pressure from Equation 1.1.by approximately 33% (close to the bottom of the wall) to 98 % (at a depth of 1.33 m below the footing).

The external stability analysis requires the estimation of vertical earth pressures developed at plane at the back end of the reinforced soil mass (location line D). These vertical pressures were obtained from measured vertical earth pressures along location line D. Figure 3.18 shows a profile of measured and assumed vertical earth pressures along location line D by the end of the construction stages (VI). Excellent agreement between the measured and predicted design values occurred at depths of 1.33 m and 2.95 m. Therefore, it can be concluded that the design procedure provides reasonable estimations for the vertical earth pressures developed along the back of the reinforced soil zone.

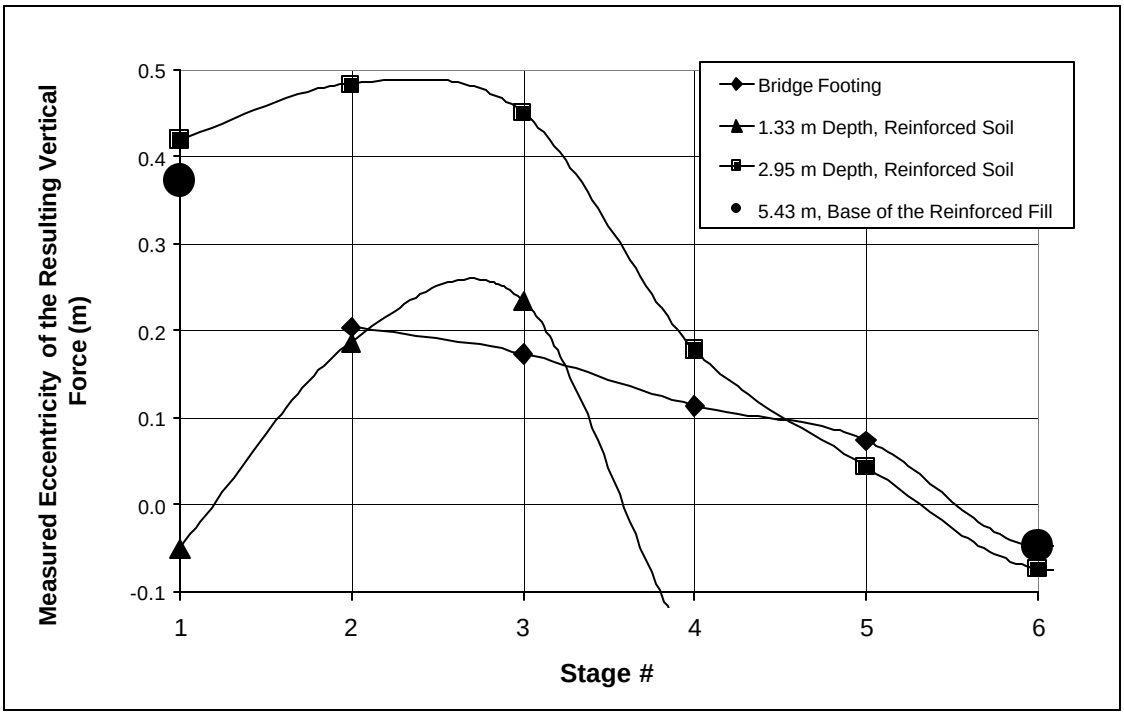

Fig. 3.14. Eccentricity Values of the Resulting Vertical Forces Acting at Different Horizontal Levels inside the Front GRS Wall.

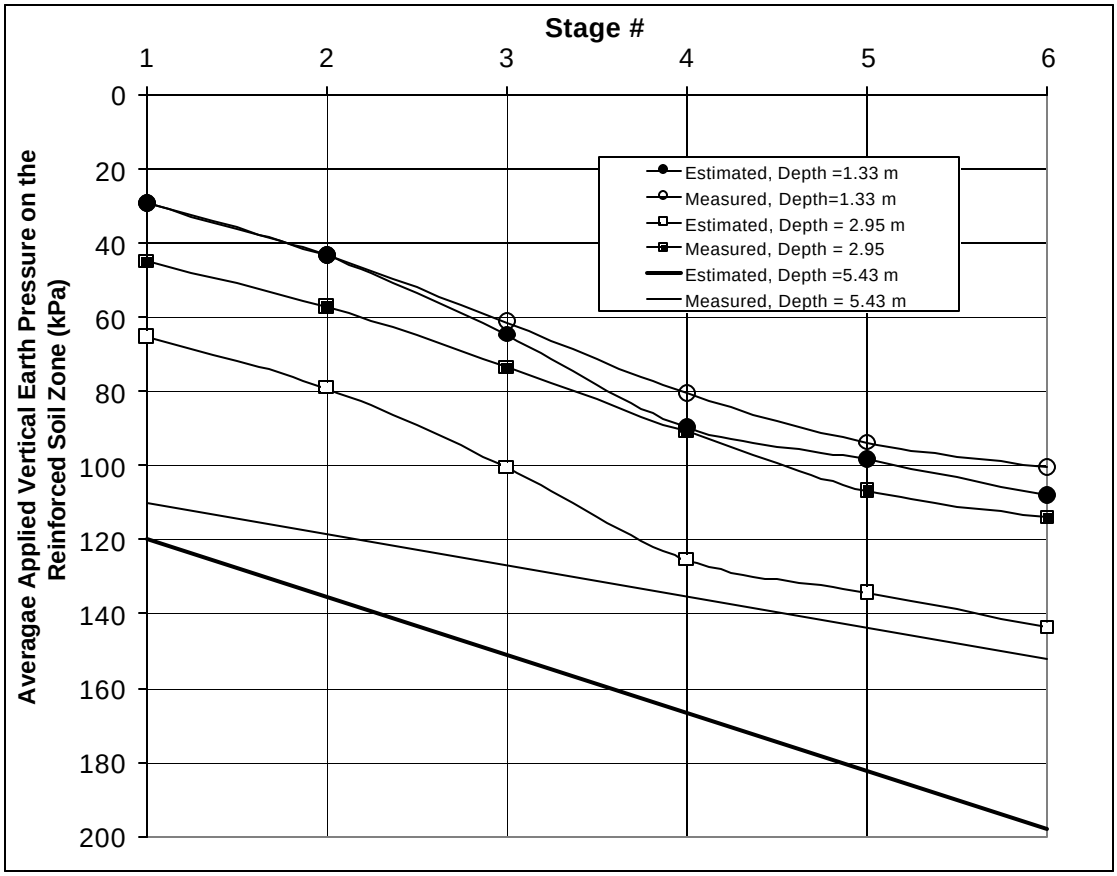

Fig. 3.15. Measured and Applied Average Vertical Earth Pressures at Different Horizontal Levels inside the Front GRS Wall.

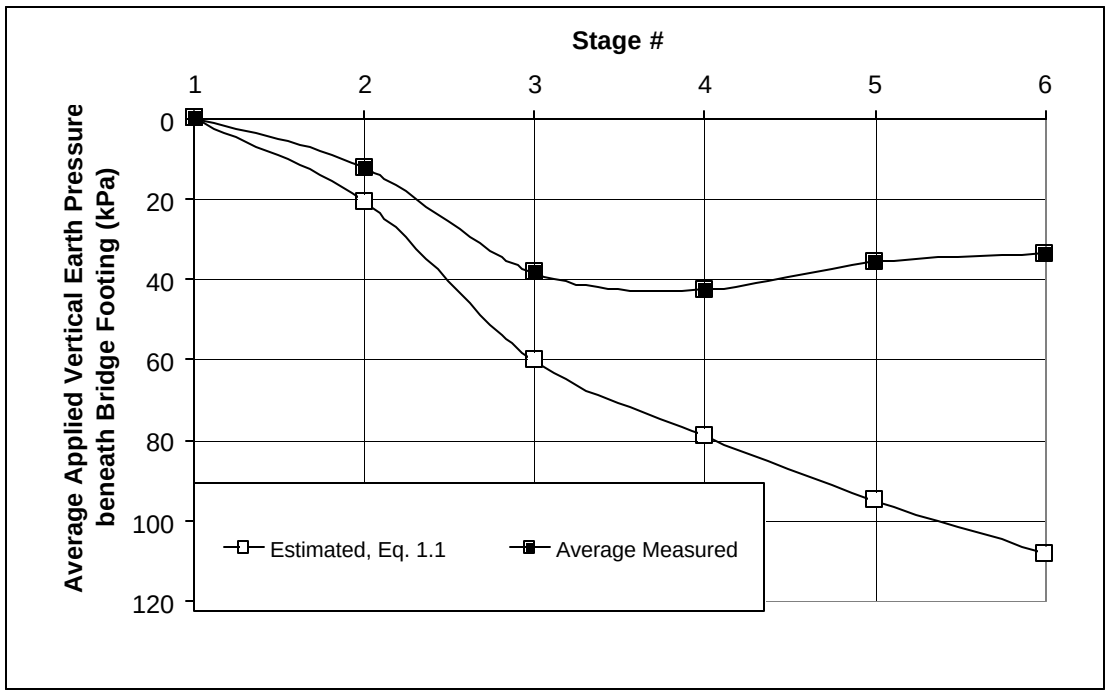

Fig. 3.16. Measured and Estimated Applied Vertical Earth Pressures Beneath the Bridge Footing.

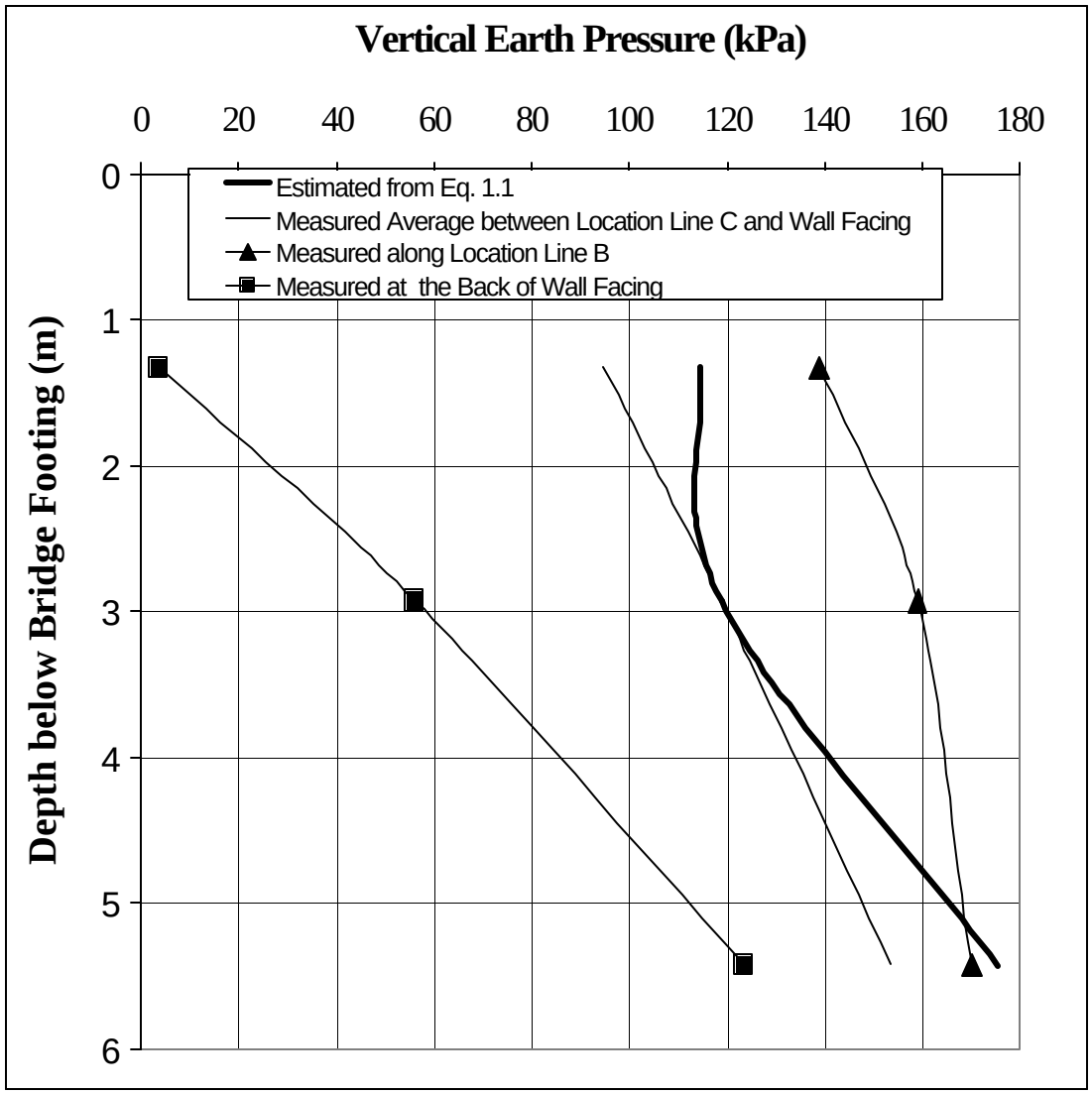

Fig. 3.17. Assumed and Measured Vertical Earth Pressures Beneath the Bridge Footing by the End of Construction.

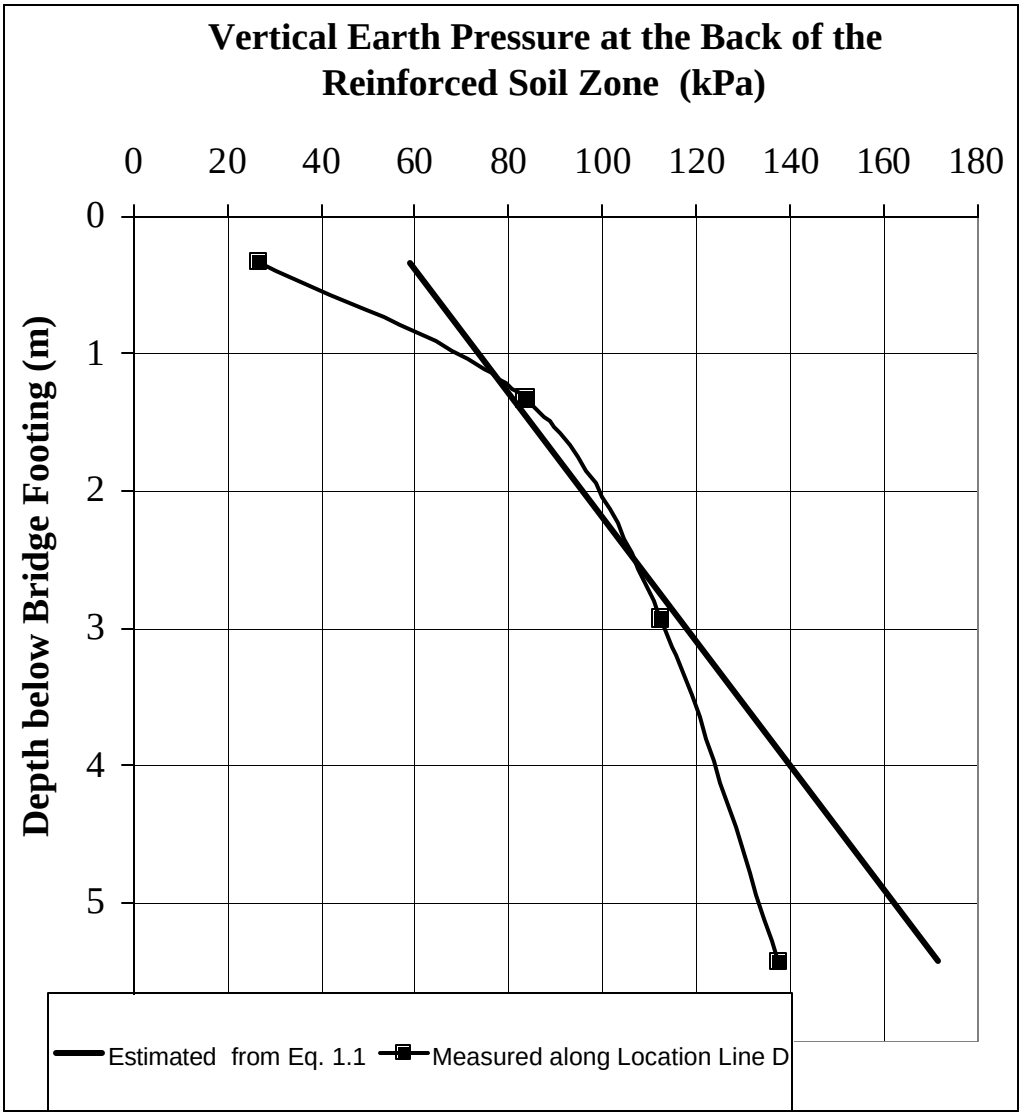

Fig. 3.18. Assumed and Measured Vertical Earth Pressures at the Back of the Reinforced Soil Zone by the End of Construction Stages.

4 LATERAL EARTH PRESSURES AGAINST THE FRONT WALL FACING

4.1 Introduction

Six gages were employed to measure distribution of lateral earth pressures against the facing of the front GRS wall (below the bridge footing) during all monitored stages. One pressure cell was placed along Section 400 of the Phase I Structure (P2, Figure 1.5) and five pressure cells were placed along Section 800 of the Phase II Structure (Table 1.1 and Figure 1.6).

4.2 Results of Pressure Cell P2 Placed along Section 400 during Construction

Measurements for lateral earth pressure on the wall facing of Section 400 (Phase I Structure) from pressure cell P2 were collected manually during all construction stages. Table 4.1 and Figure 4.1 summarize these measurements and the corresponding estimated horizontal and vertical earth pressures at the location of P2 gage (Equations 1.4 and 1.1). Ratios of measured lateral earth pressure to estimated vertical earth pressure are also listed in Table 4.1. This ratio was 2.01 for the first measurement, when just 0.1 m of backfill had been placed and compacted on top of P2 gage, much higher than the design estimated ratio of 0.31 (Table 4.1 and Figure 4.1). As reported in the literature (Section 1.5.3), it seems that compaction operations created lateral earth pressure on the facing that were locked-in after the compaction load was released. The measured lateral earth pressures and the ratio decreased in the subsequent two measurements when an additional 0.8 m of the backfill (vertical earth pressure of 17.7 kPa) was placed (Table 4.1). The decrease in horizontal earth pressure on the facing can be attributed to a small outward displacement of the facing (wall yielding). As additional backfill was placed, the lateral earth pressure on the facing increased but the ratio decreased. A constant ratio of approximately 0.11 was achieved from the end of Stage I to Stage VI. This ratio (0.11) is much less than the estimated design value of 0.31. This implies that current design procedures overestimate the loads carried by the facing.

Table 4.1. Measured and Estimated Lateral Earth Pressures against the Front Wall Facing of Section 400 (Measured from Pressure Cell P2).

Stage #	Estimated Vertical Earth Pressure from Eq. 1.1. (kPa)	Measured Lateral Earth Pressure on the Wall Facing (kPa)	Ratio of Lateral to Vertical Earth Pressure	Estimated Lateral Earth Pressure from Equation 1.4 (kPa)
I	0	0		0
I	2.3	4.5	2.01	0.7
I	11.3	2.8	0.25	3.49
I	20.3	2.7	0.13	6.28
I	24.7	4.8	0.19	7.67
I	47.2	5.6	0.12	14.64
I	62.9	7.3	0.12	19.5
II	75.7	8.5	0.11	23.45
IV	111.6	11.4	0.10	34.6
VI	129.6	14.7	0.11	40.4
VII	149.9	15.0	0.10	46.5

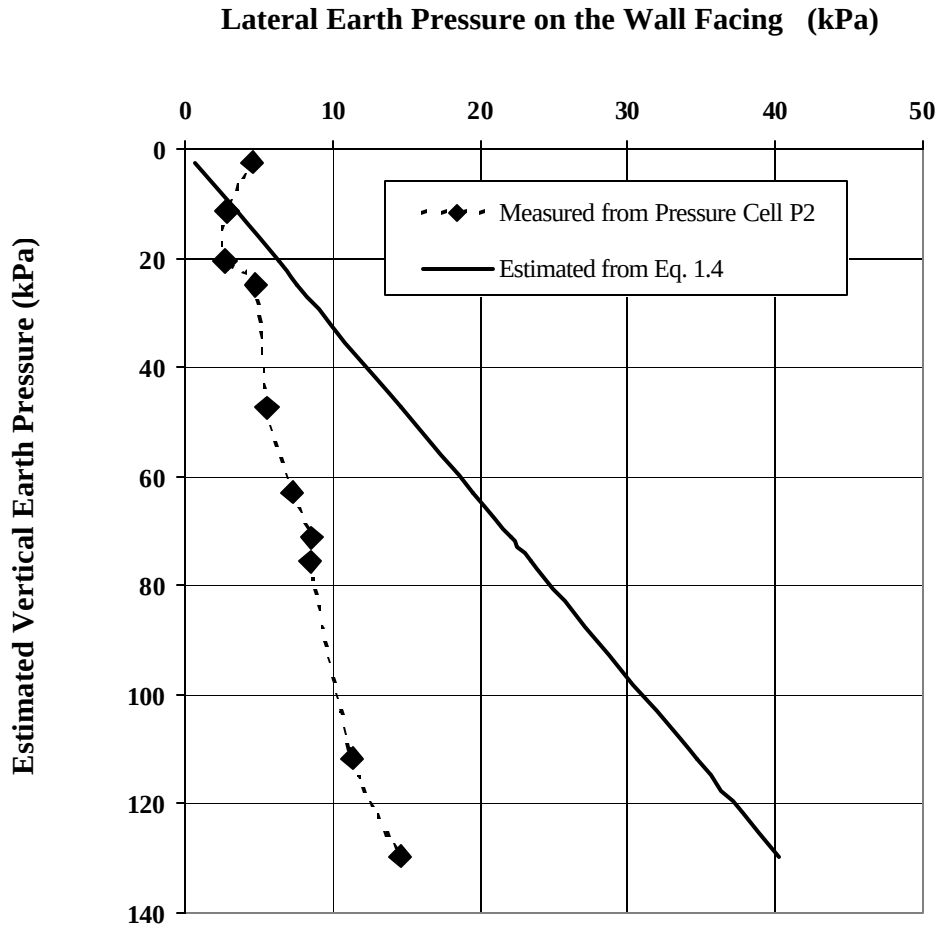

Figure 4.1. Measured and Estimated Lateral Earth Pressures against the Front Wall Facing of Section 400 during Construction (Measured from Pressure Cell P2).

4.3 Results of Pressure Cells Placed along Section 800 during Construction

Figures 4.2 and 4.3 show the time records of the measured lateral earth pressure against the wall facing of Section 800 during all construction stages (i.e., from days # 55 to day # 180 from Jan. 1., 1999). Continuous abrupt (not smooth) changes in the measured data (Figures 4.2 and 4.3) can be attributed to changes in air and backfill temperature and continuous movements of the wall facing. When 0.7 m of

backfill was placed and compacted over gages 11HN and 11HS during wall construction (Stage I), a sharp increase in the horizontal lateral earth pressure of 5.5 kPa was developed (Figure 4.3). The corresponding ratio between lateral earth pressure and vertical earth pressure is 0.611, higher than the estimated design ratio of 0.31. This could be attributed to the locked-in influence of the compaction operations as discussed before.

The measured lateral earth pressures against the wall facing at the end of each construction stage from each gage are summarized in Table 4.2 and Figure 4.4. Figure 4.5 shows vertical profiles of the measured and estimated lateral earth pressure against the wall facing by the end of front wall construction (Stage I) and by the end of all construction stages (Stage VI). These profiles are erratic showing no clear trend with the depth. This can be attributed to differences in the movement of the segmental wall at different levels. Figure 4.5a indicates that the compaction-induced stresses by the end of wall construction (Stage I Construction) remained at the top layer of the wall.

Gage 12H, located close to the top of the wall directly beneath the bridge footing, registered very small lateral earth pressure during all construction stages. This suggests the wall facing directly below the bridge footing did not feel the surcharge loads applied during placement of the bridge superstructure (Stages II to VI). It is possible that the top reinforced soil zone of the wall experienced relatively large lateral displacements during placement of the bridge superstructure, allowing the geogrid reinforcements to be mobilized and support most of the lateral earth pressure loads, thus taking the lateral earth pressure off the wall facing.

Most of the gages responded well to loading during Stages II to IV, especially gages 9H and 11HS (Figures 4.2 to 4.4 and Table 4.2). Sharp increases in the measured lateral earth pressures can be noticed in Figures 4.2 and 4.3 around days 69 and 70 when girders were placed (Stage III). It seems that the wall facing supported relatively large lateral earth pressures during these stages because the wall system was relatively rigid during Stages II, III, and IV (see Chapters 2 and 5).

During Stage V, the measured lateral earth pressure on the wall facing decreased for gages 9H, 11HN, and 11HS and showed no change for Gage 7H (see Figure 4.4 and Table 4.2). The reduction in the lateral earth pressures can be attributed to the relatively large lateral movements of the reinforced soil wall system during Stage V (see Chapter 2). These movements allowed the geogrid reinforcements to be mobilized and support a larger proportion of the lateral earth pressure loads, thus taking off the lateral earth pressure from the wall facing. This behavior also correlates very well with the measured vertical earth pressure (Chapter 3) and geogrid strains (Chapter 5) close to the wall facing during Stage V.

As increasing vertical loads were applied during Stage VI, the lateral earth pressures against the wall facing increased again (Figure 4.4). A ratio between the lateral and vertical earth pressure of approximately 0.04 to 0.08 was achieved towards the end of all construction stages (Stage VI). This ratio is much smaller than the ratio of 0.31 assumed in the design process. Figure 4.5b indicates clearly that the design procedures overestimate considerably the lateral earth loads carried by the facing.

Except for gage 7H, changes in the lateral earth pressure on the wall facing induced by placements of the bridge superstructures (Stages II to VI) were small (Figure 6.4). This response correlates very well with the small increase in the measured vertical earth pressure close to the wall facing due to the placement of the bridge superstructure (Chapter 3) and could be attributed to the large wall movements during Stage V (see Chapter 2).

Table 4.2. Measured Lateral Earth Pressures against the Front Wall Facing of Section 800 at the End of Each Monitored Stage.

Stage	I	II	III	IV	V	VI	VII
Gage #							
7H*	0.5	0.5	1.0	2.0	2.0	4.4	5.9
9H	1	1.5	4.0	6.0	0.5	2.4	3.1
11HN	6.0	6.5	6.7	7.0	6.0	8.5	9.3
11HS	5.0	6.5	8.0	9.0	6.0	7.8	8.4
12H	0	0.5	0.5	0.5	0.5	1.5	0.6
*Gage placed at elevation of 2.74 m above leveling pad but first data was collected at elevation of 4.27 m (see Table 2.5)							

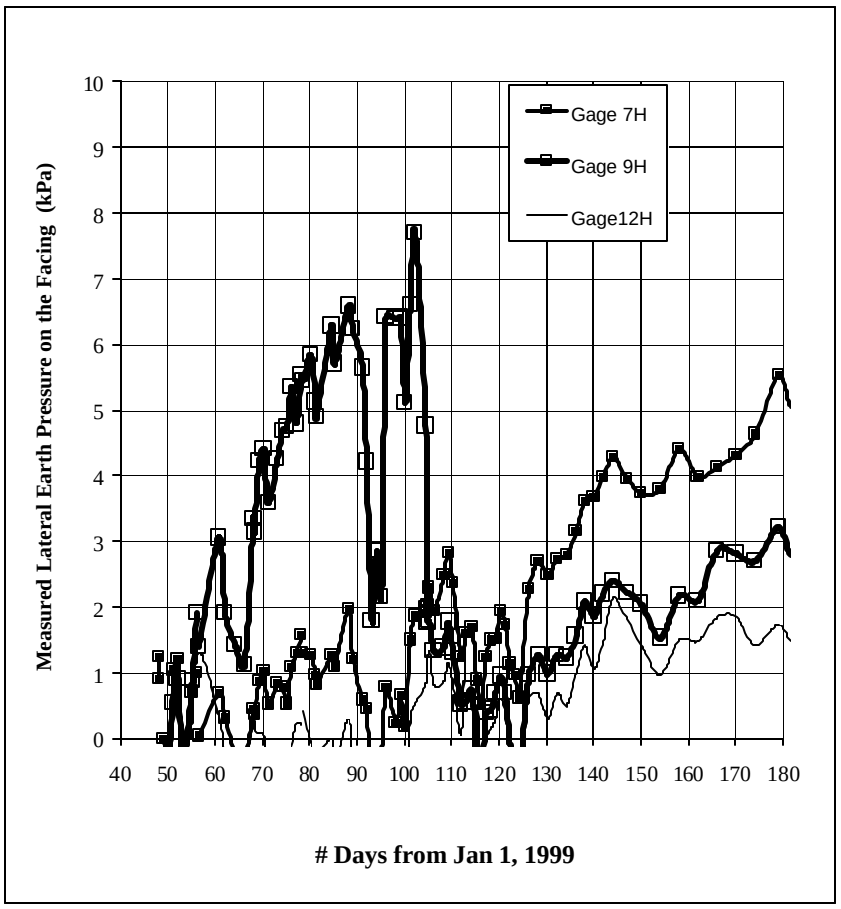

Figure 4.2. Time Records for the Measured Lateral Earth Pressure against the Wall Facing of Section 800 during all Construction Stages (from Gages 7H, 9H, and 12 H).

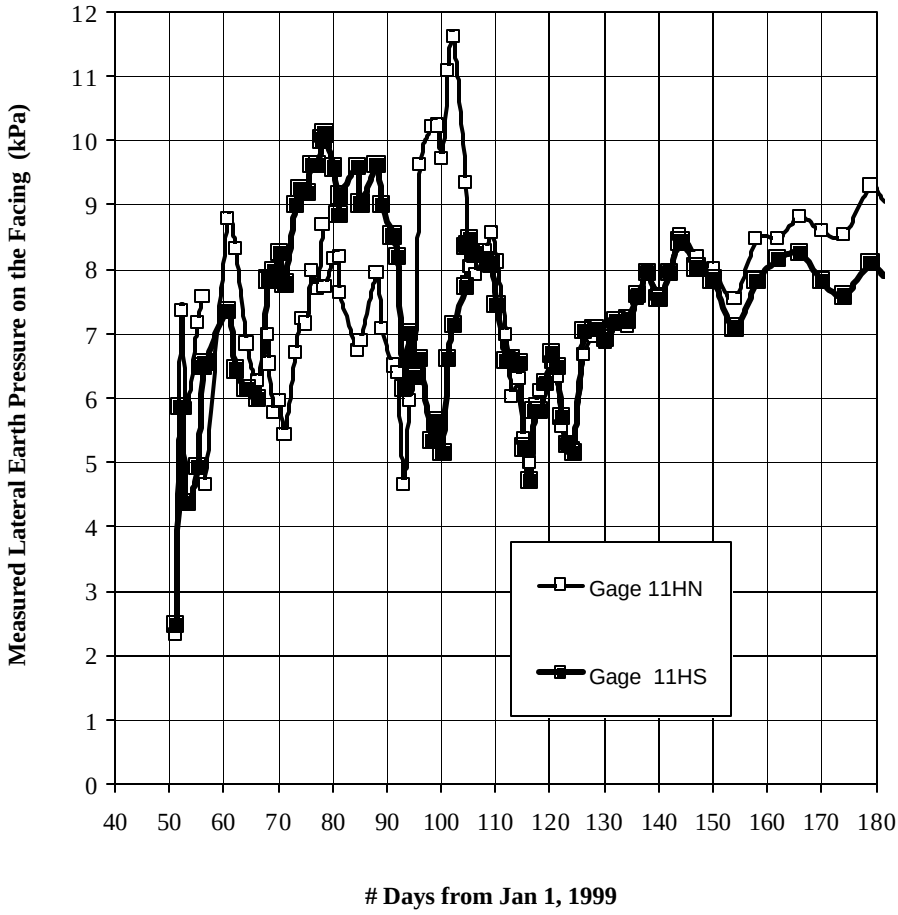

Figure 4.3. Time Records for the Measured Lateral Earth Pressure against the Front Wall Facing of Section 800 during all Construction Stages (from Gages 11 HN and 11HS).

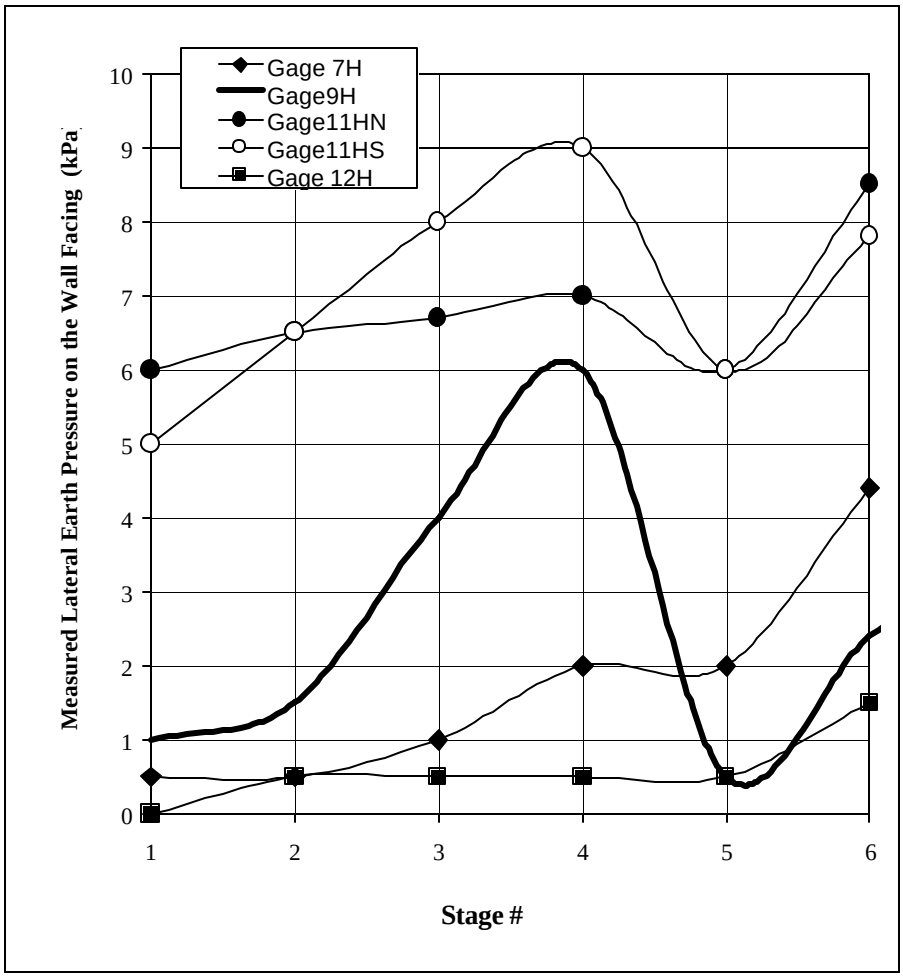

Figure 4.4. Lateral Earth Pressure against the Front Wall Facing of Section 800 Measured by the End of each Construction Stage.

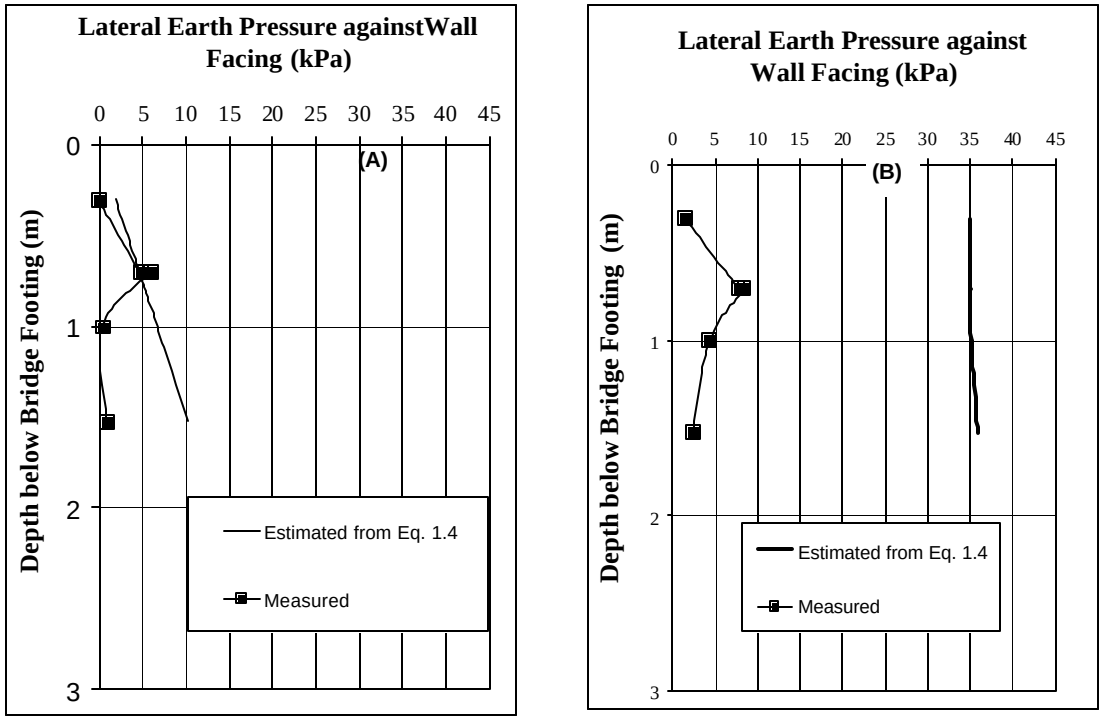

Figure 4.5. Measured and Estimated Profiles of Lateral Earth Pressure against the Front Wall Facing of Section 800: a) by the End of Front GRS Wall Construction (Stage I), and b) by the End of all Construction Stages (Stage VI).

4.4 Results while Structure was in Service (Stage VII)

Typical time records for the measured lateral earth pressure against the wall facing while the bridge was in service for one year (Stage VII, days 180 to 545 from Jan. 1, 1999) are shown in Figure 4.6. The fluctuations in the measured values can be attributed to changes in air and backfill temperature and continuous movements of the wall facing. Tables 4.1 and 4.2 list the values of the measured lateral earth pressures for Stage VII. The Stage VII results in the tables represent average values of data measured over a year while the bridge was in service. Along Section 400 (Table 4.1) the measured increase in lateral earth pressure during Stage VII was a very small value of 0.3 kPa. Along Section 800 (Table 4.2) the measured increase in lateral earth pressure was also small for most of the gages (less than 0.7 kPa, except Gage 7H). The increase in lateral earth pressure while the structure was in service was relatively large at the location of Gage 7H (1.5 kPa, see Table 4.2). The small increase in the measured lateral earth pressure during Stage VII along Section 800 occurred immediately after opening the bridge to traffic (see Figure 4.6), possibly due to placement of minor structures on the bridge structure (even after opening the bridge to traffic).

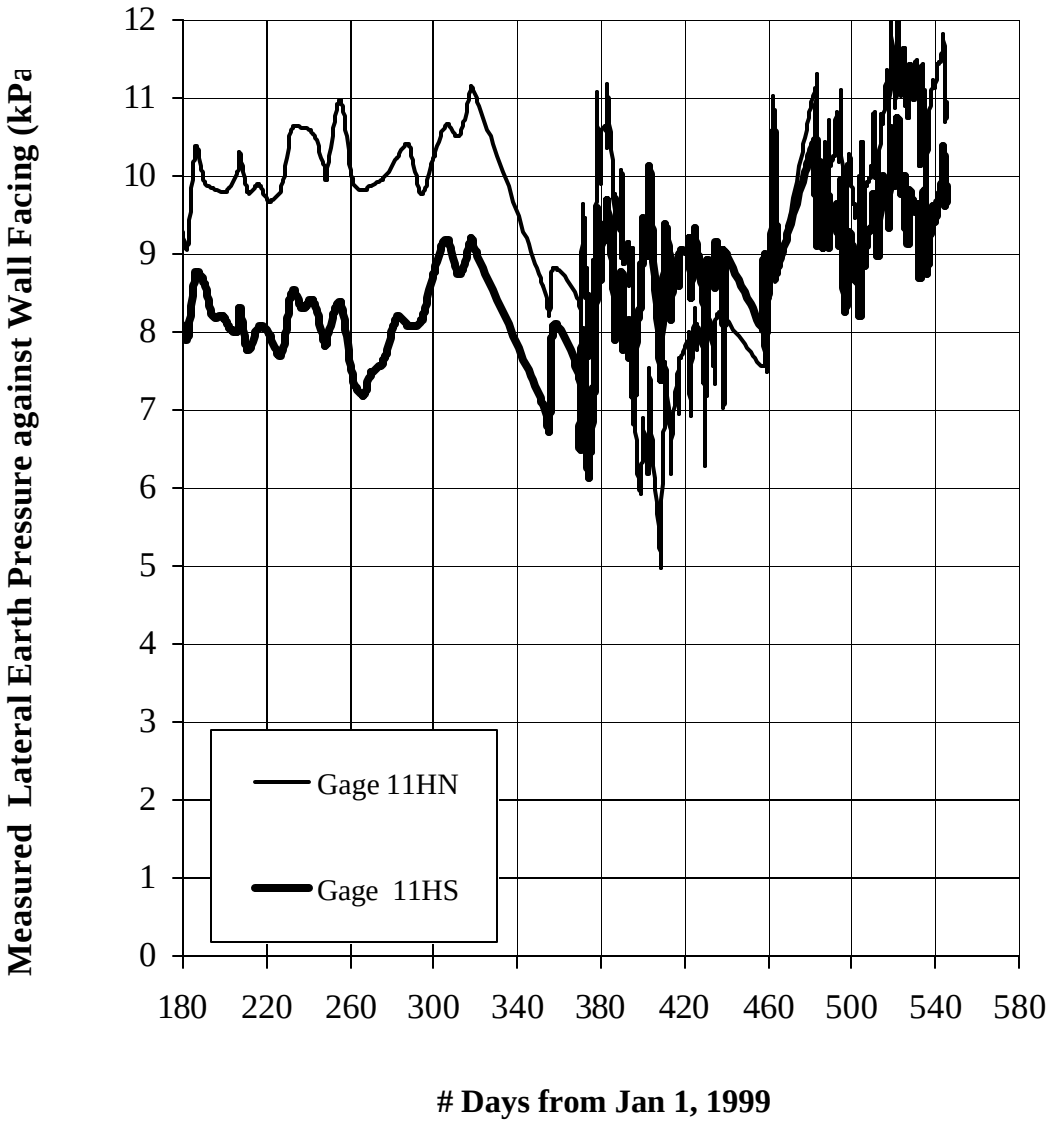

Figure 4.6. Typical Time Records for the Measured Lateral Earth Pressure against the Front Wall Facing of Section 800 while the Structure was in Service.

4.5 Consistency of the Measured Data

The consistency of the measured data is investigated by comparing the results of Gages 11HN and 11HS, placed at the same elevation. Figure 4.6 indicates that the results from these two gages run parallel and very close to each other. The measured lateral earth pressures from gages 11HN and 11HS and other gages are not seem to be influenced by seasonal changes in temperatures (see Figure 4.6). The measured lateral earth pressures on the facing correlate with the applied loads during various construction stages as discussed in previous sections. Sharp increases in the measured lateral earth pressures can be noticed in Figures 4.2 and 4.3 around days 69 and 70 when girders were placed (Stage III). As will be summarized in Chapter 6, the measured lateral earth pressures correlate well with the vertical earth pressures and geogrid lateral strain measured close to the wall facing. Based on the above discussion, it is fair to conclude that the measured results for the lateral earth pressure on the wall facing are reliable and consistent during the construction stages.

4.6 Summary and Assessment of the Design Procedure

Compaction operations induced comparatively large earth pressure against the wall facing. Some of the compaction induced pressure remained locked-in after removal of the vertical compaction loads. Large ratios of lateral to vertical earth pressure of 2.01 and 0.61 were measured along sections 400 and 800, respectively, during initial stages of placement and compaction of backfill over the gages (assumed value in the design is 0.31). The design procedure (Equation 1.4) does not account for the influence of compaction. It therefore underestimated the developed lateral earth pressure against the wall facing during initial stages of backfill placement and compaction. For facing with low connection strength or low interface shear strength, the compaction loads might cause excessive deformation or improper alignment to the facing. It is estimated that the compaction-induced lateral earth pressures on the wall facing exceed the assumed active earth pressure over a depth, approximately, less than 1 m. The ratio between lateral to vertical earth pressure dropped to an almost constant value of 0.11 (Table 4.1) after almost 2 meters of backfill were placed and compacted over the gage.

The measured changes in lateral earth pressure against the wall facing while the structure was in service were small and much lower than the values estimated in the design. Live loads due to traffic loading

account for a scenario such as a line of fully loaded trucks suddenly stopping on top of the bridge during a traffic jam. It seems this scenario did not occur during Stage VII because the instruments certainly did not capture it. In other words, the collected data cannot verify design assumptions regarding the effect of live traffic load on the horizontal loading of the wall facing and therefore will not be utilized for assessment of the design procedure. The lateral earth pressures against wall facing measured by end of construction will be utilized for assessment of the design procedure. These data were proven reliable in the previous section.

Table 4.3 summarizes the measured and estimated (Eq. 1.4) lateral earth pressure by the end of all construction stages from gages placed along Sections 400 and 800, and the ratio between measured to estimated values. The measured lateral earth pressures against the wall facing range from 4.2 % to 36.4% of the values estimated in the design. The ratio between lateral to vertical earth pressure at the end of construction stages was 0.11 for section 400 and 0.04 to 0.08 for Section 800 (estimated ratio in the design is 0.31). Hence, it can be concluded the current design procedure overestimates the lateral earth pressures against the front GRS wall facing by almost three times.

The very low earth pressure measured against the wall facing suggests a behavior close to the behavior of a GRS wall with a yielding lateral boundary rather than with a rigid lateral boundary (McGown et al., 1998, see Section 1.5.4). The relatively flexible wall system allowed for the comparatively larger mobilization of the friction resistance of the backfill and the support of more lateral earth pressure by reinforcements, thus taking more lateral earth pressure off the wall facing. Smaller lateral earth pressures were measured against the wall facing along Section 800 than along Section 400. The large difference occurred, most likely, because Section 800 experienced more lateral movements than Section 400 (see Chapter 2). The lateral earth pressures against the wall facing of section 800 declined significantly during Stage V construction when the wall facing experienced large outward displacements (see Chapter 2).

The design procedure may incorrectly estimate the lateral earth pressure against the wall facing because:

- The true shear strength of the backfill is higher than what is assumed in the design (see section 1.5.2). A backfill with higher shear strength will produce smaller lateral earth pressure.

- The wall behavior and response was close to the behavior of GRS walls with yielding lateral boundary, thus reducing the earth pressure against the wall facing as discussed previously.

Table 4.3. Measured and Estimated Lateral Earth Pressure (kPa) against the Front Wall Facing by the End of Construction.

Gage #	By the end of Construction (End of Stage VI)		
	Estimated	Measured	Percentage Ratio of Measured to Estimated Values (%)
7H	38.8	4.4	11.3
9H	35.9	2.4	6.7
11HN	34.9	8.5	24.3
11HS	34.9	7.8	22.3
12H	35	1.5	4.2
P2	40.4	14.7	36.4

5. GEOGRID STRAINS IN THE FRONT GRS WALL

5.1 Introduction

Figure 1.6 and Table 1.3 show the locations of all strain gages placed along Section 800 (Phase II Structure) to measure distribution of geogrid lateral strains inside the front GRS wall (below the bridge footing) during all monitored stages. Strain gages attached to geogrid layers # 2, # 6, # 10, and #12 (Figure 1.6) will be referred to as, respectively, layer 2 gages, layer 6 gages, layer 10 gages, and layer 12 gages. Layers 12, 10, 6, and 2 gages were placed at depths of 0.61 m, 1.43 m, 3.05 m, and 4.68 m, respectively, below the bridge footing. Layer 12 gages were placed 0.61 m below the bridge footing. The outward displacements of the front GRS wall facing inferred from strain gages were presented and discussed in Chapter 2.

5.2 Typical Geogrid Strains during Placement and Compaction of the Backfill

Figure 5.1 shows time records of the geogrid strains measured from layer 6 gages during construction of the front GRS wall (Stage I). These data were collected every six minutes to monitor the development of geogrid strains during construction activities. It is interesting to notice that changes to the geogrid strains occurred during working hours and no changes occurred during the evening and night hours (when no work was taking place). These changes seemed to be sharp and occurred in a very small short period (i.e., changes were not distributed over the entire working hours during which backfill was placed and compacted). These changes did not fluctuate.

Figure 5.2 shows the measured strains from geogrid layer 6 during construction of the front GRS wall (Stage 1) versus the estimated applied vertical earth pressure over geogrid layer 6 (Eq. 1.1). The changes in geogrid strains correlate very well with the applied load. Significant increases in geogrid strains occurred during placement and compaction of the initial 1 m of backfill over the gages (~20 kPa in Figure 5.2), especially close to the wall facing (along Location Line A). Comparatively, smaller geogrid strains developed during the rest of Stage 1 Construction. During the compaction and

placement of 1 m of backfill, the responses in geogrid strains were different from Gage 6SBN and Gage 6SBS, which were placed at the same location (Figure 5.2). However, the response from these two gages in subsequent stages was almost parallel. The large increases in geogrid strains and differences in the measured geogrid strains for gages placed at the same location following placement and compaction of backfill over the gages can be attributed to several factors:

- Locked-in strains induced by compaction loads (see Section 1.5.3). The influence of compaction loading might vary across the geogrid layers.
- Presence of slack in the geogrid and differences in initial tensioning of the geogrid.
- Non-stable or erroneous 1st reading (reference) due to the sensitivity of the gages and flexibility of the geogrid layers.
- Bending of the geogrid. If the geogrid layer is placed on uneven ground or experiencing any flexural loading (may be due to uneven backfill settlement or settlement of backfill relative to the facing) one side of the geogrid (top or bottom) will be in tension as the other will be in compression.

The strain gages placed along Section 800 were ordered with high sensitivity (Geokon Model 4050) because the measured geogrid strains on Phase I Structure were small (Abu-Hejleh et al., 2000). During construction stages, several strain gages went off the scale and maxed out yielding no reading. The combination of gage sensitivity, flexibility of the geogrid (i.e., can easily experience vertical deformation), installation, and backfill compaction operation produced the loss of several strain gages.

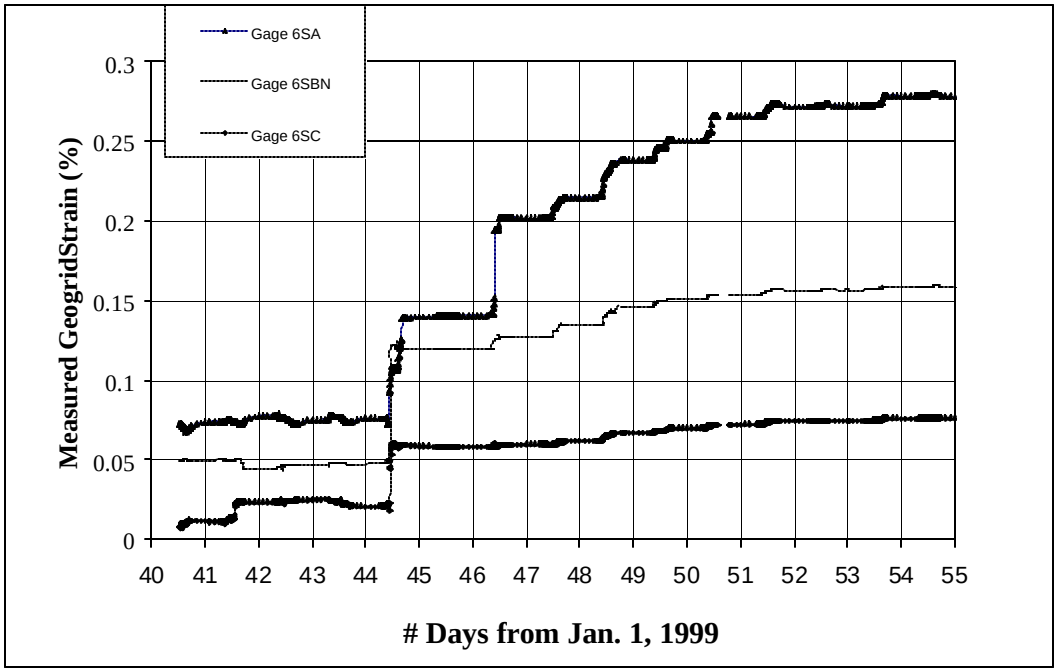

Fig. 5.1. Typical Time Records for Measured Geogrid Strains during Construction of the Front GRS Wall (Stage I).

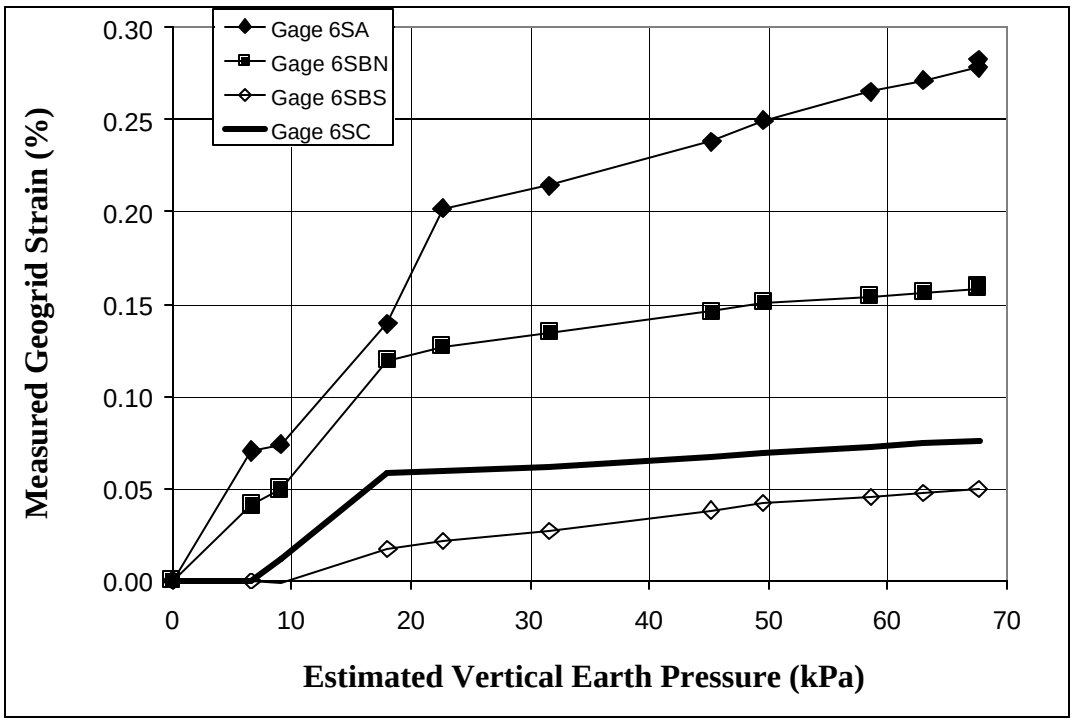

Fig. 5.2. Typical Measured Geogrid Strains vs. Vertical Earth Pressure during Construction of the Front GRS Wall (Stage I).

5.3 Results of Layer 2 Strain Gages during all Construction Stages

Figures 5.3 shows time records for the geogrid strain results measured during all construction stages at geogrid layer 2 (Figure 1.3). Sharp increases of geogrid strains occurred following placement and compaction of the backfill along Location Lines A and B. In all subsequent construction stages, small changes in geogrid strains occurred for gages placed along Location Lines B and C. The measured geogrid strains along Location Line A continued to increase and exceeded those measured along Location Lines B and C (Figure 5.3). Just before the end of Stage I Construction, Gage 2SA went off the scale and maxed out (Figure 5.3). Transmission from Gage 2SB was also lost by the end of construction Stage VI (Figure 5.3).

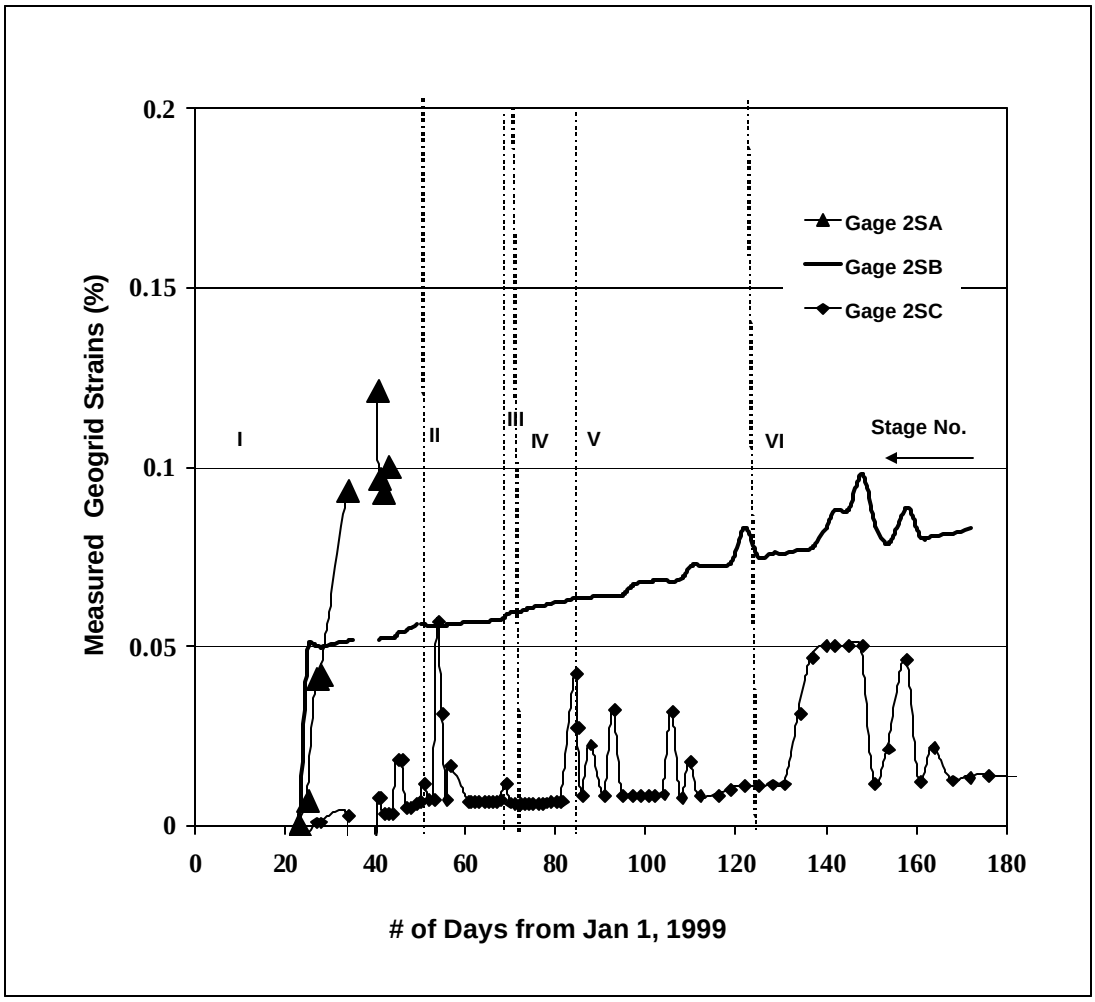

Fig. 5.3. Measured Strains along Geogrid Layer 2 during all Construction Stages.

5.4 Results of Layers 6 and 10 Gages during all Construction Stages

Figures 5.4 and 5.5 show time records for the geogrid strain results measured during all construction stages from geogrid layers 6 and 10, respectively. Gage 6SBN exceeded the measuring range at the end of Stage VI (Figure 5.4). The strain readings from Gage 6SA exceeded the measuring range during Stage IV, seemed to fall down and become within the measuring range at the end of Stage V and most of Stage VI, but exceeded the measuring range by the end of Stage VI (Figure 5.4). The missing strain data for Gages 6SBN and 6SA at the end of Stage VI were estimated based on extrapolation from their data at previous stages and from strain data obtained from Gage 6SBS. A summary of the obtained strains along geogrid layers 6 and 10 at different construction stages is shown in Figure 5.6. The geogrid strain measurements at different stages as a function of the applied vertical earth pressures over geogrid layers 6 and 10 (Eq. 1.1) are shown in Figure 5.7. The geogrid strain measurements at locations lines A and B were extrapolated to estimate the geogrid strains at the rear side of the wall facing. Horizontal profiles of the total geogrid strains, and *change*s in geogrid strains developed due to the placement of the bridge superstructure (Stages II to VI from Stage I), measured from layers 6 and 10 gages, are given in Figures 5.8 and 5.9, respectively.

Gage 10SD registered the development of a very small compressive strain in geogrid following the initial placement and compaction backfill over that gage (Figure 5.5 and 5.6). This could be attributed to bending of the geogrid layer and/or non-stable or erroneous 1st reading (reference reading). It is possible also that the compressive strains measured in the geogrid were real. It is difficult to imagine the development of compression strains in the geogrid while it was isolated in the air, but it could be possible when geogrid became an integral part of the reinforced soil mass. This gage experienced an increase of geogrid tensile strains when additional backfill was placed and during all subsequent construction stages, but registered very small compressive strains in the geogrid by end of construction stages. This, as discussed before, could be attributed to erroneous reference readings.

During Stages II to VI, geogrid layers 6 and 10 at different Location Lines responded with comparatively small deformations and strains to the increasing vertical earth pressures (Figures 5.6 and

5.7, see Chapter 2). The highest strains occurred close to the wall facing during Construction Stages I through IV (Figure 5.8).

During Stages V and VI, the GRS system along layers 6 and 10 appears to have responded with comparatively large strains and displacements to the increasing level of applied vertical earth pressures (Figures 5.6 and 5.7, see Chapter 2). As shown in Figure 5.9, the change in geogrid tensile strains at Location Line A (behind wall facing) due to the placement of the bridge superstructure (Stage II to VI from Stage I) slightly increased along geogrid layer 6 and declined sharply along geogrid layer 10. Most of the geogrid tensile straining during Stage V occurred inside the interior portion of the reinforced soil mass along Location Line B for layer 6 (Figure 5.4 and 5.6) and along Location Lines C and B for layer 10 (Figures 5.5 and 5.6). By the end of Stage VI, the maximum strain occurred at Location Line C for layer 10 (Figure 5.8b and 5.9b). Along geogrid layer 6, the maximum strain occurred at Location Line A (0.4%) which was slightly higher than that measured along Location Line B (0.37%) as demonstrated in Figure 5.8a. However, the increase in geogrid tensile strains due to the placement of the bridge superstructure (Stages II to VI) for layer 6 (Figure 5.9a) at Location Line B (0.23%) was much larger than that at Location Line A (0.097%).

Along layer 10, the geogrid tensile strains at Location Line A dropped during Stages V and VI, while the strains at Location Lines C and B were increasing at a comparatively very high rate during these two stages (Figure 5.5 and 5.6). This severe reduction in geogrid strain at Location Line A close to the wall facing measured from gage 10SA correlates very well with the reduction of both the measured lateral earth pressure against the wall facing from Gage 11HN (see previous Chapter) and the measured vertical earth pressures behind the wall facing from Gage10VA (see Chapter 3). The significant increase of geogrid tensile strain along Location Lines B and C from Gage 10SB and 10SC during Stage V correlates well with the significant increase in vertical earth pressures measured from Gages 10VBN and 10VC (Figure 3.6).

Along geogrid layer 6, a very small increase in the geogrid tensile strains occurred at Location Line A during Stage V (Figure 5.6a). This seems to correlate well with the no change in the measured lateral

earth pressure against the wall facing from Gage 7H during this stage. At the same time, the strains at Location Line B were increasing at a comparatively high rate (Figure 5.4). This correlates well with the comparatively high rate of increases in the measured vertical earth pressure from Gage 6VBN during this stage (Figure 3.4).

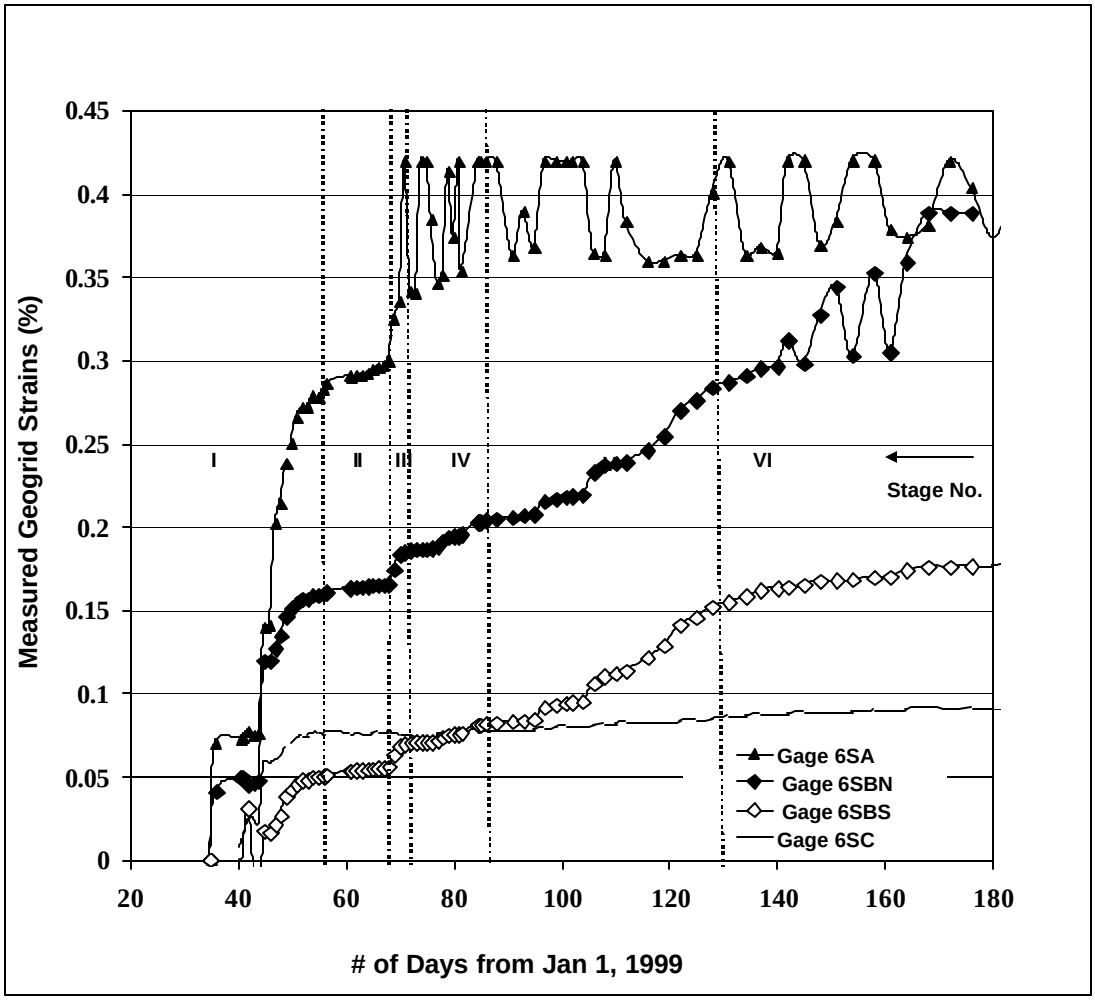

Fig. 5.4. Measured Strains along Geogrid Layer 6 during all Construction Stages.

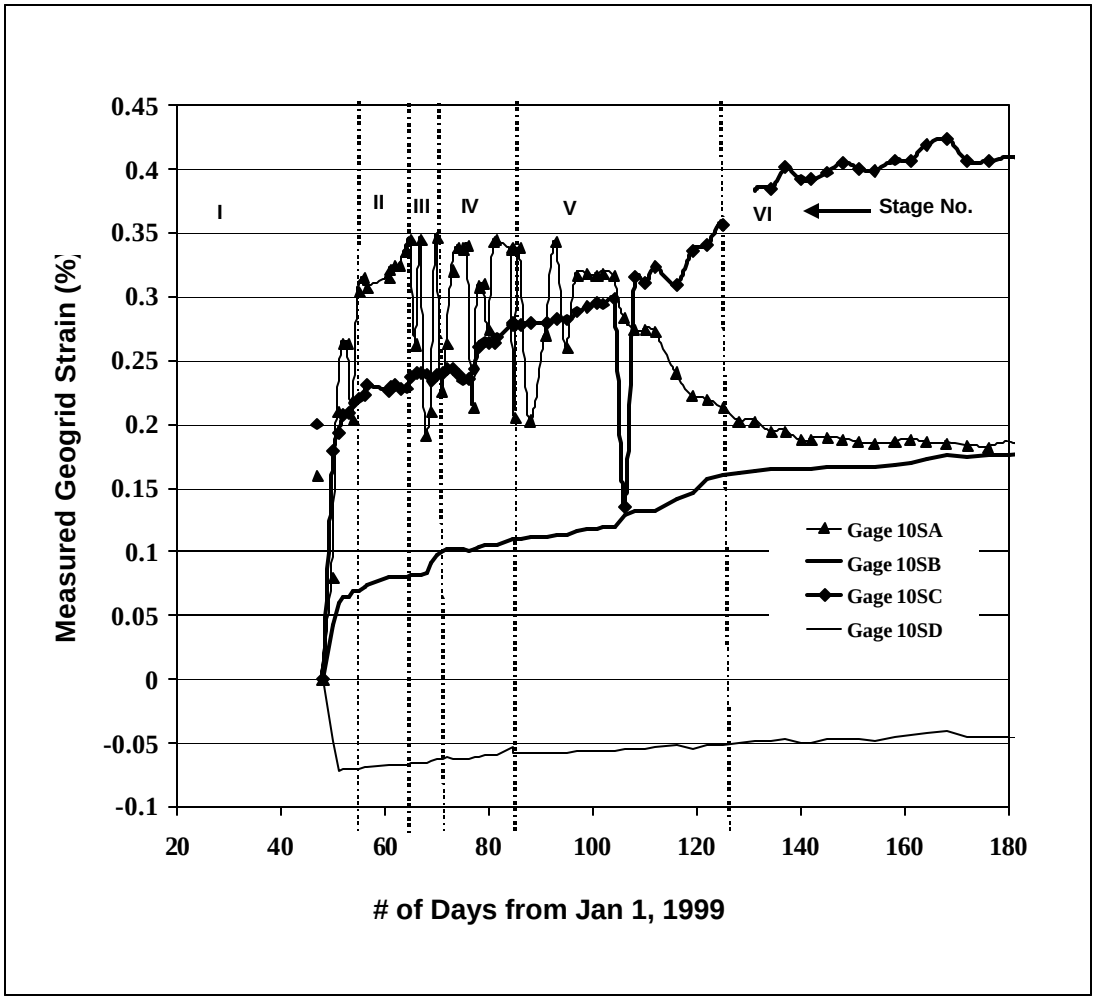

Fig. 5.5. Measured Strains along Geogrid Layer 10 during all Construction Stages.

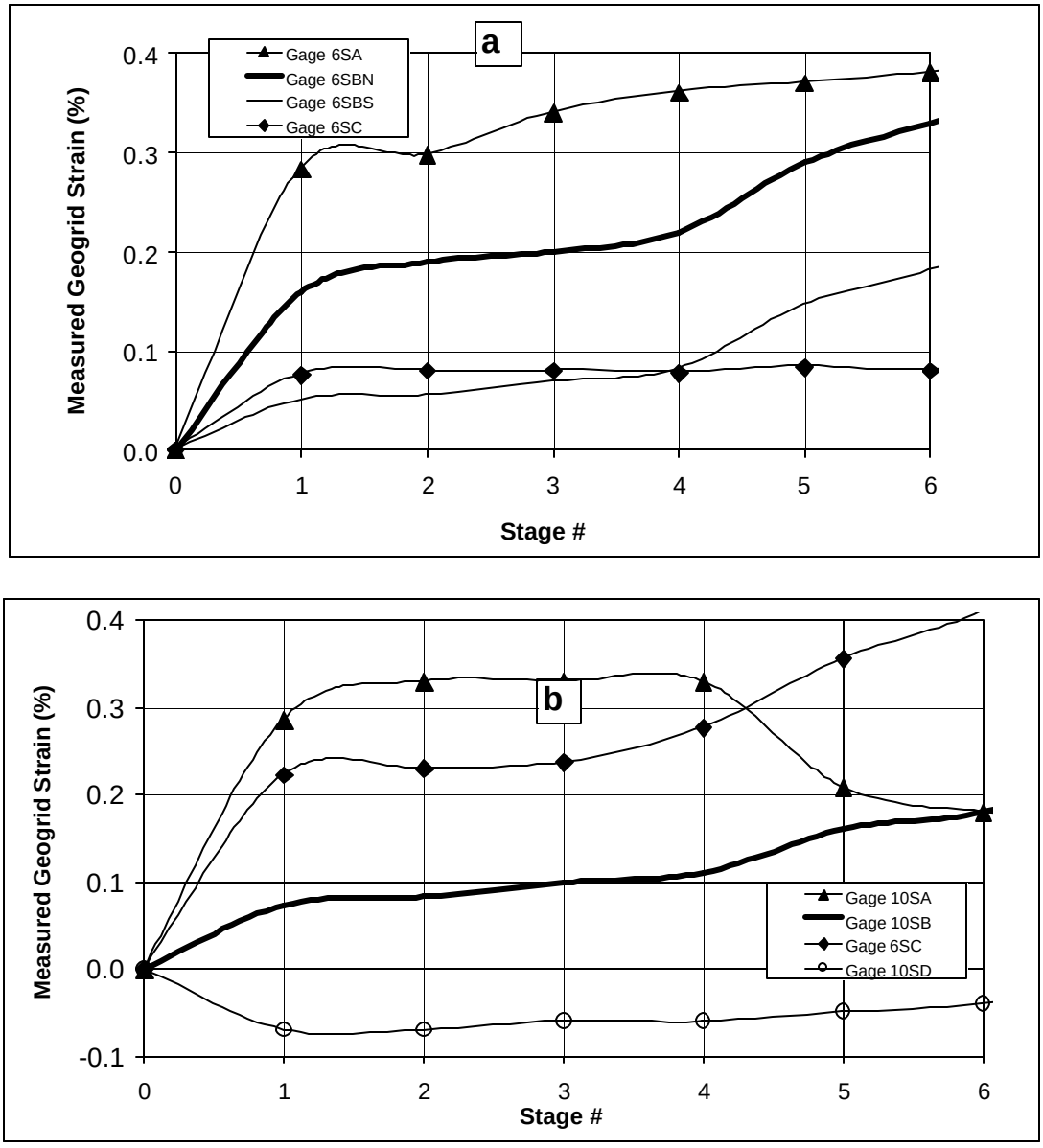

Fig. 5.6. Measured Geogrid Strains at Various Construction Stages along a) Geogrid Layers 6, and b) Geogrid Layer 10.

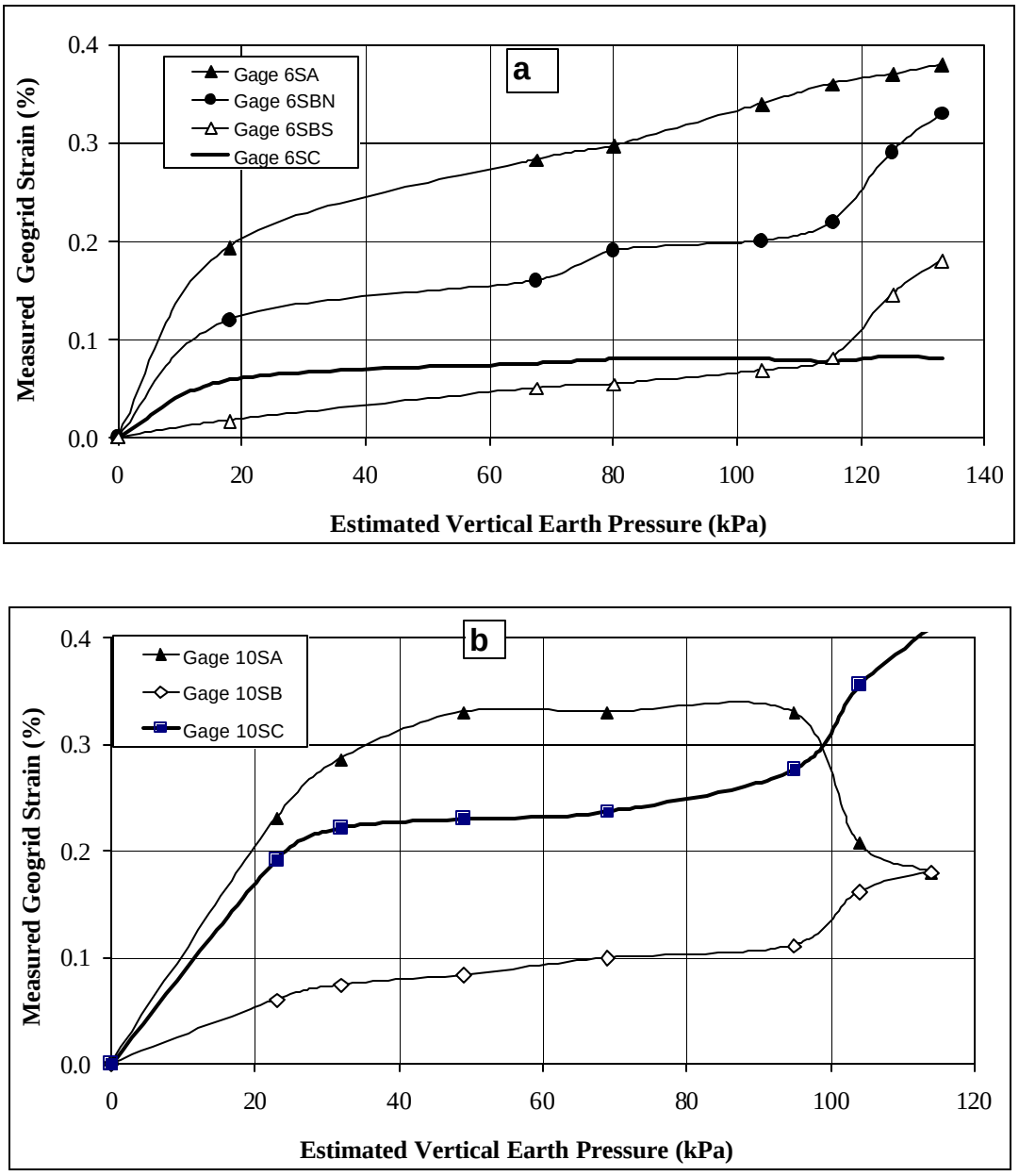

Fig. 5.7. Measured Geogrid Strains vs. Vertical Earth Pressure during all Construction Stages along a) Geogrid Layer 6, and b) Geogrid Layer 10. Note : 3rd data point refers to Stage I Construction, 4th data to Stage II and so on.

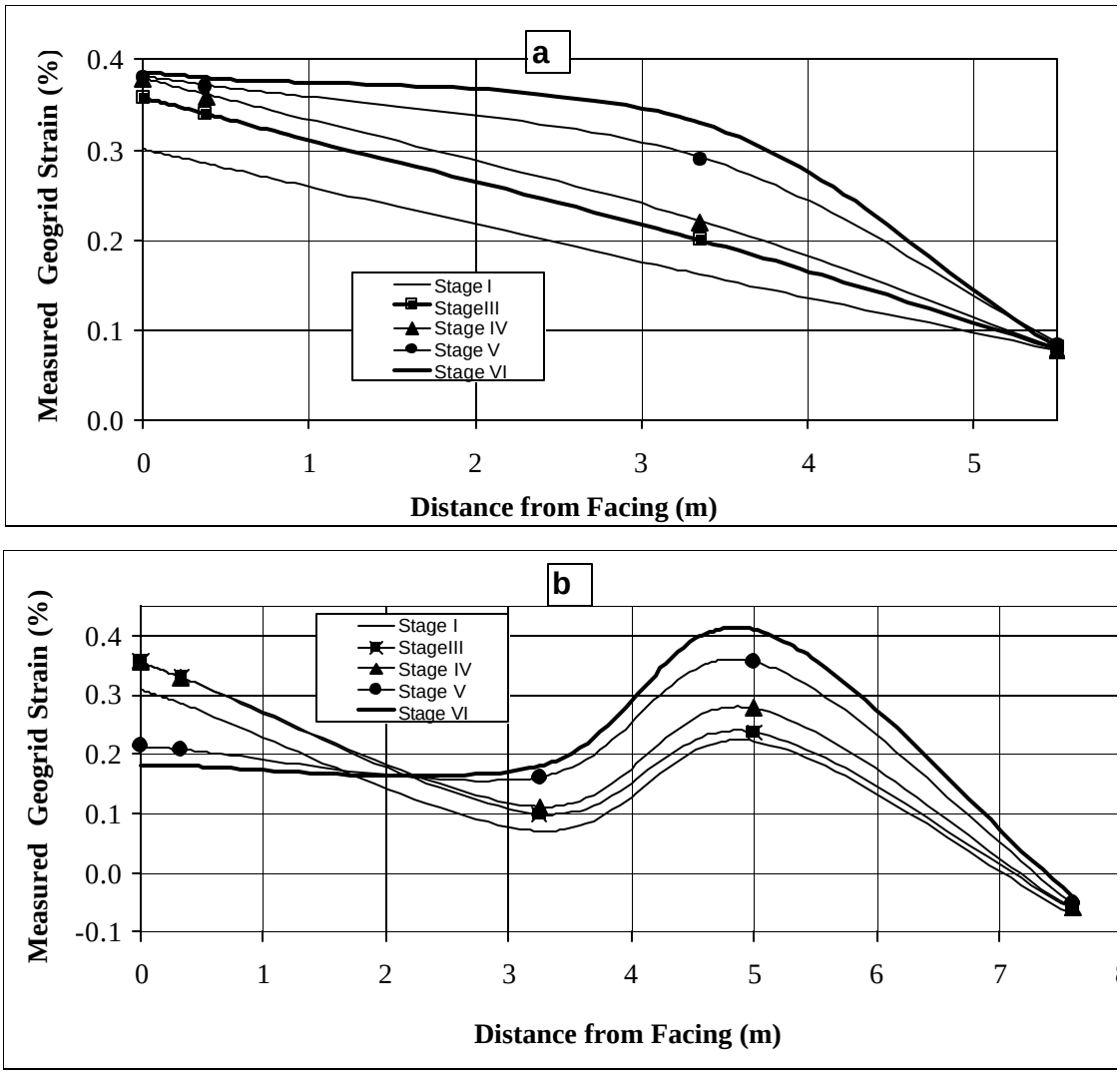

Fig. 5.8. Horizontal Profiles of the Measured Total Geogrid Strains during Various Construction Stages along: a) Geogrid Layer 6, and b) Geogrid Layer 10.

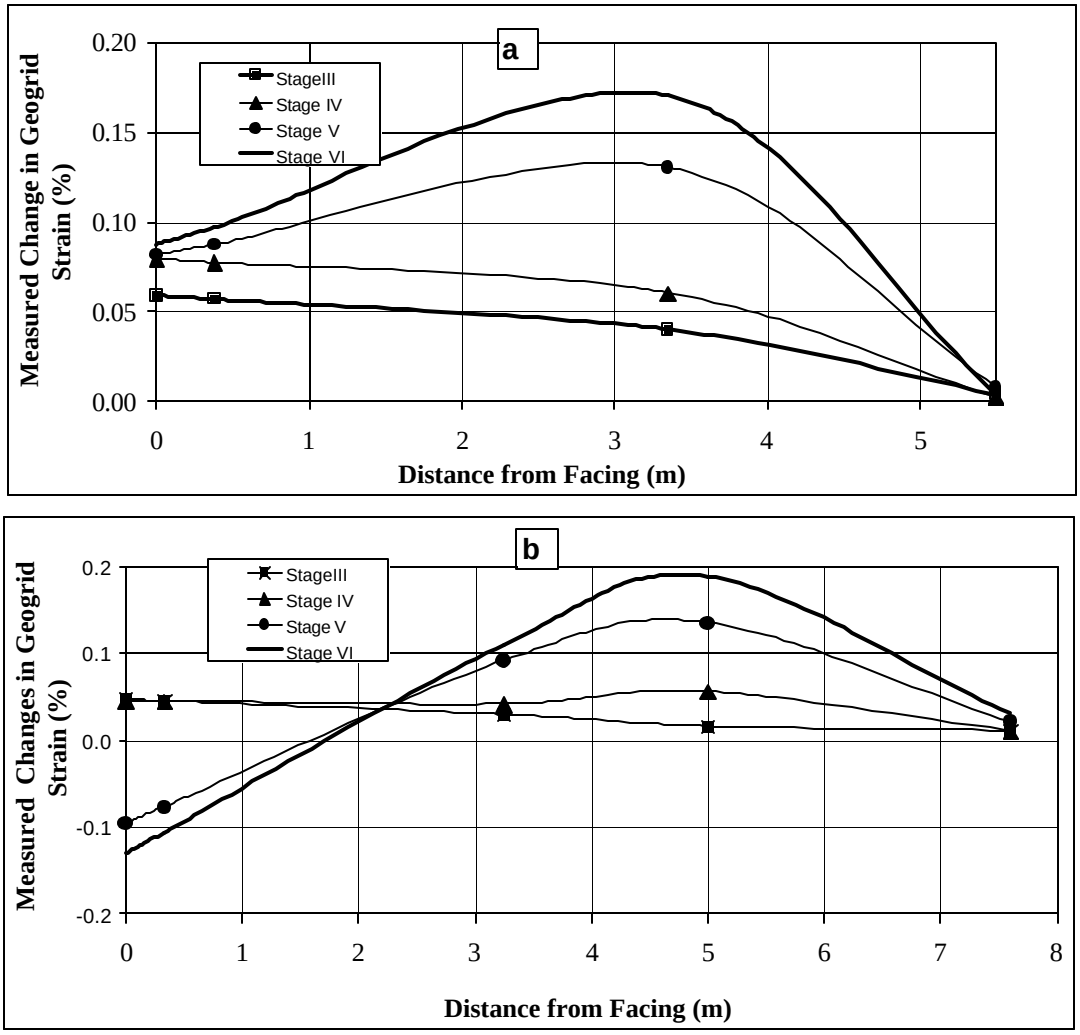

Fig. 5.9. Horizontal Profiles of the Measured Changes in Geogrid Strains during Placement of the Bridge Superstructure (Stages II to VI) from Stage I along: a) Geogrid Layer 6, and b) Geogrid Layer 10.

5.5 Results of Layer 12 Gages during all Construction Stages

Figures 5.10 shows time records for the measured strain data along geogrid layer 12 during all construction stages along Location Lines B and D. Due to the placement and compaction of 0.61 m of backfill over the gages (end of Stage I Construction), very sharp and significant increases in geogrid strains were measured: 0.44% along Location Line B and 0.18% along Location Line D (Figure 5.10). These large changes are questionable and unlikely to be representative of the axial/lateral trains experienced by the geogrid beneath the bridge footing. Large changes in the measured geogrid strains occurred during Stages III (placement of girders) and IV (placement of backfill behind the abutment wall). These changes are larger than those that occurred for geogrid layers 6 and 10 during the same stages, as expected. Very sharp reduction of the tensile geogrid strains was observed during Stage V (0.5% for Gage 12SB and 0.39% for Gage 12SD). This correlates very well with the observed sharp reduction of vertical earth pressures beneath the bridge footing during Stage V (see Chapter 3). Geogrid layer 12 was subjected to increasing tensile strains at Location Lines B and D during the final construction stage (Stage VI, Figure 5.10). Gage 12SD registered final very small compressive strains in the geogrid by the end of the construction stages, which could be attributed to erroneous reference readings.

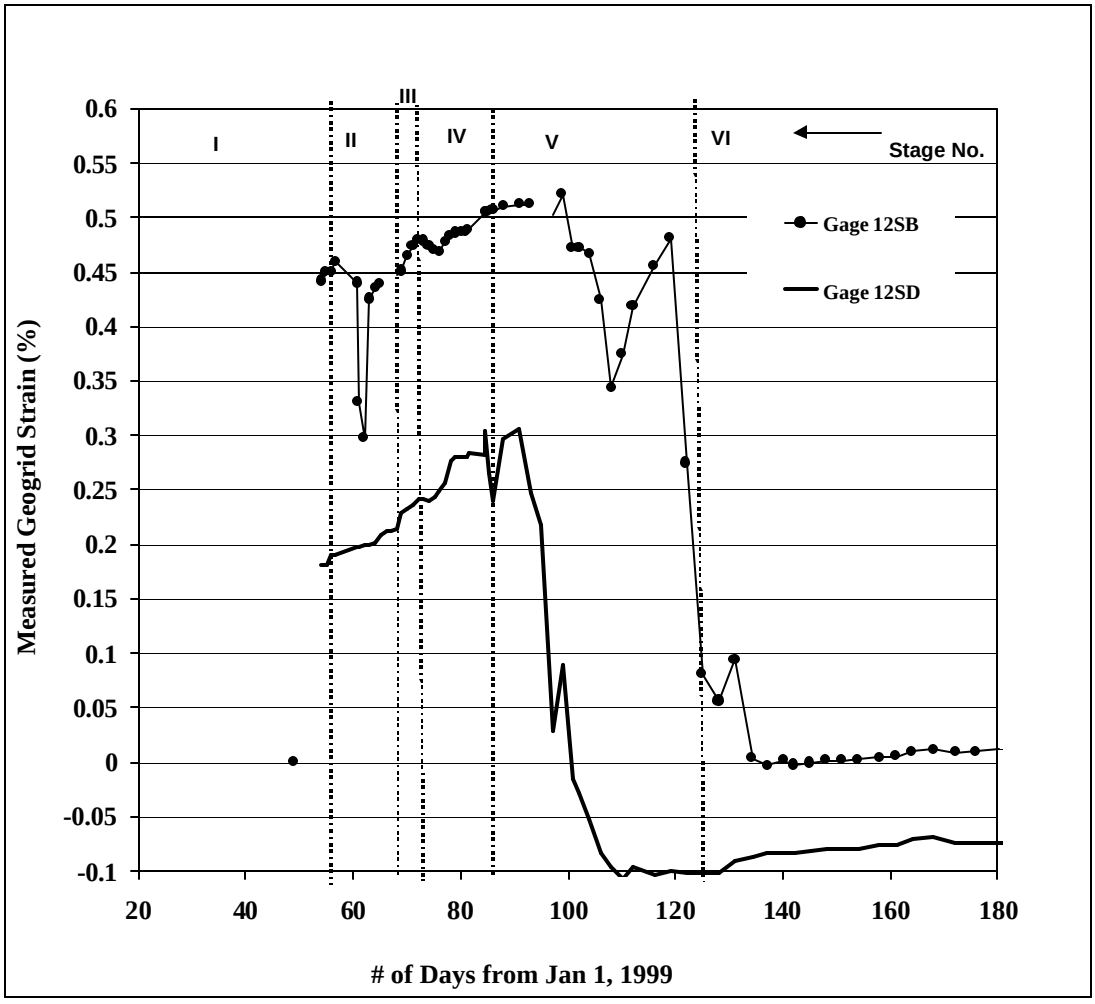

Fig. 5.10. Measured Strains along Geogrid Layer 12 during all Construction Stages.

5.6 Measured Results while the Structure was in Service (Stage VII)

Figures 5.11, 5.12, and 5.13 show time history records of the collected geogrid strain measurements along geogrid layers 6, 10, and 12, respectively, after opening the structure to traffic during Stage VII (days 180 to 545 from Jan. 1., 1999). Gage 10SC exceeded the measuring range during Stage VII and therefore was lost (Figure 5.12). The developed post-construction geogrid tensile strains (Figures 5.11 to 5.13) for all monitored geogrid layers were very small from approximately June 1999 to January 2000 and became negligible from approximately January 2000 to June 2000 (i.e., strains leveled out and remained approximately constant during this period). The geogrid strain measurements compare very favorably with the movements of the facing column of the front GRS wall obtained through

surveying and inclinometer, which showed relatively small (though not negligible) post-construction displacements from June 1999 to January 2000, and negligible post-construction movements from January to June 2000 (see Chapter 2).

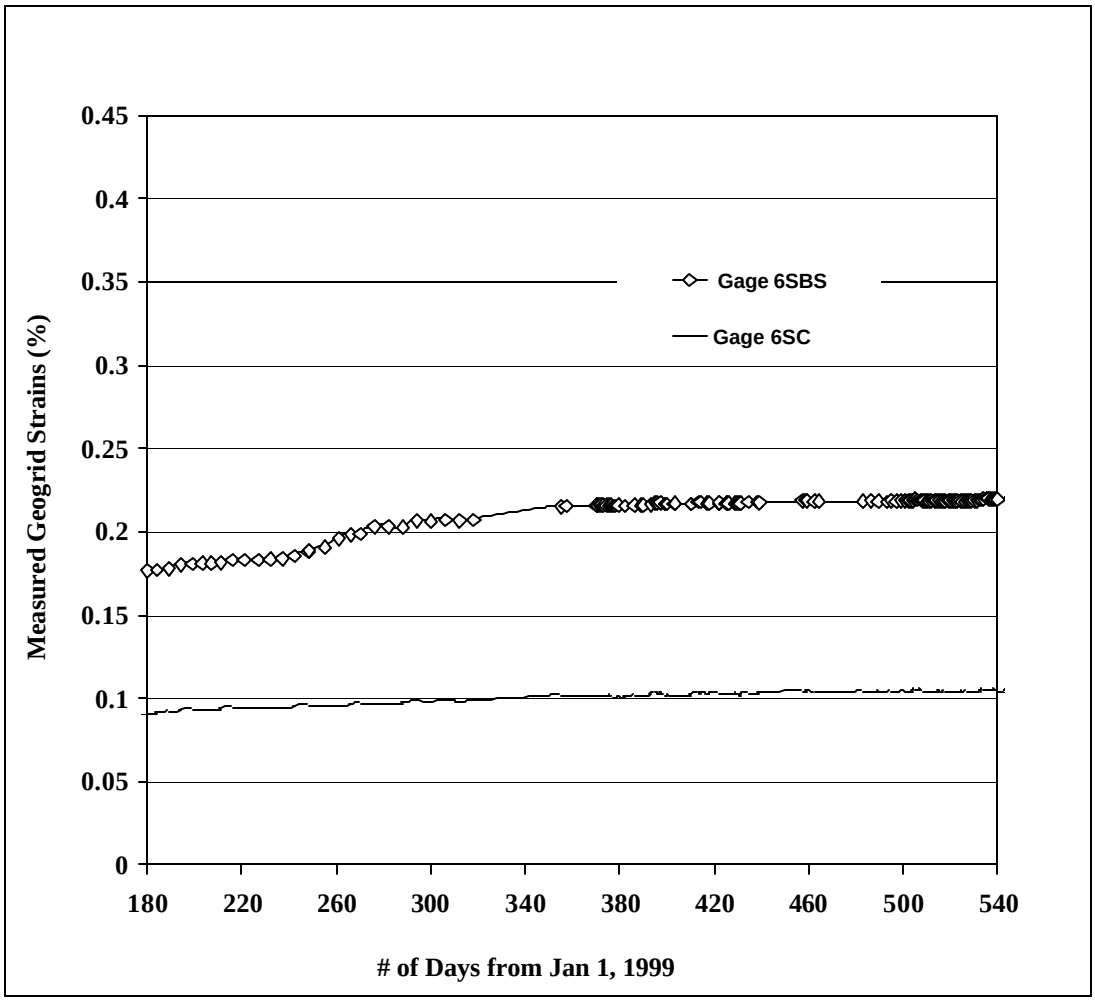

Fig. 5.11. Measured Strains along Geogrid Layer 6 while Structure was in Service (Stage VII).

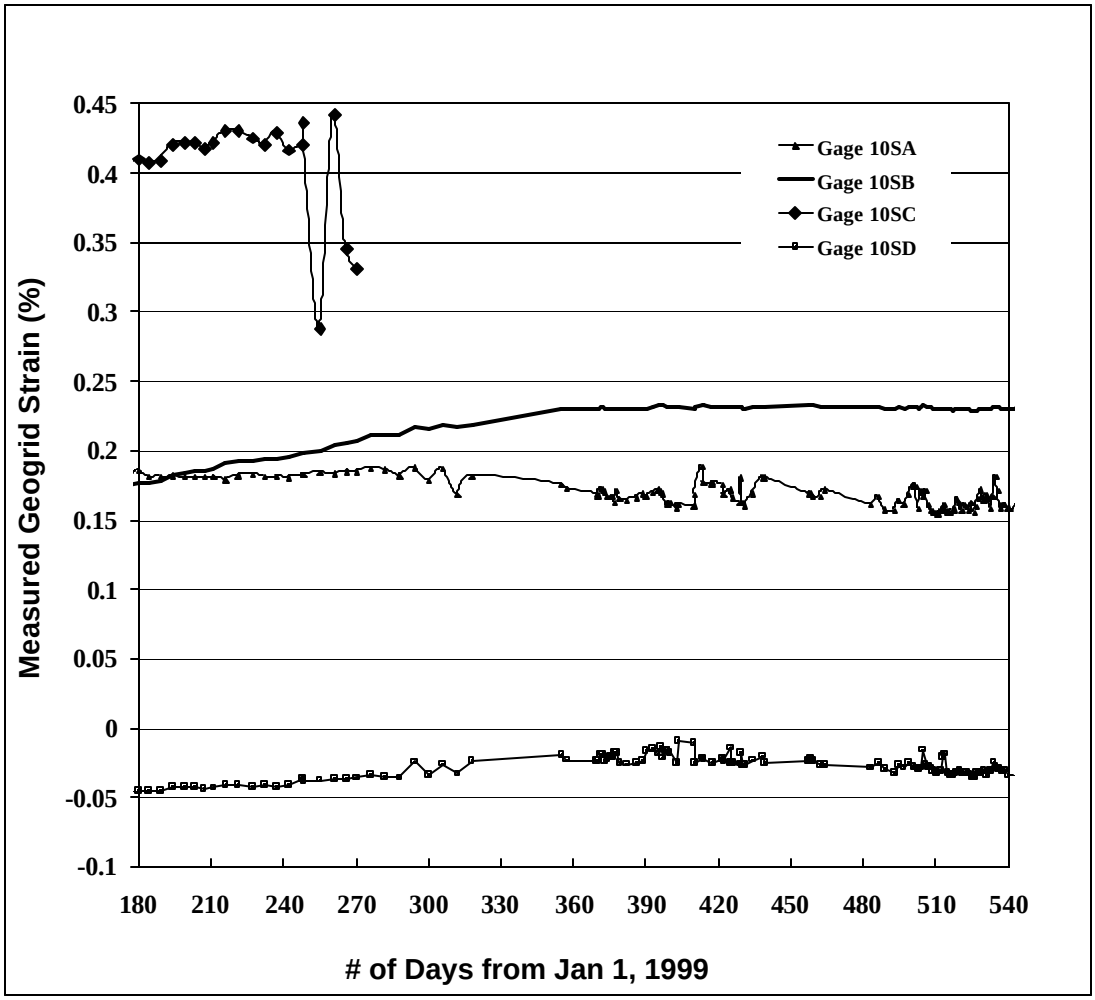

Fig. 5.12. Measured Strains along Geogrid Layer 10 while Structure was in Service.

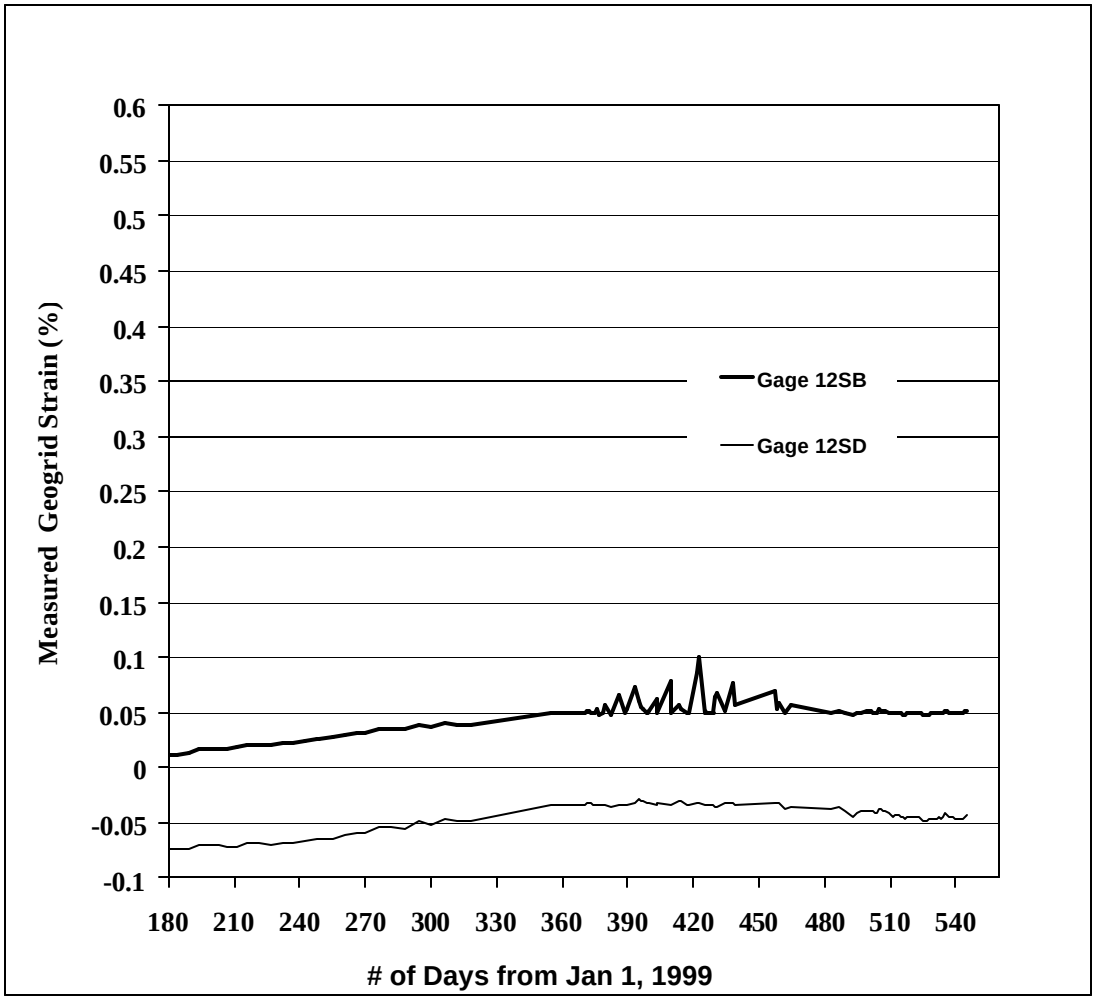

Fig. 5.13. Measured Strains along Geogrid Layer 12 While Structure was in Service.

5.7 Summary and Discussion of the Measured Results

Table 5.1 summarizes the geogrid strains measured from all gages during all construction stages. Table 5.1 also summarizes the geogrid strains developed due to the placement of the bridge superstructure (Stages II to VI), referred to as "changes from Stage I." Table 5.2 summarizes the geogrid strains measured by the end of the construction stages (Stage VI) and after opening the bridge to traffic (Stage VII). The data listed for Stage VII correspond to 6 months and 12 months after opening the bridge structure to traffic. Table 5.2 also summarizes the geogrid strains developed after opening the bridge to traffic, referred to as "changes from Stage VI." The data obtained by extrapolation are highlighted in Tables 5.1 and 5.2. For geogrid layer 2, located in the lower zone of the wall, the highest strains occurred at Location Line A (close to the wall facing) during all construction and post-construction stages (Table 5.1). At Location Lines B and C of geogrid layer 2, Location Line C of geogrid layer 6 (located in the middle zone of the wall), and Location Line D of geogrid layer 10 (located in the upper zone of the wall), very small changes in geogrid tensile strain were measured during all monitored stages (Table 5.1). This is because the lateral boundary of the soil along these locations was fully confined by the adjacent soil, allowing no loads to be supported by the geogrid. The geogrid layers along different locations and depths experienced increasing geogrid tensile strains and forces during and after construction (Tables 5.1 and 5.2). The maximum reliable registered geogrid strain was 0.5% (Table 5.2).

Sharp increases in geogrid tensile strains were measured following placement and compaction of the first two meters of backfill over gages. Strain gages results for geogrid layers 6 and 10 suggest that, out of the total geogrid strains induced during all monitored stages, approximately 50% occurred during placement and compaction of the initial 2 m of backfill (approximately 40 kPa vertical earth pressure) above these geogrid layers (see Figure 5.2 and Tables 5.1 and Table 5.2). This was attributed primarily to the influence of compaction that created large locked-in lateral geogrid and soil strains after removal of the compaction vertical loads. Other factors that might contribute to these large increases in geogrid strains are presence of slack, bending of the geogrid reinforcement and non-stable or erroneous reference reading (reference reading). To eliminate/alleviate these error causes, it is suggested to take

the reference readings for geogrid strain data after approximately 0.4 m of backfill is placed and compacted.

During Stages II to VI, the GRS system along geogrid layers 6 and 10 responded with comparatively small deformations and strains to the increasing vertical earth pressures. A possible reason for this behavior is the influence of compaction experienced in the previous stage. An additional potential justification is the fact that Construction Stages II to IV of Section 800 took place during the winter season. Buttry et al. (1996) reported a comparatively more rigid behavior for a GRS structure during the winter season (see Section 1.5.2). For geogrid layers 6 and 10, the highest strains occurred close to the wall facing during Construction Stages I through IV. This could be attributed to the relatively stiff connection between the facing and geogrid reinforcements during these stages and rigid behavior of the wall system (Section 1.5.3). Beneath the bridge footing, changes in the measured geogrid strains during Stages II to VI were larger than those that occurred for layers 6 and 10. This could be a sign of comparatively larger lateral movements beneath the bridge footing, resulting in relatively larger mobilization of the soil friction resistance and tensile resistance of the geogrid reinforcements.

During Stages V and VI, the GRS system along layers 6 and 10 responded with comparatively large strains and displacements to the increasing level of applied vertical earth pressures. Thawing and wetting of the backfill, as well as disappearance of the compaction influence, may have led to softening of the backfill during these stages (see observations reported by Buttry et al., 1996 in Section 1.5.2). Most of the geogrid tensile straining of layers 6 and 10 occurred inside the interior portion of the reinforced soil mass along Location Line B for layer 6 and along Location Line C for layer 10, where measured geogrid strains were increasing at a comparatively very high rate The stretching movement of the reinforced soil mass at these locations allowed for more of the lateral earth pressure to be supported by the geogrid reinforcements at these locations.

The geogrid tensile strains dropped during Stage V at locations behind the wall facing along geogrid layer 10 and beneath the bridge footing along Location Lines B and D. This is a sign of the reinforced soil mass subjected to lateral compressive loads at these locations that reduced the geogrid tensile loads. This response is strongly correlated with the measured vertical and lateral earth pressures from

other gages, suggesting it is reliable. This response could also be attributed to the lateral movement of the reinforced soil mass and possible settlement and rotation of the bridge footing relative to the more rigid wall facing during Stage V. This movement, most likely, led to the redistribution (increase and decrease) of geogrid tensile loads and vertical earth pressure loads in the reinforced soil mass.

The developed post-construction (1 year) geogrid tensile strains were very small (0 to 0.09%, see Table 5.2) and become negligible from approximately January 2000 to June 2000.

5.8 Consistency of the Measured Geogrid Strain Data

More research is needed to explain the reduction of geogrid tensile strain data and vertical earth pressure beneath the bridge footing that occurred during Stage V. Also, there is no measured geogrid strain data along Location Lines A and C beneath the bridge footing so that a complete picture of the geogrid strain distribution beneath the bridge footing could be obtained. For these reasons, the measured lateral strain data along geogrid layer 12 will not be analyzed further.

Previous sections concluded that the measured changes in lateral strains of geogrid layers 6 and 10 correlate very well with the applied loads and the measured response from pressure cells employed to measure vertical and lateral earth pressures. The geogrid strain measurements compare very favorably with the movements of the facing column of the front GRS wall obtained through surveying and inclinometer and show excellent agreement with the movements obtained after opening the structure to traffic (see Chapter 2). Based on the above discussion, it is fair to conclude that the measured results for the changes in geogrid lateral strains for layers 6 and 10 are consistent and representative of the actual response. Therefore, these data are found appropriate for comparison with the assumed design values.

Table 5.1: Measured Geogrid Strains (%) during all Construction Stages.

Stage #	I	II		III		IV		V		VI	
		Ch. = Change from Stage I (Wall construction) Values									
Gage #		Ch.	Total	Ch.	Total	Ch.	Total	Ch.	Total	Ch.	Total
Layer 2 Gages											
2SA	(0.24)										
2SB	0.06	0	0.06	0	0.06	0	0.06	0.02	0.08	0.02	0.08
2SC	0.01	0	0.01	0	0.01	0	0.01	0	0.01	0	0.01
Layer 6 Gages											
6SA	0.28	0.02	0.3	0.06	0.34	(0.08)	(0.36)	0.09	0.37	0.1	0.38
6SBN	0.16	0.03	0.19	0.04	0.20	0.06	0.22	0.13	0.29	0.17	0.33
6SBS	0.05	0.01	0.06	0.02	0.07	0.03	0.08	0.1	0.15	0.13	0.18
6SC	0.08	0	0.08	0	0.08	0	0.08	0	0.08	0	0.08
Layer 10 Gages											
10SA	0.29	0.04	0.33	0.04	0.33	0.04	0.33	-.08	0.21	-.11	0.18
10SB	0.07	0.01	0.08	0.03	0.10	0.04	0.11	0.09	0.16	0.11	0.18
10SC	0.22	0.01	0.23	0.02	0.24	0.06	0.28	0.14	0.36	0.19	0.41
10SD	-.07	0	-.07	0.01	-.06	0.01	-.06	0.02	-.05	0.03	-.04
Layer 12 Gages											
12SB	0.44	0	0.44	0.14	0.58	0.18	0.62	-.33	0.11	-.32	0.12
12SD	0.18	0.02	0.20	0.06	0.24	0.11	0.29	-.28	-.10	-.25	-.07

Data between parenthesis are for missing data estimated with extrapolation

Table 5.2: Measured Geogrid Strains (%) while Structure was in Service.

Monitored Stage #	End of Construction (Stage VI)	While Structure in Service (Stage VII)			
		After 6 months		After 12 months	
		Change from Stage VI	Total	Change from Stage VI	Total
Gage #	**Layer 6 Gages**				
6SA	0.38	(0.02)	(0.40)	(0.02)	(0.40)
6SBN	0.33	(0.04)	(0.37)	(0.04)	(0.37)
6SBS	0.18	0.04	0.22	0.04	0.22
6SC	0.08	0.02	0.10	0.03	0.11
	Layer 10 Gages				
10SA	0.18	-0.01	0.17	-0.01	0.17
10SB	0.18	0.05	0.23	0.05	0.23
10SC	0.41	(0.09)	(0.50)	(0.09)	(0.50)
10SD	-0.04	0.03	-0.01	0.01	-0.03
	Layer 12 Gages				
12SB	0.12	0.05	0.17	0.04	0.16
12SD	-0.07	0.04	-.03	0.03	-.04

Note: Data between parenthesis are for missing data estimated with extrapolation

5.9 Internal Stability Analysis of the Front GRS Wall

The analysis of the measured geogrid strain data requires the determination of the value and location of the maximum tensile forces in each geogrid layer to gain insight into the potential breakage of geogrid reinforcements. The maximum measured geogrid tensile strains across geogrid layers 6 and 10 at different construction stages were used to estimate the maximum geogrid tensile forces. The analysis also requires the determination of the connection forces between blocks and geogrid layer to gain insight in the potential breakage of connections. The geogrid strains at the rear side of the wall facing for geogrid layers 6 and 10 at different construction stages were used to estimate the connection forces between the blocks and geogrid. The geogrid tensile loads were obtained directly from the load-strain curve measured for UX 6 Tensar geogrid using ASTM D4595 method. Neglecting the time-dependent response of the geogrid or creep in estimating the geogrid loads will be validated in the next section. For the strain range measured in our study (less than 1%) the load-strain curve was linear and the applied geogrid tensile force was 2000 kN/m @1% strain.

5.9.1 Tensile Forces in the Geogrid Layers and Connections

Results for the maximum tensile forces and connection forces along geogrid layers 6 and 10 versus the applied vertical earth pressure on these layers during different construction stages are shown in Figures 5.14a and 5.14b. Predictions for the maximum tensile forces and connection forces in geogrid layers 6 and 10 as given in AASHTO 5.8.4.1C (using Equations 1.3 and 1.5) are also shown in Figure 5.14. If AASHTO predictions are reasonable, all measured curves shown in Figure 5.14 should be close to the AASHTO curve. Tables 5.3 and 5.4 summarize the measured maximum geogrid axial tensile forces and connection forces, respectively, by the end of the construction stages and 12 months after opening the bridge to traffic, along with the estimated values from the design (Equations 1.3 and 1.5). The ratio (%) of the measured geogrid maximum tensile forces and connection forces to the AASHTO estimated values are also shown in Tables 5.3 and 5.4. The results of Figure 5.14 and Tables 5.3 and 5.4 suggest that:

- The design procedure did not account for the compaction-induced stresses developed in the geogrid reinforcements and connections during interim construction stages of the front wall. The geogrid maximum tensile forces and connection forces measured at any horizontal level during placement and compaction of 1 m of backfill over that level are up to two times of those estimated in the design (Figure 5.14).

- Figure 5.14a and Table 5.3 show that the design procedure overestimated the required maximum geogrid tensile forces measured by the end of the construction stages. The measured maximum geogrid tensile forces range from 43% to 57% of the forces estimated in the design. This could be attributed to true shear strength of the backfill being higher than assumed in the design. It is also possible that the facing supported some of the applied lateral earth pressure, which was not accounted for in the design.

- Figure 5.14b and Table 5.4 show that the design procedure overestimated the required connection forces measured at the end of the construction stages. The measured connection forces range from 19% to 47% of the connection loads estimated in the design. The difference could be attributed to

two factors: (1) actual shear strength of the backfill was higher than assumed in the design, and (2) relatively flexible facing and connection that allowed for comparatively larger mobilization of the friction resistance of the backfill and the support of more lateral earth pressure by reinforcements, thus taking more of the lateral earth pressure off the facing and connections. Results of Table 5.4 suggest that the lateral boundary of the wall yielded more at geogrid layer 10 than at layer 6. The more flexible connection at layer 10 could be attributed to smaller vertical loads (smaller restrain) acting on the block facing of layer 10.

- The post-construction geogrid tensile strains may be developed due to traffic loads or/and creep. If the post-construction geogrid strains were developed due to traffic loads only (not from creep), then the developed maximum geogrid tensile forces while the structure was in service increased by 1.8 kN/m for layer 10 and 0.4 kN/m for layer 6 (Table 5.3). These measured forces range from 16% to 57% of the reinforcement loads estimated in design. Hence, the design overestimated the reinforcement loads due to traffic load by almost two times (assuming no creep-induced strains). If the post-construction geogrid strains were developed due to creep (no traffic load), they are very small (zero to 0.09%) when compared to the creep limit for the geogrid reinforcement, and they leveled out and become constant from January to June 2000 (long-term creep deformations are negligible). However, CDOT design procedure employs a creep reduction factor of 2.7 to determine the geogrid long-term design strength from the geogrid ultimate strength. This is a very high reduction factor that should be adjusted or estimated more rationally.

Table 5.3: The Design and Measured Maximum Geogrid Tensile Forces.

Geogrid Layer #	Estimated Max. Geogrid Tensile Force (kN/m)	Measured Max. Geogrid Tensile Force (kN/m)	Percentage Ratio of Measured to Estimated
End of Construction			
6	16.5	7.7	47%
10	14.3	8.2	57%
After Opening Bridge to Traffic			
6	19.0	8.1	43%
10	17.5	10	57%

Table 5.4: Design and Measured Connection Forces.

Geogrid Layer #	Estimated Connection Force (kN/m)	Measured Connection Force (kN/m)	Percentage Ratio of Measured to Estimated
End of Construction			
6	16.5	7.7	47%
10	14.3	3.6	25
After Opening Bridge to Traffic			
6	19.0	8.1	43%
10	17.5	3.3	19

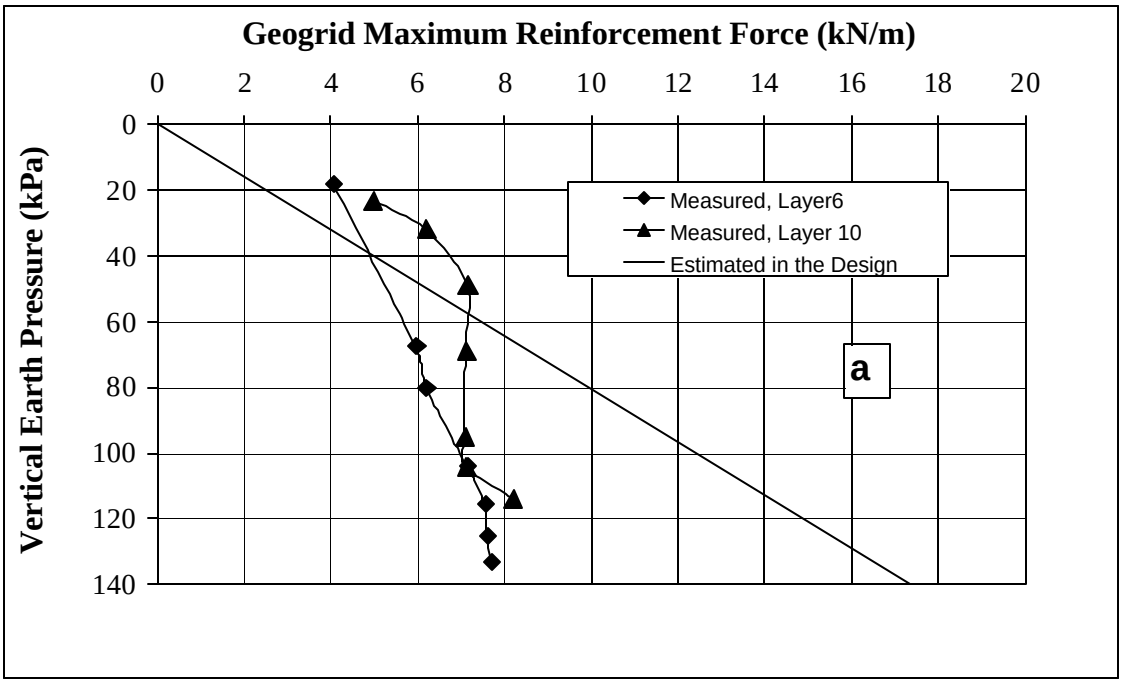

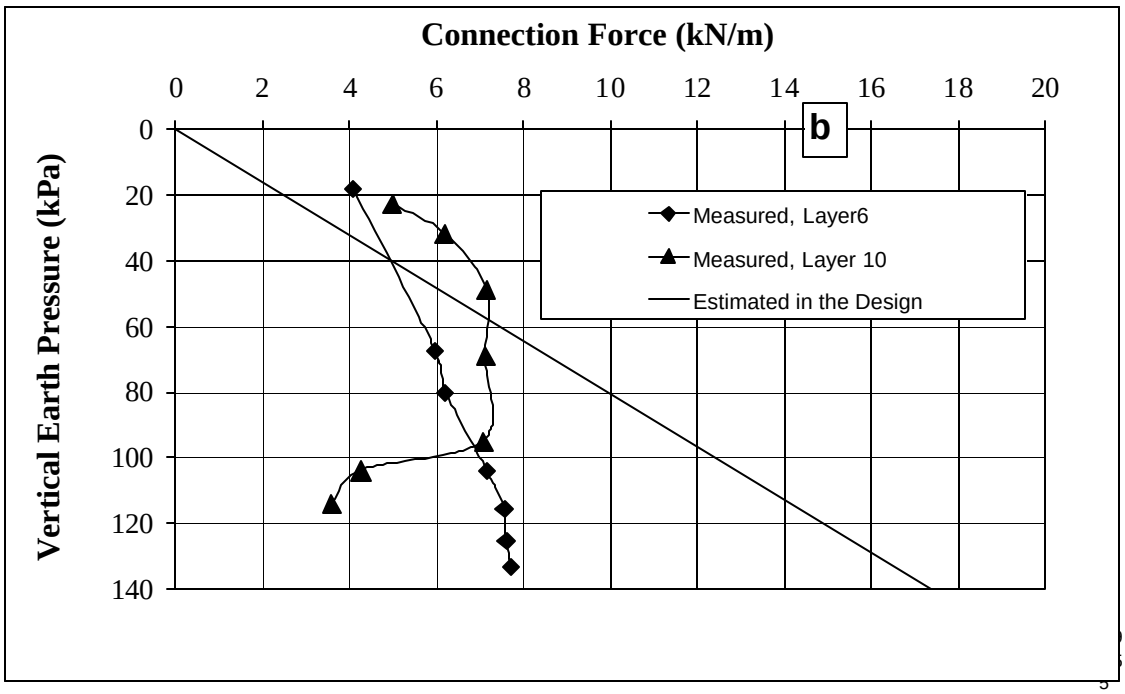

Fig. 5.14. Measured and AASHTO Predicted Results along Geogrid Layers 6 and 10: a) Maximum Geogrid Tensile Forces, and b) Connection Forces.

5.9.2 Reinforcements Internal Stability with Respect to Pullout Failure

Reinforcement stability requires that the reinforcement pullout resistance be larger than the geogrid applied maximum tensile force. Information on the measured geogrid maximum tensile forces was presented in the previous section. During construction, the comparatively large compaction-induced tensile geogrid forces might exceed the relatively low pullout capacity of the upper geogrid layers.

Location of the maximum tensile force line is needed to estimate the embedment length of the reinforcement in the resistance zone to reinforcement pullout failure. The reinforcement pullout resistance is linearly related to the reinforcement embedment length. Location of the potential failure surface is assumed by AASHTO to coincide with the maximum tensile forces line. The location of this line for GRS walls, with no surcharge load and constructed with extensible reinforcements is shown in Figure 5.15 (Elias and Christopher, 1997). For a structure like the Founders/Meadows structure, where a reinforced soil wall directly supports a high surcharge load, AASHTO's 1996 specifications recommend the embedment length beneath the bridge footing to be the length of reinforcements beyond the back edge of the bridge footing.

The locations of the maximum geogrid strains across geogrid layers 2, 6, and 10 were employed to determine the location of the maximum tensile forces line (i.e., the locus of the maximum tensile force in each reinforcement layer). For geogrid layer 6, the obtained maximum geogrid strain by the end of Stage VII (see Table 5.1) at Location Line A (0.40%) was very close to that at Location Line B (0.37%). However, the increases in geogrid tensile strains due to the placement of the bridge superstructure (more reliable strains are obtained in this range) were higher at Location Line B (0.17%) than at Location Line A (0.097%, see Table 5.1). Therefore, Location Line B was selected as the location where the maximum tensile strains occurred for layer 6. The results, as summarized in Figure 5.15, suggest that the maximum tension line can be assumed to be bilinear. It starts at the toe of the wall and extends through a straight line to the back edge of the bridge footing at the mid height of the wall, and from there extends vertically to the back edge of the bridge footing. This finding is in support of AASHTO recommendation presented before.

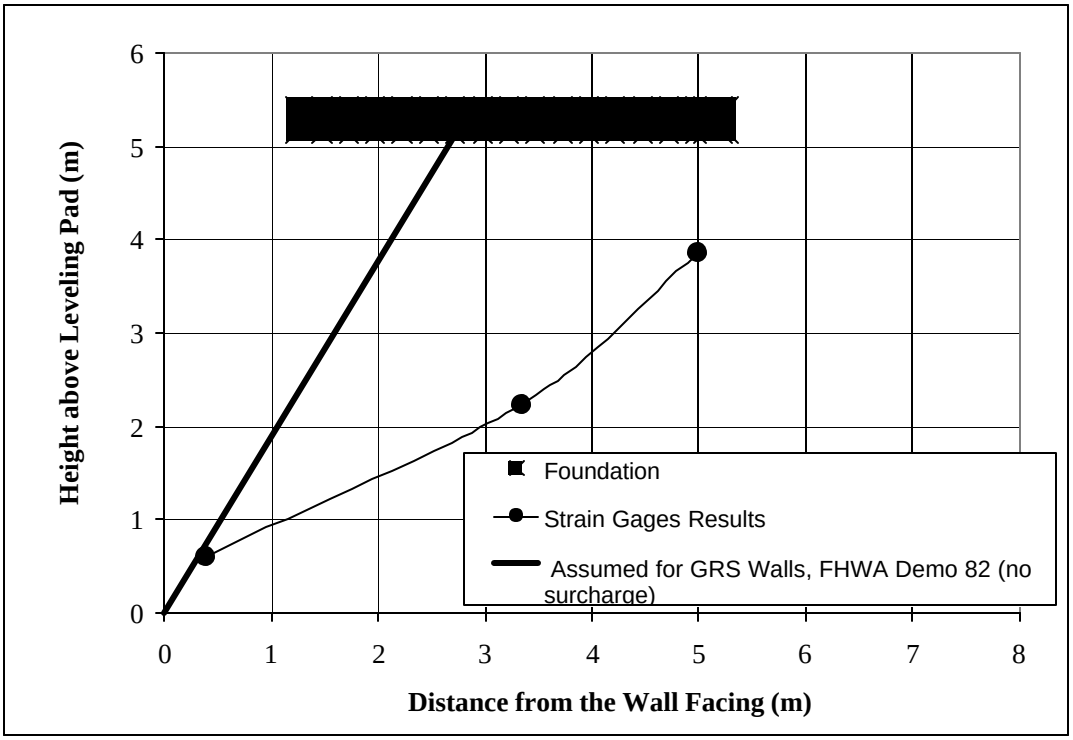

Fig. 5.15. Measured Location of the Maximum Tension Line (i.e., Potential Failure Line), Obtained from the Measured Geogrid Strain Data.

6. SUMMARY AND ASSESSMENT OF THE DESIGN AND PERFORMANCE OF THE FRONT GRS WALL

6.1 Overview

CDOT successfully completed the construction of the new Founders/Meadows Bridge in June of 1999. The Founders/Meadows structure is the first major bridge in the United States built on footings supported directly by a geosynthetic-reinforced soil system, eliminating the use of traditional deep foundations (piles and caissons) altogether. Figure 6.1 shows a typical cross-section through the "front GRS wall" and "abutment GRS wall," illustrating that the front GRS wall provides direct support for the bridge and embankment behind the abutment wall. A key element in the design was the need to support the high concentrated loads from the bridge footing and to alleviate the bridge bump problem. In addition, this kind of bridge support allows for construction in stages and comparatively smaller construction working areas. The Founders/Meadows Bridge was considered experimental, and comprehensive material testing, instrumentation, and monitoring programs were incorporated into the construction operations. These programs would allow assessment of the overall structure performance and evaluation of the suitability of CDOT and AASHTO design procedures and assumptions for the use of the front GRS wall as a measure to support the bridge footings, and, in conjunction with the abutment GRS wall, to alleviate the bridge bump problem.

The first report of this study (Abu-Hejleh et al., 2000) presented the design, materials, construction, and instrumentation of the Founders/Meadows structure. This second report presents a summary and analysis of the collected instrumentation data and assessment of the performance and design for the front GRS wall. This wall supports directly the bridge structure and the embankment behind the bridge wall (Figure 6.1). Recommendations for design and construction of future GRS abutments are furnished in the Executive Summary.

The overall instrumentation program was conducted in two phases: Phases I and II, which correspond, respectively, to the construction of the Phase I Structure (from July to December 1998) and Phase II

Structure (from January to June 1999). Instrumented sections 200, 400 (Figure 6.1) are located at the center of Phase I Structure and Section 800 (Figure 6.2) is located at the center of Phase II Structure. These sections were instrumented with survey targets, an inclinometer, and strain gages to measure movements of the facings of the front GRS wall and settlement of the bridge footing along Phase I and Phase II Structures (Figures 6.1 and 6.2). One gage (P2) was placed in the middle zone of the front wall (Figure 6.1) to obtain data for lateral earth pressure against the front wall facing of Section 400. The front GRS wall along Section 800 of the Phase II Structure was heavily instrumented with pressure cells and strain gages (Figure 6.2). Five gages to measure lateral earth pressure against the front wall facing were placed in the middle and upper zones of the front wall facing (Figure 6.2). Gages to measure distributions of vertical earth and geogrid strain were placed along three zones inside the front GRS wall (Figure 6.2): the upper zone of the wall (near the bridge footing, around geogrid layers 12 and 13), the middle zone of the wall (around geogrid layers 6 and 10), and the lower zone (near the base of the wall). These gages were placed along four critical vertical Location Lines (Figure 6.2): vertical Location Line A is very close to the wall facing, vertical Location Line B is close to the centerline of the bridge abutment wall, vertical Location Line C is close to the back edge of the bridge footing, and vertical Location Line D is behind the bridge footing (~7.5 m from the facing). The performance data presented in this report for the front GRS walls were collected during construction of the front GRS wall (Stage I, see Figure 6.1), during placement of the bridge superstructure (Stages II to VI, see Figure 6.1), and while the structure was in service for 18 months (Stage VII).

6.2 Measured Front Wall Response during Construction of the Front Wall

Construction of the front GRS wall went from July 16, 1998 to September 12 (warm season) for the Phase I Structure (Sections 200 and 400), and from January 19, 1999 to February 24, 1999 (cold season) for the Phase II Structure (Section 800). The maximum measured front wall outward displacement induced by wall construction was 12 mm, which corresponds to 0.2 % of the front wall height (Table 2.1). The measured settlement of the leveling pad supporting the front wall facing was approximately 8 mm (Table 2.1).

Measurements for vertical earth pressure inside the reinforced soil mass of Section 800 suggest that compaction induced vertical earth pressures ranging from 20 to 35 kPa (Figure 3.1). During placement and compaction of the first 1 m of backfill over the gages, sharp increases in geogrid strains (Figures 5.1 and 5.2) and lateral earth pressure against the wall facing (Table 4.1, Figure 4.3) were measured by these gages. Ratios of the measured lateral earth pressures to the design estimated values were as high as two. This response was attributed primarily to the influence of compaction that created large geogrid strains and earth pressures against the wall facing. Some or all of the compaction-induced pressures and strains remained locked-in after removal of the compaction vertical loads. Strain gage results for geogrid layers 6 and 10 suggest that, out of the total wall outward displacements and maximum geogrid strains induced during all monitored stages, approximately 50% occurred during placement and compaction of the initial 2 meters of backfill above these geogrid layers (see Figures 5.2 and 2.2, and Tables 2.1, Tables 5.1 and 5.2). The measured tensile strains of geogrid layers 6 and 10 (Section 800) dropped to the values estimated in the design after almost two to three meters of backfill were placed and compacted (Figure 5.14). The ratio between lateral to vertical earth pressure dropped to the ratio estimated in the design (0.31) after one meter of backfill was placed and compacted and it further dropped to a value of 0.11 after almost two meters of backfill were placed and compacted (from Gage P2 in Section 400 shown in Figure 6.1, see Table 6.1).

6.3 Measured Front Wall Response during Placement of the Bridge Superstructure

Monitoring stages (Figure 6.1) include placement of the bridge footing and girders seat (Stage II), placement of girders (Stage III), placement of reinforced backfill behind the abutment wall (Stage IV), placement of the bridge deck (Stage V), and placement of minor structures (Stage VI). These stages were completed on December 16, 1998 for the Phase I Structure (Sections 200 and 400), and on June 30, 1999 for the Phase II Structure (Section 800). The total average vertical contact stress directly underneath the bridge footing by the end of Stage VI was estimated as 115 kPa.

The maximum front wall outward displacement and bridge footing settlement induced by placement of the bridge superstructure were 10 and 13 mm, respectively. These movements correspond, respectively, to 0.17% and 0.29 % of the front wall height (Table 2.1). The measured settlement of the leveling pad supporting the front wall facing was approximately 7 mm (Table 2.1). It was observed that displacements induced in Section 800 were higher than those at Section 400 (Figure 2.3). This was attributed to a different construction season for both sections (summer to fall for Section 400, and winter to spring for Section 800) and a different construction sequence (Stage IV before Stage III for Section 400).

The measured response of the front GRS wall along Section 800 of Phase II Structure during placement of the bridge superstructure during Stages II to IV was significantly different from the measured response during Stage V, as detailed below.

6.3.1 Wall Response along Section 800 during Construction Stages II to IV

During these stages, the front GRS wall system along geogrid layers 6 and 10 (middle zone of the wall, Figure 6.2) responded with comparatively small deformations and strains to the increasing vertical earth pressures (Figures 2.2 and 5.7). A possible reason for this behavior is the influence of compaction experienced in the previous stage. An additional potential justification is the fact that Construction Stages II to IV of Section 800 took place during the winter season. Due to the relatively rigid behavior of the wall system during these stages, the wall facing supported relatively large lateral earth pressures against the wall facing (Table 4.2, Figure 4.4) and the maximum geogrid tensile strains occurred close to the wall facing (Figure 5.8). Along the levels of geogrid layers 6 and 10, there was excellent agreement between the applied and measured average vertical earth pressure during these stages, suggesting no transfer of bridge vertical loads to the wall facing at these levels (Figure 3.15).

Beneath the bridge footing (upper zone of the front wall), changes in the measured geogrid strains during Stages II to IV were larger than those that occurred at geogrid layers 6 and 10 (Table 5.1, Figure 5.10). There was almost 40 kPa difference between the applied and measured average vertical earth pressure in that zone (Figure 3.16). At the level beneath the bridge footing, the measured lateral earth

pressures against the wall facing were negligible (Gage 12H, Table 4.2). It is speculated that the reinforced soil zone beneath the bridge footing experienced significant lateral deformations (as evidenced by large increases of geogrid tensile strains) and settlement during these stages. This movement, most likely, caused the transfer of portion of the applied bridge vertical loads to the relatively more rigid wall facing, and minimized the lateral earth pressure against the wall facing.

6.3.2 Wall Response along Section 800 during Construction Stages V and VI

During these stages, the front GRS wall along layers 6 and 10 responded with comparatively large strains and displacements to the increasing level of applied vertical earth pressures (Figures 2.2 and 5.7). Thawing and wetting of the backfill, as well as disappearance of the compaction influence, may have led to softening of the backfill during these stages. The following additional observations were noticed during Stage V:

- The measured vertical earth pressures directly behind the wall facing dropped sharply at all levels (lower, middle, and upper zones, Figure 3.11 and Table 3.1). The measured lateral earth pressures against the wall facing (Table 4.2, Figure 4.4) and geogrid tensile strains (Table 5.1 and Figure 5.6) dropped for locations close to geogrid layer 10 (close to the upper zone of the wall) and remained approximately constant at locations close to geogrid layer 6 (middle zone of the wall).
- Location Lines B and C of geogrid layers 6 and 10 (the middle, interior portion of the front wall) experienced large increases of vertical earth pressures (Table 3.1) and geogrid tensile strains (Table 5.1). Most of the geogrid tensile straining occurred along vertical Location Line B for geogrid layer 6 and along vertical Location Line C for layer 10. The increase in vertical earth pressure was higher at vertical Location Line B than at C. The difference between the applied and measured average vertical earth pressure was very small (Figure 3.15). This response suggests that the reinforced soil mass between geogrid layers 6 and 10 supported most of the applied loads (i.e., no transfer of load to the wall facing).
- Both the geogrid tensile strains (Figure 5.10 and Table 5.1) and vertical earth pressure beneath the bridge footing (Figure 3.9 and Table 3.1) dropped sharply during Stage V. The difference between the applied and measured average vertical earth pressure beneath the bridge footing increased from

40 kPa to 60 kPa (Figure 3.16). At the level beneath the bridge footing, the measured lateral earth pressure against the wall facing remained negligible (Gage 12H, Table 4.2). It is speculated that some of the applied bridge loads at the horizontal level directly below the bridge footing were transferred to the wall facing.

By the end of all construction stages (Stage VI), the measured vertical earth pressures (Table 3.1) and geogrid tensile strains (Table 5.1) behind the wall facing (vertical Location Line A), and the lateral earth pressure against the wall facing (Table 4.2) became very close to, or even less, than the values measured by the end of Stage I Construction. In other words, the measured changes in loads behind the wall facing due to the placement of the bridge superstructure were very small. Geogrid strains were highest at vertical Location Line C for geogrid layer 10, at vertical Location Line B for layer 6 (see Figures 5.8 and 5.9), and behind the wall facing for geogrid layer 2 (Figure 5.3). The distribution of vertical earth pressures directly beneath the bridge footing was almost uniform (Figure 3.10). At other levels (geogrid layers 0, 6, and 10), the vertical earth pressure distribution differed significantly from location to location (Figures 3.3, 3.5, and 3.7 and Table 3.1). The lowest vertical earth pressure occurred close to the wall facing and the highest vertical earth pressure occurred along vertical Location Line B, the centerline of the bridge abutment. This distribution was approximately symmetrical around the center of the reinforced soil zone (~3.75 m from rear side of the facing). Ratios between measured lateral earth pressures against the wall facing in the upper half of the wall and estimated vertical earth pressure range from 0.04 to 0.11, way below the value estimated in the design (0.31). The maximum registered geogrid tensile strain by the end of all construction stages was 0.41% (Table 5.1), almost half the value expected in the design.

It can be concluded that the comparatively large movements of the front GRS structure experienced during Stage V significantly influenced the distribution of stresses and strains inside the reinforced soil mass of the front wall, especially close to the wall facing and directly beneath the bridge footing. This movement mobilized the backfill shear resistance and reinforcement tensile resistance (see Section 1.5.3), and led to:

- Reduction of the comparatively large: vertical earth pressure developed behind the facing, lateral earth pressure against the wall facing, and connection loads between reinforcement and blocks.
- Transfer of the large vertical earth pressures and reinforcement loads developed behind the wall facing to locations deeper inside the reinforced soil zone (except for the zone beneath the bridge footing).
- For the uppermost zone of the front wall below the bridge footing, it is speculated that a large portion of the applied bridge loads were transferred to the wall facing due to differential settlement between the reinforced backfill and the more rigid wall facing.

6.4 Measured Front Wall Response while the Structure was in Service

The post-construction stage (Stage VII) was completed on June 2000 (lasted 1 year for Phase II Structure and 18 months for Phase I Structure). The total average vertical contact stress directly underneath the bridge footing during this stage was estimated as 150 kPa.

The maximum registered front wall outward displacement and bridge footing settlement induced while the bridge was in service (Stage VII) were 13 and 10 mm, respectively. These movements correspond, respectively, to 0.22% and 0.17% of the front wall height (Table 2.1). The measured settlement of the leveling pad supporting the front wall facing was approximately 5 mm (Table 2.1). From the time of opening the bridge to traffic (December 1998 for the Phase I Structure and June 1999 for the Phase II Structure) until January 2000, the structure showed continued movements (Table 2.1 and Figure 2.4). However, from January 2000 to June of 2000, the measured movement results along all sections from different techniques suggest that the front GRS wall and bridge footing experienced negligible movements (Table 2.1 and Figure 2.4). The developed post-construction geogrid tensile strains for all monitored geogrid layers along Section 800 were very small from approximately June 1999 to January 2000 (0 to 0.09%, Table 5.2) and became negligible from approximately January 2000 to June 2000 (Figures 5.11, 5.12 and 5.13). For Section 800 of Phase II Structure, the monitored influence of traffic loads on the vertical loading of the reinforced soil mass (Table 3.2 and Figure 3.13) and horizontal loading of the wall facing (Figure 4.6, Tables 3.1 and 3.2) was very small.

6.5 Assessment of the Performance and Design of the Front GRS Wall

The measured changes in the vertical earth pressure in the reinforced soil mass and lateral earth pressure against the wall facing while the structure was in service were much lower than the values estimated in the design. Live loads due to traffic loading account for a scenario such as a line of fully loaded trucks suddenly stopping on top of the bridge during a traffic jam. If this scenario happened during Stage VII, our instruments certainly did not capture it. These performance data cannot be used to investigate design assumptions regarding the effect of live loads due to traffic. It was demonstrated in this study that all measured performance data for the structure during the construction stages are consistent and representative of the overall actual response experienced by the front GRS wall. The performance data that will be utilized in the assessment of the design and performance of the front GRS wall are:

- The vertical earth pressures in the reinforced soil mass and lateral earth pressures against the wall facing measured by the end of construction stages (Stage VI). These data were mostly collected along Section 800.
- The measured geogrid tensile strains (Section 800) and facing movement (Sections 200, 400, and 800) measured by the end of construction (Stage VI) and by the end of the post-construction stage (Stage VII, while the structure was in service).

Assessment of the external stability of the front GRS structure (overturning, sliding, and bearing capacity) assumed the reinforced soil zone to extend from the facing to vertical Location Line D, located approximately 7.5 m from the facing. Connection loads between reinforcements and facing blocks were obtained from geogrid strain measurements at the facing.

6.5.1 Movements of the Front GRS Wall

- The measured maximum outward displacement of the front GRS wall and settlement of the bridge footing due to placement of the bridge superstructure were, respectively, 11 mm (20 mm expected in the design) and 13 mm (25 mm expected in the design).
- The maximum *total* settlement recorded for the bridge footing was 23 mm, which is roughly a third of the AASHTO specified maximum tolerable *differential* settlement (70 mm) and a fourth of the

value assigned in the design for adequate clearance between I-25 and the bottom of the bridge superstructure (100 mm).

- The long-term outward displacement of the front wall facing and settlement of the bridge footing ceased from January to June 2000 (Table 2.1).

6.5.2 Internal Stability of the Reinforced Soil Mass

- The maximum tension line can be assumed to be bilinear. It starts at the toe of the wall and extends through a straight line to the back edge of the bridge footing at the mid height of the wall, and from there extends vertically to the back edge of the bridge footing (Figure 5.15).
- The design procedure provides a good estimation of the average vertical earth pressure acting within the potential failure zone. Along the potential failure line, the design underestimates the vertical earth pressures at locations beneath the bridge footing by approximately 20%, and overestimates them at locations close to the toe of the wall by approximately 33% (Figure 3.17).
- The design procedure did not account for the compaction-induced stresses developed in the geogrid reinforcements during interim construction stages of the front wall. The geogrid maximum tensile forces measured during placement and compaction of 1 meter of backfill are up to twice those estimated in the design (Figure 5.14a and Figure 5.2). During construction, the comparatively large compaction-induced tensile geogrid forces might exceed the relatively low pullout capacity of the upper geogrid layers. In order to anchor the reinforcements against potential reinforcement pullout during the compaction operations, it is suggested to drive steel bars through the back of the reinforcements into the backfill.
- The design procedure overestimated the maximum geogrid tensile forces for geogrid layers 6 and 10 measured after construction was completed (Figure 5.14a and Table 5.3). The measured maximum geogrid tensile forces range from 43% to 57% of the design values. This could be attributed to the fact that actual backfill shear strength is higher than the assumed value in the design. It is also possible that the facing supported some of the applied lateral earth pressure, which was not accounted for in the design.
- The post-construction geogrid tensile strains may be developed due to traffic loads or/and creep. If the post-construction geogrid strains were developed due to traffic loads only (not from creep), then

the measured maximum geogrid forces ranges from 16% to 57% of the reinforcement loads estimated in the design (Table 5.3). Hence, the design overestimated the reinforcement loads due to traffic load by almost two times (assuming no creep-induced strains). If the post-construction geogrid strains were developed due to creep (not from traffic loads), these strains are relatively very small (zero to 0.09%, Table 5.2), and they leveled out and became constant (Figures 5.11, 5.12, and 5.13) from January to June 2000 (i.e., long-term creep deformations were negligible). However, CDOT design procedure employs a very large creep reduction factor of 2.7 to determine the geogrid long-term design strength from the geogrid ultimate strength. The small post-construction creep geogrid strain could be attributed to two factors: 1) confinement of geogrid materials in well-compacted granular material that has no creep potential; and 2) the relatively small tensile loads in the geogrid reinforcements under working load conditions (maximum geogrid strain of 0.43% measured by the end of the construction stages).

6.5.3 Internal Stability of Connections and Wall Facing

- The design procedure did not account for the compaction-induced stresses developed at the connections and against the wall facing during interim construction stages of the front wall. The connection loads (Figure 5.14b) and lateral earth pressure against the wall facing (Figure 4.1 and Table 4.1) measured during placement and compaction of 1 meter of backfill are up to twice those estimated in the design. For wall facings with low connection strength or low interface shear strength, the compaction loads might cause excessive deformation or improper alignment to the facing. To prevent this unacceptable performance, it is recommended to: 1) fill the hollow core of the concrete blocks with gravel and drive temporary steel bars through block cells, 2) place a zone of crushed stone for a distance of 0.3 m behind the facing blocks, and 3) lightly compact the 3 feet behind the facing with one pass of a hand-operated compactor and keep heavy machinery 2 feet from the facing.
- The design procedure overestimated the connection forces (Figure 5.14b and Table 5.4) and lateral earth pressure against the wall facing (Table 4.3) measured after construction was completed. The measured connection forces range from 19% to 47% of the design values. The measured lateral earth pressures against the wall facing range from 4.2% to 36.4% of the design values. The

difference could be attributed to two factors: (1) actual shear strength of the backfill is higher than the assumed value in the design, and (2) relatively flexible facing and connection that allowed for comparatively larger mobilization of the shear resistance of the backfill and the support of more lateral earth pressure by reinforcements, thus taking more of the lateral earth pressure off the facing and connections.

- The measured vertical earth pressure behind the wall facing measured after construction was completed ranges from 2% (at a depth of 1.33 m below the footing) to 67% (at the bottom of the wall) of the vertical earth pressures employed in the design (Figure 3.17).
- The placement of the bridge superstructure had a small influence on the loads developed behind and against the upper half of the wall facing (Section 800, see Tables 3.1, 4.2, and 5.1).

6.5.4 External Stability of the Front GRS Wall

- The eccentricity values of the resulting vertical forces acting at different horizontal levels inside the front GRS wall measured after construction was completed are negligible (Table 3.3 and Figure 3.14). Therefore, there is not any potential for overturning the Founders/Meadows structure.
- The flexibility of the front GRS wall exhibited during Stage V (significant movement occurred to the structure) significantly enhanced the overturning stability of the structure by reducing the loads developed behind and against the wall facing.
- The most critical stage for the overturning occurred at the end of Stage III (placement of girders, see Figure 3.14). The backfill behind the bridge (placed during Stage IV) should be placed before placement of the girders to increase the forces resisting potential overturning of the reinforced soil structure.
- The measured bearing pressure at the base of the reinforced fill (Figure 3.15) by the end of construction (154 kPa) is below the expected design value (~199 kPa) and well below the tolerable bearing capacity (480 kPa).
- The measured bearing pressure below the bridge footing (Figure 3.16, 34 kPa) is way below the expected design value (115 kPa) and the allowable value (200 kPa). It is speculated that a large portion of the applied bridge loads beneath the bridge footing were transferred to the wall facing due to differential settlement between the reinforced backfill and the more rigid wall facing.

- The design procedure provides a reasonable estimate of the vertical earth pressures developed along the back of the reinforced soil zone (Figure 3.18).

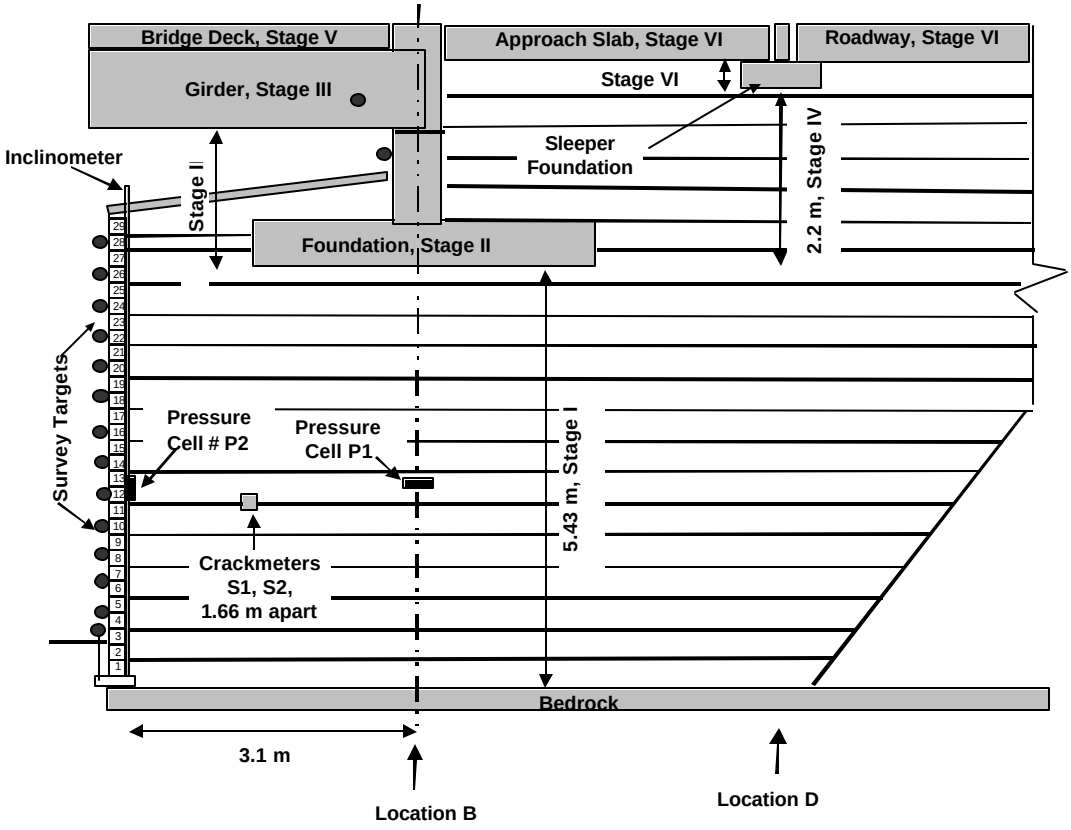

Figure 6.1. Instrumented Section 400 Showing all Monitored Construction Stages.

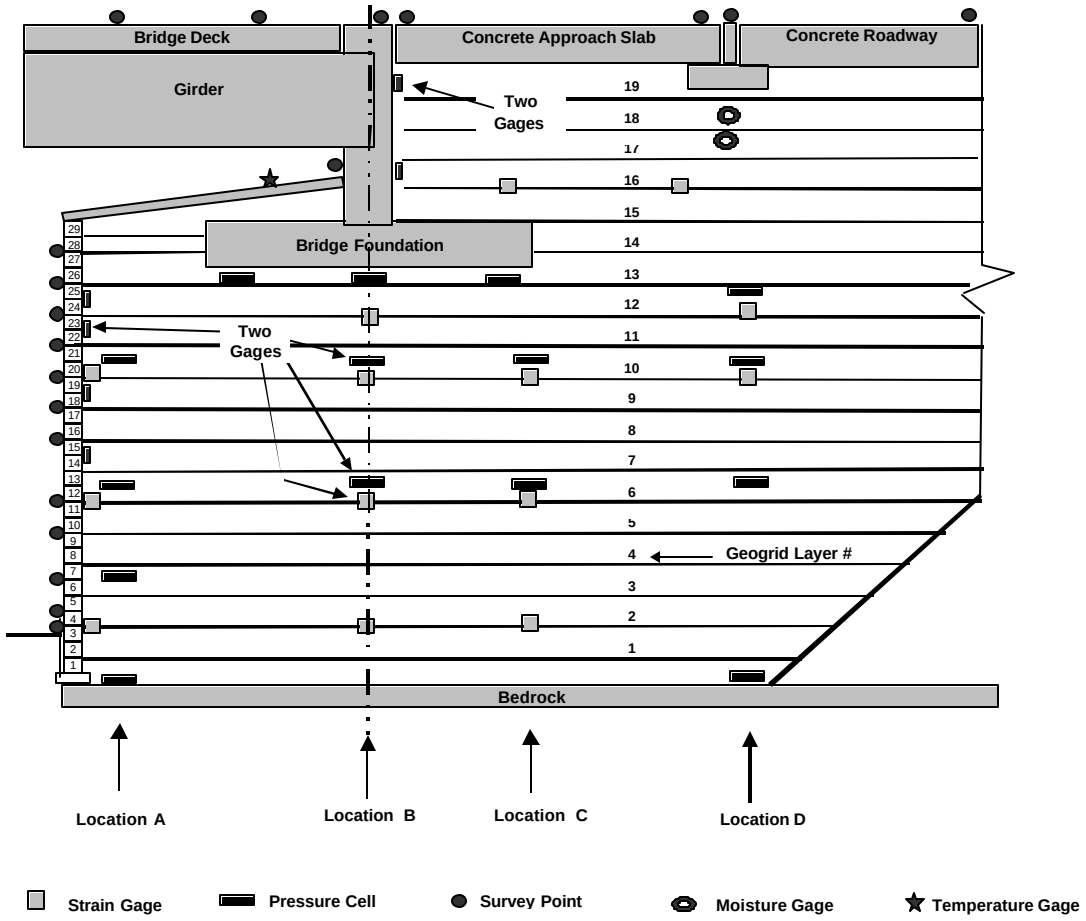

Figure 6.2. Layout and Instrumentation Program for Section 800.

REFERENCES

1. Abu-Hejleh, N., Zornberg, J., Outcalt, S., and McMullen, M. (2001). "Results and Recommendations of Forensic Investigation of Three Full-Scale GRS Abutment and Piers in Denver, Colorado." *Report No. CDOT-DTD-R-2001-6*, Colorado Department of Transportation.

2. Abu-Hejleh, N., Outcalt, S., Wang, T., and Zornberg, J. (2000). "Performance of Geosynthetic-Reinforced Walls Supporting the Founders/Meadows Bridge and Approaching Roadway Structures, Report 1: Design, Materials, Construction, Instrumentation, and Preliminary Results." *Report No. CDOT-DTD-R-2000-5*, Colorado Department of Transportation.

3. Abu-Hejleh, N., Wang, T., and Zornberg, J. (2000). "Performance of Geosynthetic-Reinforced Walls Supporting Bridge and Approaching Roadway Structures." *ASCE/Geotechnical Special Publication No. 103, Advances in Transportation and Geoenvironmental Systems Using Geosynthetics, Proceeding of Sessions of GEO-Denver 2000, Denver, USA, 218-243*

4. Adams, M. (1997). "Performance of a prestrained geosynthetic reinforced soil bridge pier." *Int. Symp. On Mechanically Stabilized Backfill,* T.H. Wu, editor, A. A. Balkema, Denver, USA, 35-53.

5. Andraws, K.Z. and Yogarajah (1994). "Effects of Reinforcement Connections on the Behaviour of Reinforced Soil Retaining Walls." *8th International Conference of the Association for Computer Methods and Advances in Geomechanics*, May, pp. 1313-1318.

6. Buttry, K., McCullough, E., Wetzel, R. (1996). "Temperature and Related Behavior in Segmental Retaining Wall System." Transportation Research Board, 1524, pp. 19-23.

7. Elias, V. and Christopher, B.R. (1997). "Mechanically Stabilized Earth Walls and Reinforced Soil Slopes, Design and Construction Guidelines." *FHWA Demo Project 82*-1, Washington DC, 367 p.

8. FHWA (1997). "Development of Protocols for Confined Extension/Creep Testing of Geosynthetic for Highways Applications." FHWA-RD-97-143. Sponsored by Turner-Fairbanks Highway Research Center.

9. FHWA (2000). "GRS Bridge Piers and Abutments." FHWA-RD-00-038. Sponsored by Turner-Fairbanks Highway Research Center.

10. Ingold, T.S. (1981) "The Effects of Compaction on Retaining Walls." *Geotechnique* 29, No.3, pp. 265-283.

11. Jewell, R.A. (1985) "Limit Equilibrium Analysis of Reinforced Soil Walls", *Proc. 11th International Conference of Soil Mechanics and Foundation Engineering*, San Francisco, Vol. 3, Balkema, Holland, pp. 1705-1708.

12. Ketchart, K. and Wu, J.T.H. (1997). "Loading Tests of GRS Bridge Pier and Abutment in Denver, Colorado." *Report No. CDOT-DTD-97-10*, Colorado Department of Transportation.

13. McGown, A., Andraws, K.Z., Pradhan, S., Khan, A.J. (1998) "Limit State Design of Geosynthetic Reinforced Soil Structures." *Sixth International Conference on Geosynthetics,* Atlanta, Georgia, March, 143-180.

14. Wu, J.T.H., and Helwany, S.M.B. (1996)."A Performance Test for Assessment of Long-Term Creep Behavior of Soil-Geosynthetic Composites." *Geosynthetic International, Vol. 3, No.1, pp. 107-124.*